MICROELECTRONICS BIOINSTRUMENTATION SYSTEMS

FINAL REPORT

October 1, 1976 to September 30, 1977

Research Grant NGR-36-027-053

Wen H. Ko, Ph.D.
Director
Engineering Design Center
Principal Investigator

Engineering Design Center
Case Institute of Technology
Case Western Reserve University
Cleveland, Ohio 44106

Table of Contents

INTRODUCTION

1. Objectives

This program involved the research, development and fabrication of microelectronic bioinstrumentation systems to be employed in the Cardiovascular Deconditioning Program. The primary objective was to design and fabricate implantable telemetry systems for long-term monitoring of animals on earth in order to collect physiological data necessary for the understanding of the mechanisms of cardiovascular deconditioning. The secondary objectives included the study of in-flight instrumentation systems, and the development of microelectronic instruments and RF powering techniques for other life science experiments in the NASA program.

2. Background

During the last two decades, there has been a tremendous advancement in microelectronics, from transistors to integrated circuits (I.C.) and then to large scale integrated circuits (L.S.I.). This has made possible the development of implantable telemetry and stimulation systems which are able to communicate signals through the body boundary by means of RF waves, while the object is assuming normal activity without restraint.

Although the feasibility of implant instruments has been repeatedly demonstrated in laboratories [1, 3] many problems are still unresolved for practical use of chronic implants. A few examples are: a) the size and weight limitation always conflicts with the requirements or desired performance of the range, the accuracy, the number of channels and the signal quality in a noisy environment; b) the power supply for long-term implants; c) the availability of microelectronic components in the implant units that can operate in micro-watt power and at a low voltage supply; and d) the most serious problem of packaging of the implant unit for chronic application in the body environment. For each specific application, practical solutions have to be developed based on a library of inconsistent information derived from various laboratory experiences.

The Engineering Design Center of Case Western Reserve University has been pioneering the research in implant instruments for the past sixteen years, and now has the complete facility to design and fabricate integrated circuits and implant systems for biomedical research. Our program on the study of implantable biomedical transducers is unique. Many skills in design, fabrication and packaging of implant devices were accumulated in our laboratory [4-6]. The effort on microelectronic instrumentation for biomedical research has been supported by NIH for the past eleven years. By using microelectronic technology, implant telemetry devices can be made smaller than an asprin tablet and weigh less than one gram. The unit operates on a power of one to five microwatts and is capable of transmitting one channel of body signal over a distance of three to ten meters to a conventional radio receiver (7).

In order to study the mechanisms of cardiovascular deconditioning continuous monitoring in animals, and later in humans, over a period greater than six months is needed. Long-term monitoring systems for the collection of physiological data on earth as well as in space flight, with minimum restraint possible, is desired. The telemetry system can be used to take measurements and transmit physiological information on-ground and in-flight over a period of several months, to observe how the cardiovascular system alters its performance with the environment. These telemetry devices can be implanted in animals and attached to the body surface of a human subject. The work during the last three years is summarized as follows:

1. Ingestible micropower telemetry system: This study includes the design of monolithic integrated circuit chips for micropower pulse frequency modulators (8) (M-5-A and M-7 circuits) and the digital processing unit for the receiver to discriminate noise from signal pulse. It consists of: a) a control logic, b) pulse, amplitude, duration and period discriminators, c) a digital counter and logic, d) a D/A converter, and e) a power supply. The packaged temperature telemetry transmitter has a diameter of 5.6 mm and a length of 7.2 mm, including a three-month-life battery.

2. Miniature pO_2 and pH sensors for potential use in space suits were explored. The miniature devices were constructed and evaluated, showing better performance than commercially available units. However, their poor stability disqualifies them for chronic applications. The results were published but the project was terminated.

3. Single frequency RF powering technique: The possibility of using a pulsed external RF field to power an implant transmitter with the same RF frequency for powering and signal transmission was investigated. Satisfactory results were obtained. This technique is especially suitable for short range telemetry from the animals strapped in chairs or moving in cages.

This technique was developed to power implanted EKG transmitters with an external coil looped over the monkey's body. The powering pulse is interrupted at regular intervals to receive EKG signals during interrupted window periods. Single channel EKG transmitters were implanted in monkeys using this technique and they have been running satisfactorily from July, 1976 to September, 1976, at Dr. Stone's facility in Galveston and at the Yerkes Regional Primate Center in Atlanta.

4. An RF powered rectangular cage which evolved from a cubic and cylindrical structure has been studied. The RF excitation is from a center rod of the cage. Our laboratory tests have shown that with three to five watts of power, an RF field is generated which is strong enough to develop eight to fifteen volts at the power detector output for implant instrument use. A detector system, using a three orthogonal coils to retrieve power from the cage at any orientation, was designed and is being evaluated. The system uses a unique structure to use three orthogonal coils while maintaining a flat package.

5. Implantable single channel EKG telemetry system: Single channel EKG transmitters and demodulator units were designed. The system is aimed at obtaining base-line information from instrumented animals. The work completed includes: a) battery powered implant transmitters that can operate for three to six months, and b) RF powered units for use on monkeys in chairs.

Units with epoxy and glass encapsulation have been fabricated. The glass units have been functioning in animals from January to June, 1976. Two improved units with greater RF strength and better receiving systems were fabricated and implanted in July, 1976, and have been functioning properly since that time.

6. Three channel RF powered telemetry units: Exploratory studies have been carried out to design a three channel system for EKG, arterial

pressure, and temperature using a single frequency RF powering technique. The bench design has been completed using discrete components and a hybrid integrated circuit version is being assembled for laboratory evaluation. This unit will be incorporated with the RF powered animal cage and three coil detector system to provide continuous monitoring of unrestrained animals in a cage.

7. Packaging techniques and animals evaluation: The single channel ECG transmitters have been evaluated in rhesus monkeys at Dr. Stone's facility in Galveston. Four battery powered, hysol epoxy-silastic packaged units were made and implanted in January and July, 1974, to develop implant techniques. Units failed several weeks later due to body fluid leakage.

A new packaging technique, utilizing a wax-polyethelene mixture was tried in September, 1974. The new units were then epoxy sealed in glass shells, the outside of which were coated with silastic and a dacron gauze wrapped around the glass capsules for suture purposes. The transmitters were RF powered. Failure analysis of the RF powered transmitter revealed that corrosion had occured. It was concluded that only a hermetically sealed transmitter would be suitable for long-term implantation.

The first hermetically sealed transmitters were sent to Dr. Stone in September, 1975. In January, 1976, two additional hermetically sealed units were shipped to Atlanta for implantation. These transmitters were shown to have difficulty after some rotation of the package in the body because powering and signal transmission strength were marginal with air core coils. In March, 1976, the transmitter was redesigned for higher output with a ferrite coil. Two modified transmitters were implanted in monkeys in July, 1976, and as of September, 1976, both transmitters continue to function properly.

PROGRAM ORGANIZATION

The principal investigator of the proposed research is Wen H. Ko, Ph. D., Director of the Engineering Design Center and Professor of Electrical Engineering and Applied Physics, and Biomedical Engineering. He was responsible for the overall operation and progress of the project. Rai-Ko Sun, Dr. Sc., Visiting Associate Professor in Electrical Engineering and Applied Physics was the co-investigator and was in charge of the technical direction of the project, and with Dr. Ko jointly supervised the engineers, graduate students and technicians. The engineers were responsible for microelectronic fabrication, including hybrid circuits and package testing. Graduate Students carried out the research projects under the direction of faculty members to perform design, testing and documentation. The technicians assisted in the assembly, packaging and evaluation.

FACILITIES

The Engineering Design Center maintains a well equiped precision machine shop suitable for miniaturization work. The equipment includes four precision lathes which range from a jeweler's lathe to a 14 inch diameter lathe, a jig borer, drill presses, milling machines, a hand saw, a honing machine, a belt sander, an ultrasonic cleaner, a miniature drill press, an arbor press, surface grinders, and a cutter grinder. Seven other machine shops; including a complete sheetmetal facility, a wood-working shop, and a glass shop; are available on campus.

The Microelectronics Laboratory houses the complete equipment for solid state electronic device, integrated circuit fabrication, and hybrid integrated circuit assembly. The biopolar diffusion line has the capability to fabricate standard transistors and IC circuits. An ion implantation machine, annealing furnaces, and high vacuum evaporation units forms the facility for processing MOS line of circuits and devices. The thick film hybrid circuit line consists of silk screen printer, ceramic firing furnace, crystal and ceramic cutting and lapping machine. An Implant Device Packaging laboratory is being established to have an epoxy molding chamber, laser sealers for glass and metal, and a clean room for implant assembly.

The Applied Neural Control Laboratory is equipped to handle animal testing and evaluation. The laboratory's major emphasis lies in the area of design and development of assistive devices for the disabled. The Engineering Design Center also supports a small-animal facility of its own used by three faculty members from clinical departments of our medical school.

Besides the three major facilities mentioned above, the Engineering Design Center supports various other smaller laboratories which are equipped to aid in the processing, assembly, and bench testing of the telemetry systems developed for this project.

REFERENCES

1. McKay, R.S. Biomedical Telemetry. C.A. Caceres, Ed., New York: Press, 1970.

2. Ko, W.H. and Neuman, M. "Implant Biotelemetry and Microelectronics." Science, Vol. 156, No. 3773, April 21, 1976, pp. 351-360.

3. Fryer, T.B. and Sandler, H. "A Review of Implant Telemetry Systems." Biotelemetry, 1(6), pp. 351-374.

4. Ko, W.H., Ramseth, D., and Yon, E. "A Multiple Channel Monolithic Integrated Circuit Biomedical Telemetry System." 23rd ACEMB, November, 1970.

5. Hoffmann, A. and Ko, W.H. "Design and Fabrication of a PAM/FM Multiple Channel Telemetry System." Twenty-eighth Annual Conference on Engineering in Medicine and Biology, New Orleans, Louisiana, September 20-24, 1975.

6. Ko, W.H. NASA Annual Reports for NASA Grant Number NGR-36-027-053, 1974, 1975.

7. Poon, C.W. "An Ingestible Temperature Telemetry System." M.S. Thesis, June, 1975.

8. Guvenc, M.G. and Ko, W.H. "A Micropower Modulator Chip for Temperature and Biopotential Telemetry." Twenty-eighth Annual Conference on Engineering in Medicine and Biology, New Orleans, Louisiana, September 20-24, 1975.

PROGRESS REPORTS

NGR-36-027-053

October 1, 1976 to September 30, 1977

Priviledged Communication
Wen H. Ko, Ph. D.

SINGLE FREQUENCY RF POWERED ECG TELEMETRY SYSTEM

Introduction

The need for small and long-term telemetry transmitters, which could be used to transmit physiological information from small animals used in various biomedical experiments, imposes difficult restrictions on the construction of such devices. If the use of the implanted volume of present telemetry units is analyzed, it can be seen that the battery or equivalent energy storage generally occupies 50% of the volume, the electronics 25%, and the remainder is usually taken by the radio frequency (RF) tank circuit; antennas; connectors and similar accessories. It is therefore apparent that miniaturization of the electronics itself will not be the complete answer to the problem. Investigation carried out in the Microelectronics Laboratory at the Engineering Design Center, in the past few years, has proven the feasibility of using an RF field to power the implanted transmitter externally; especially when short range telemetry is used for data transmission from animals strapped in chairs or moving in cages. The telemetry system using the external source of energy transmitted into the implant has the additional advantage in not being limited in operation by battery lifetime and can therefore operate for the total life span of the implanted electronic devices.

In order to reduce the volume of the implant unit and to simplify the total equipment needed for such short range telemetry, an approach was developed using a single RF frequency for energy transfer and signal transmission. Only one tank circuit is used in the implant unit for both functions; the RF energy absorption and data transmission. This is acomplished by time sharing multiplexing as shown on the system block diagram in Figure 1.

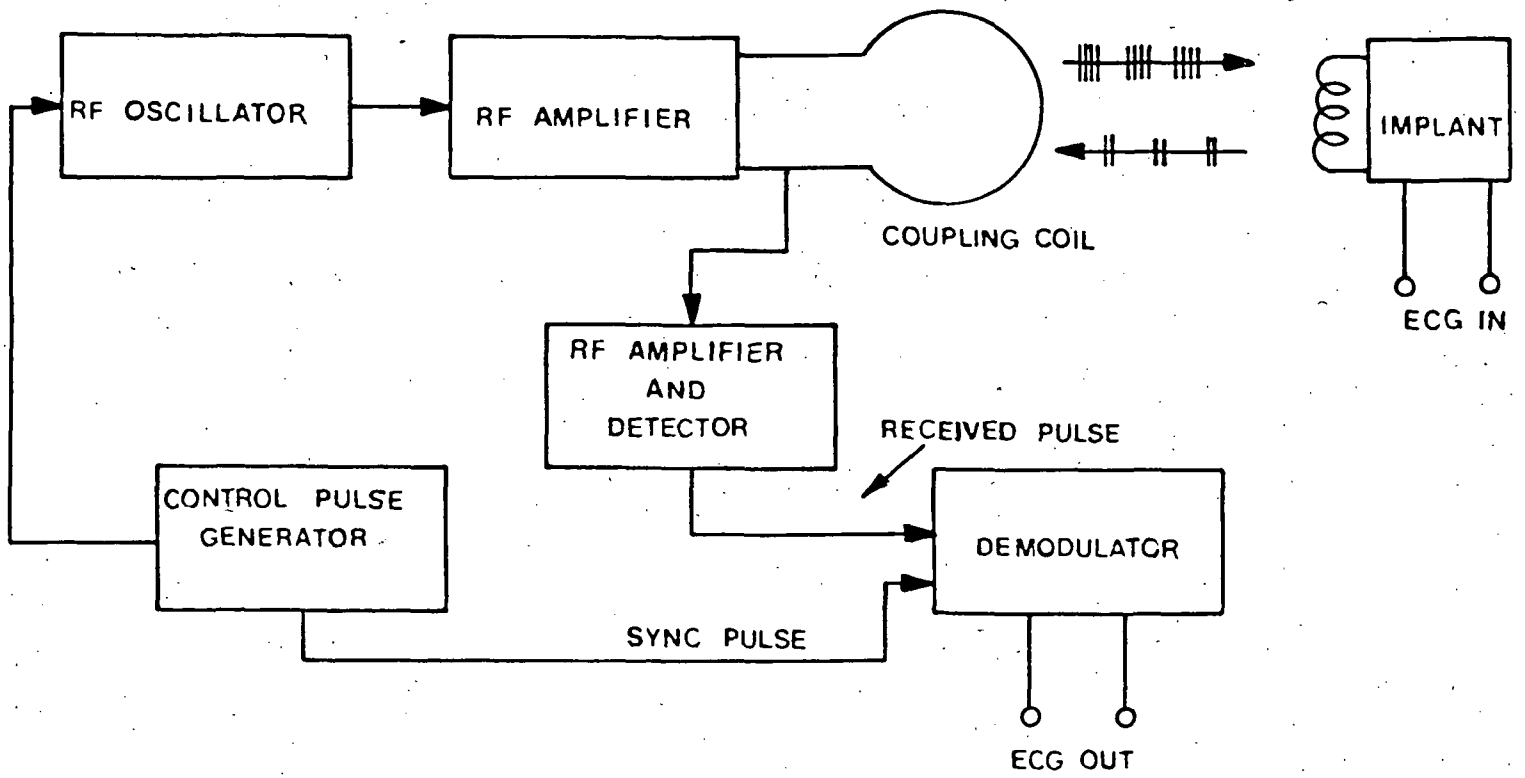

FIGURE 1 BLOCK DIAGRAM OF RF TELEMETRY SYSTEM

System Description

The system was used to transmit the ECG from a Rhesus monkey strapped in a chair for the study of the deconditioning of the cardiovascular system when the subject is exposed to a weightless condition for an extended period. The animal experiments were carried out at the Marine Biomedical Institute (University of Texas, Galveston). The RF coupling coil is an eight inch diameter loop, it was slipped over a chair and the monkey and the axis of the implant tank coil.

The RF signal generated by the RF Oscillator is pulse modulated, by the output of the Control Pulse Generator, to form an interrupted RF pulse train. This RF pulse train is amplified by the RF Power Amplifier to the desired power level and then is delivered to the coupling coil to power the implant. During the RF powering phase, the external RF power is coupled to the implant tank circuit, and the induced voltage and power is rectified and stored in a capacitor to provide the dc power supply for the implant electronic circuits. When the RF powering pulse ends, the implant electronics is turned on, the ECG signal is sampled, and a narrow pulse is transmitted from the implant to the external coupling coil. The information is transmitted by narrow pulse position modulated pulses. The time delay between the trailing edge of the RF powering pulse and the transmitted signal pulse form the implant is proportional to the amplitude of the input, in this case the ECG signal. Only one tank circuit is used in the implant unit for both RF power reception and signal transmission.

The signal transmitted by the implant is received by the same coupling coil for RF powering and is fed to the RF Amplifier through an isolation network. The signal is then detected and fed to the demodulator with the synchronization pulse from the Control Pulse Generator. The recovered biological signal (ECG) is further amplified and a low impedance voltage output is provided for recording or display.

Referring to the timing diagram in Figure 2, the RF energy is stored in the implant during the power phase, t_p and the information is transmitted during the signal phase, t_s. The time delay, t_1, is proportional to the input level of the implant and carries the desired information. The synchronization pulse for modulation in the implant unit is derived

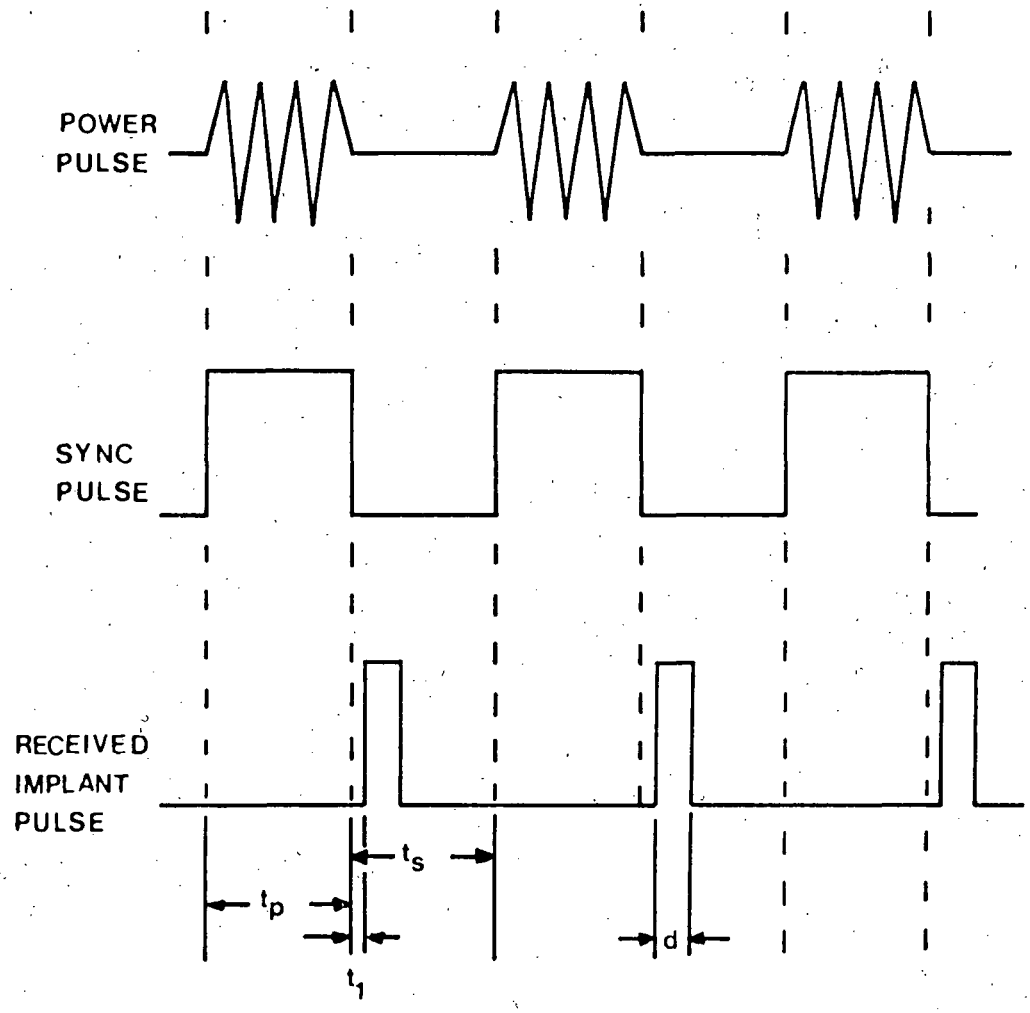

FIGURE 2 TIMING DIAGRAM

from the trailing edge of the power pulse; therefore, the system is insensitive to small variations in the duration and period of the power pulse. The value of the signal phase, t_s is selected with consideration of the maximum expected delay from the implant and power storage capability of the implant circuit. If "d" is the width of the transmitted pulse from the implant and t_{lm} is the maximum expected delay, then the condition for proper operation is $t_p > t_{lm}+d$. Furthermore, due to the power supply regulation consideration it is desirable that energy consumption during t_s be only a small fraction of the total stored energy in the capacitor. Hence, t_s should not be much larger than $t_{lm}+d$.

The time duration of the power phase, t_p, is not critical as long as it is adequate to restore all the energy consumed during the signal phase, t_s. Any variation of t_p will not introduce error into the transmitted signal. The value of "d" is determined by considering the power consumption of the implant, range of transmission, and the signal bandwidth of the RF amplifiers and the detectors of the external circuit.

Implant Unit

The most important section of the implant transmitter is the oscillator. The same tank circuit has to be used for RF power detection and also for oscillation and transmission of the signal. In addition, the circuit has to generate a trigger pulse coinciding with the trailing edge of the RF power pulse which is needed for synchronization of the modulator. The complete circuit diagram for the oscillator is give in Figure 3, the tank circuit is composed of L, C_1 and C_2.

The gate-drain junction of JFET Q_1, acts as a diode during power phase t_p, when Q_2 is turned off. Q_1 serves as the RF power detector. The rectified RF charge is stored in C_5 and the voltage is stabilized by the zener diode, D_2. This stored power provides the power for the implant circuit. A separate RF detector, D_1 and C_3, is used to generate the sync pulse for the modulator. When Q_2 is turned on by the modulator, during transmission period d, the RF signal is radiated or coupled to the external circuit through the tank circuit. Q_1 operates as a conventional Colpitts oscillator.

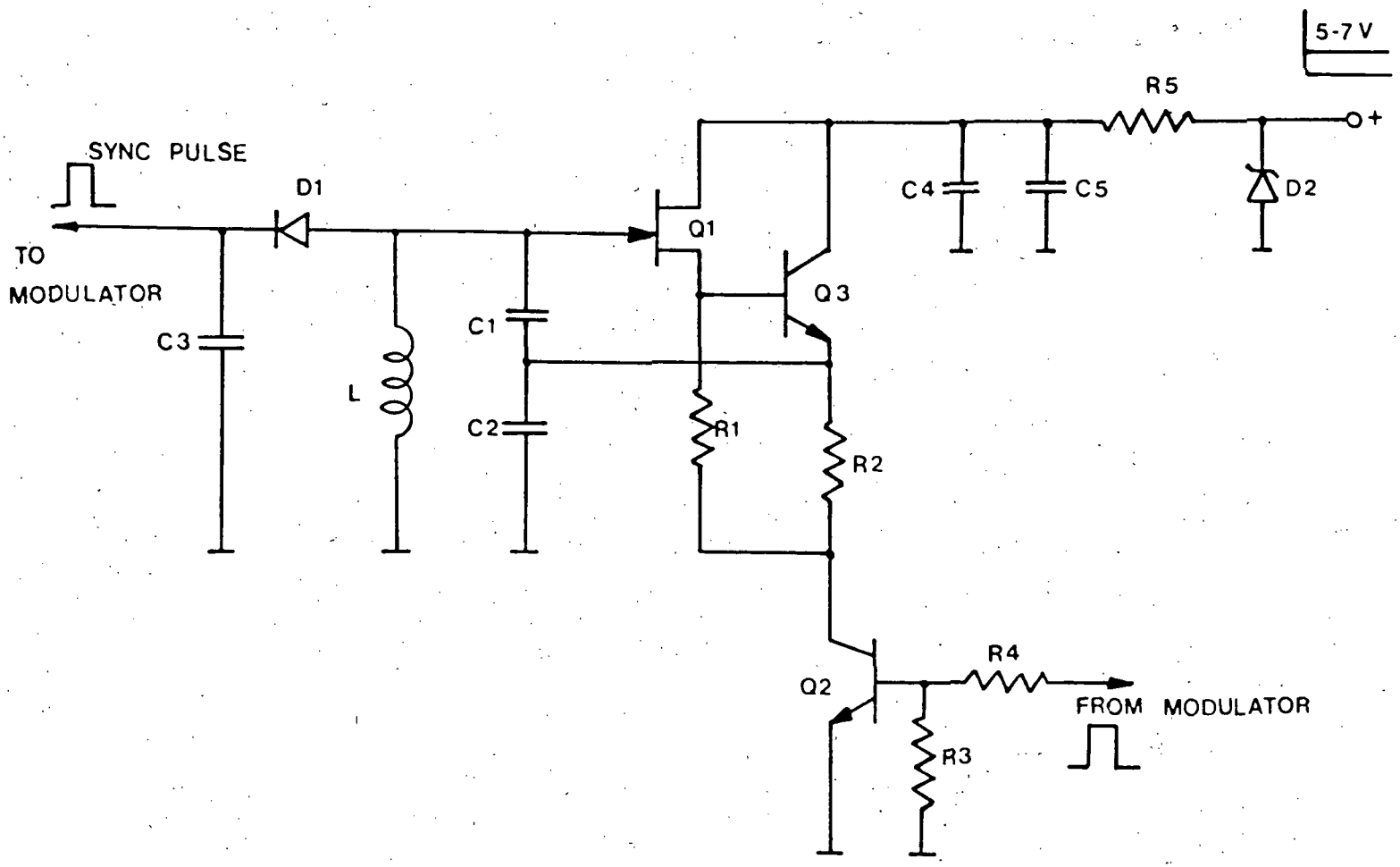

FIGURE 3 OSCILLATOR CIRCUIT DIAGRAM

The modulator section, shown in Figure 4, accomplishes the pulse position modulation through the use of a Miller integrator (Q_4). The voltage ramp generated at the collector of Q_4 (after the trailing edge of the RF power pulse) is terminated as soon as Q_5 is saturated. The integration time is therefore proportional to the voltage at the base of Q_5, which is the input from the signal amplifier to the modulator. When Q_5 is saturated, Q_4 and Q_6 turn off and a 20 μs spike pulse appears at the modulator output, Q_{10}, to the oscillator. This pulse then triggers Q_2 and the oscillator and a 20 μs RF pulse is transmitted from the implant. This modulator output pulse also turns on Q_7 which short circuits the modulator input to prevent retriggering of the modulator. The modulating signal input is obtained from the amplifier and its circuit diagram is shown in Figure 5.

The amplifier uses a standard micropower operational amplifier chip. The unique feature is the use of diodes for input level shifting. Since the amplifier operates from a single supply, the input circuits must be properly biased. This biasing is accomplished through the two diodes to conserve power and to have a short settling time. A bypass capacitor is used to filter out RF signals during the power phase, t_p, to prevent saturation of the amplifier.

The implant electronics are packaged in three flatpacks with the RF tank coil wound on a ferrite core as shown in the photograph in Figure 6. A hermetically sealed glass-metal package was developed to prevent body fluid from leaking into the implant. The package is a 10mm diameter and 43 mm long capsule, and incorporates a glass-to-kovar seal and a transistor header. The header is coated with medical grade silastic and is soldered to the kovar section. A photograph of the packaged transmitter before encapsulation is shown in Figure 7.

The Demodulator

The coupling coil shown in Figure 1 is used to receive the transmitted signal from the implant. The power reception and signal transmission frequencies for the implant are nearly the same (35 and 45 MHz, respectively). The coupling coil is tuned to the power transfer frequency and

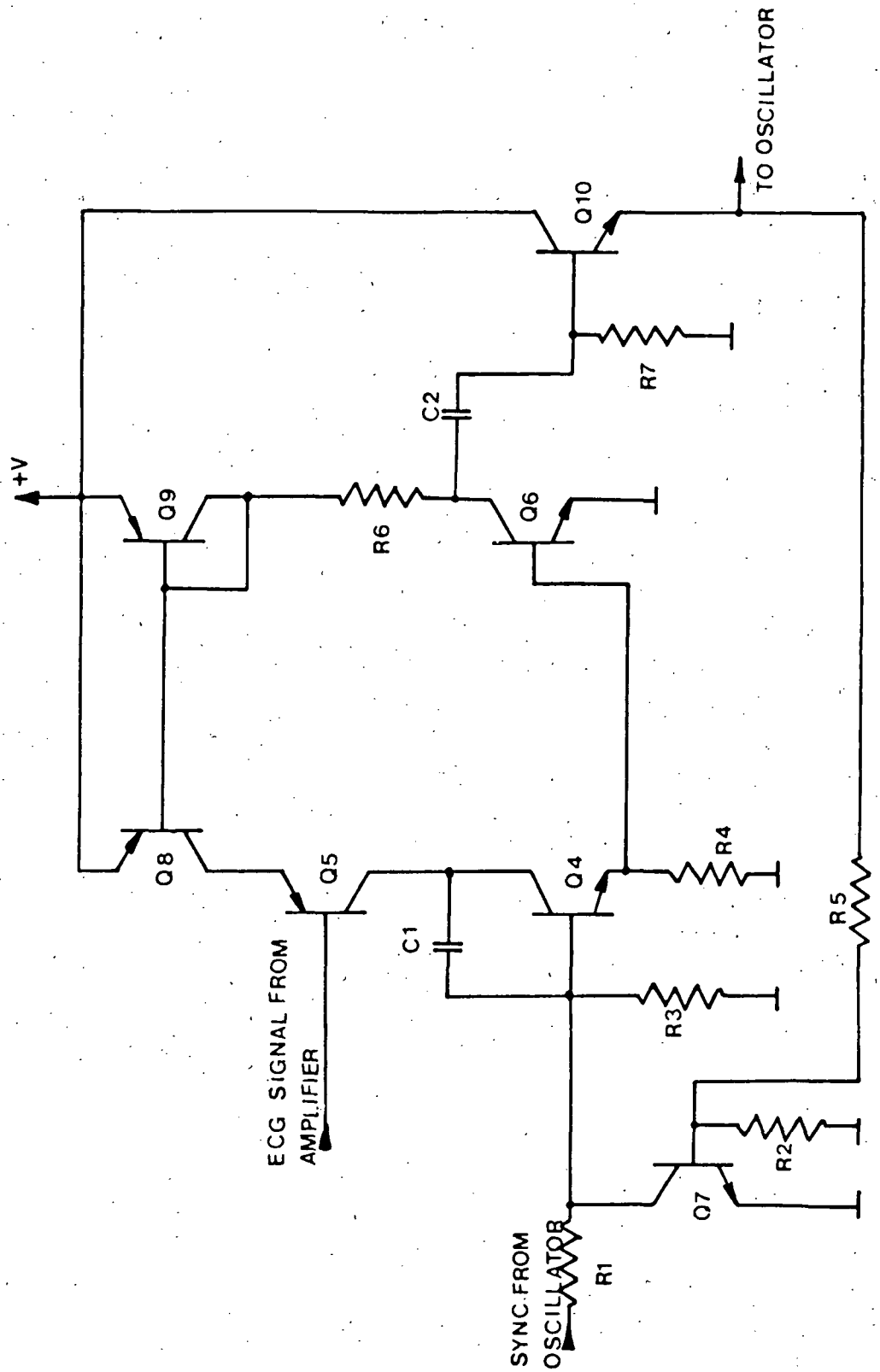

FIGURE 4 MODULATOR CIRCUIT DIAGRAM

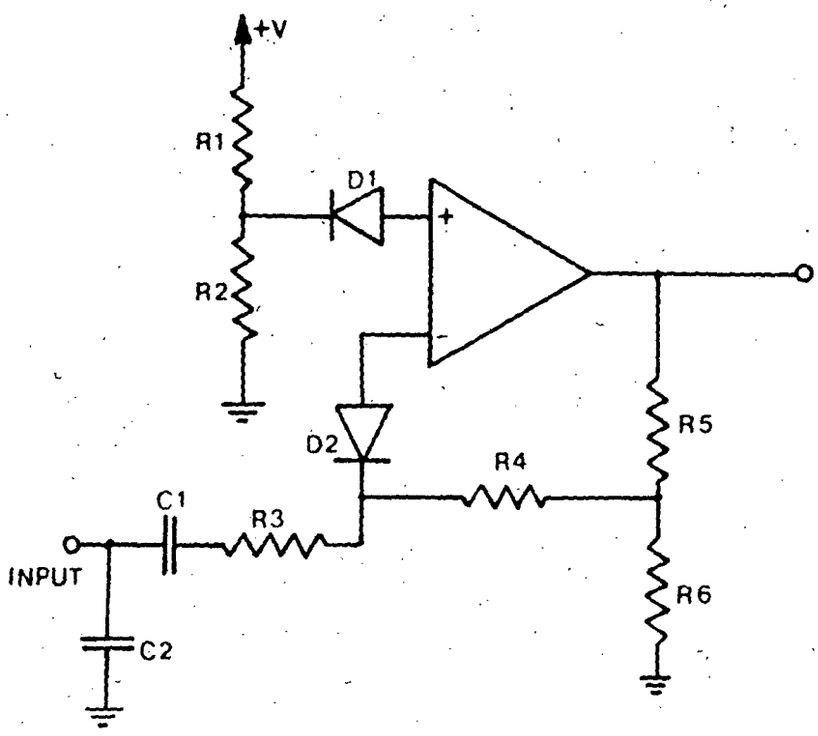

FIGURE 5 MODULATOR AMPLIFIER
CIRCUIT DIAGRAM

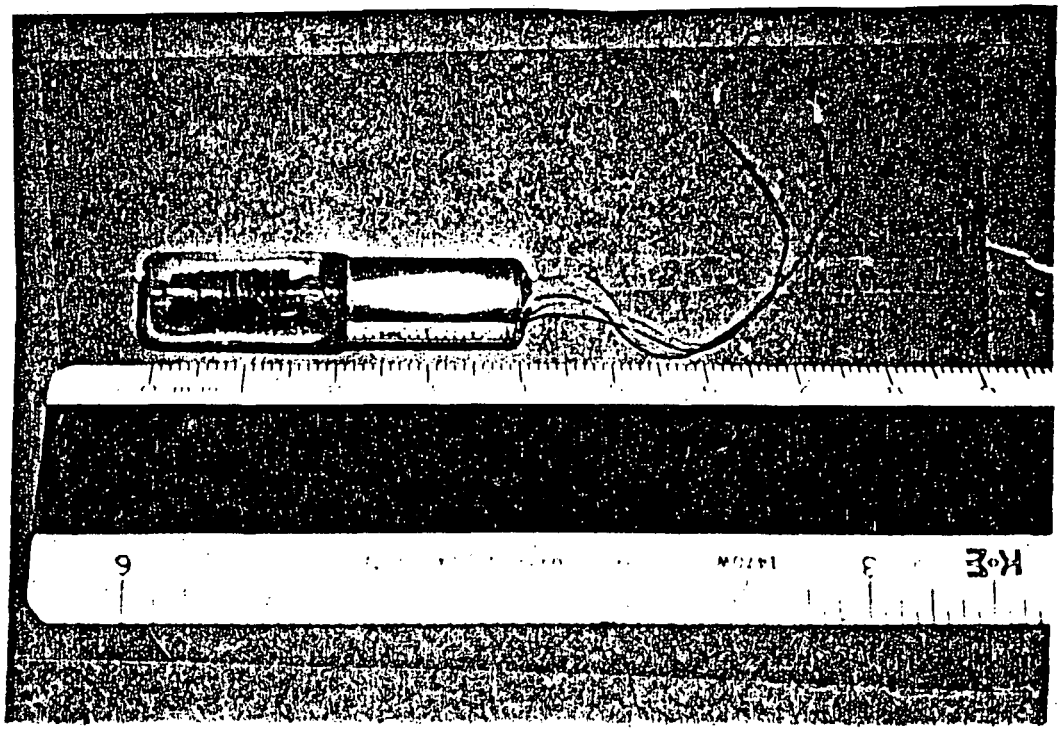

FIGURE 6

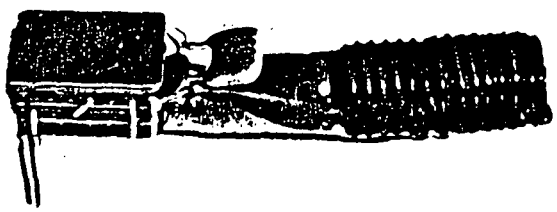

FIGURE 7 PACKAGED TRANSMITTER BEFORE ENCAPSULATION

is not far from the data transmission frequency. The close proximity between the coupling coil and the implant tank circuit (necessary for good power transfer) provides a very strong received signal. The only circuit necessary to detect the implant signal is a simple RF amplifier tuned to the implant transmitter frequency and a diode detector (one transistor). The RF amplifier and detector have a wide enough bandwidth to eliminate the need for external tuning adjustments. The rest of the demodulating system is straightforward, and is shown in the block diagram given in Figure 8.

In order to demodulate the pulse position modulated signal, the PPM pulse is used to sample a ramp voltage which is synchronous with the RF power and the ramp in the implant modulator.

Results

As was mentioned earlier, animal experiments on rhesus monkeys were carried out by Dr. H.L. Stone of the Marine Biomedical Institute. Two transmitters were implanted. Figure 9 shows two recordings; one taken immediately after implantation and one a month after implantation. Evaluation of the recorded data indicated that the transmitters exhibited a fairly high input noise level (50 μV peak). Investigation of the problem revealed that the diodes used to level shift the inputs in the amplifier added a considerable amount of noise to the system. Therefore, the amplifier was redesigned to eliminate the diodes. Instead of level shifting the inputs, a negative supply is generated from the RF detector. A schematic of the improved amplifier design is shown in Figure 10.

Diode D and capacitor C provide a filtered negative voltage. The voltage is regulated to -0.6 volts by diode D2. This amplifier circuit exhibits an equivalent input noise level of 5 μV peak at a signal bandwidth of 200 Hz.

Two transmitters were constructed with this new amplifier design and implanted in the rhesus monkeys. Figure 11 shows two recordings; one immediately after implantation and one a week after implantation. These recordings show considerably less baseline noise than the previous units.

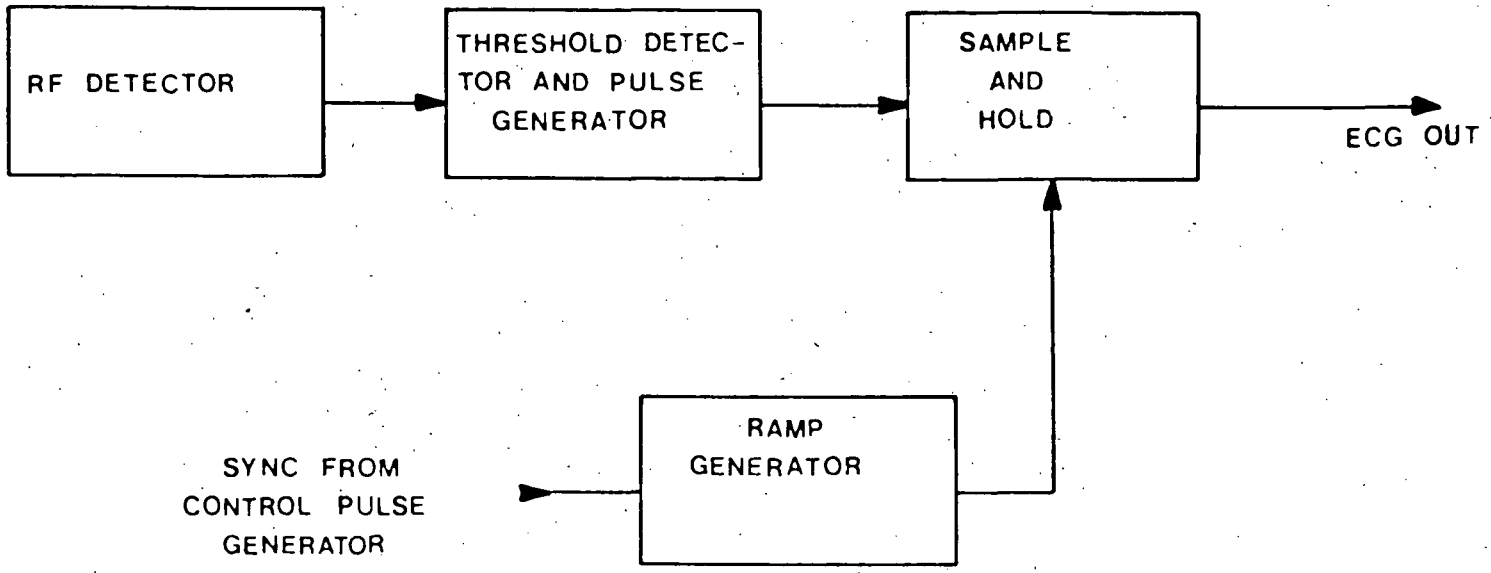

FIGURE 8 DEMODULATOR BLOCK DIAGRAM

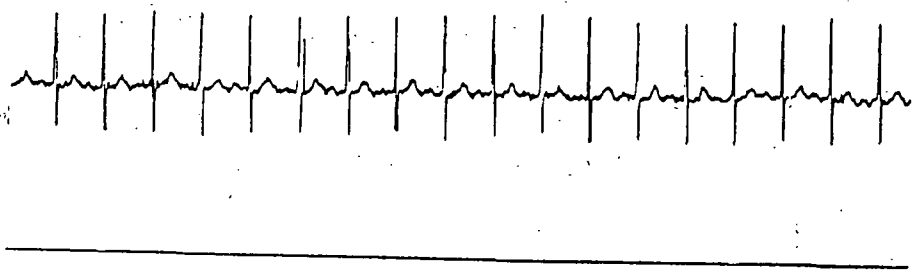

FIGURE 9a EKG RECORDING TAKEN IMMEDIATELY AFTER IMPLANTATION

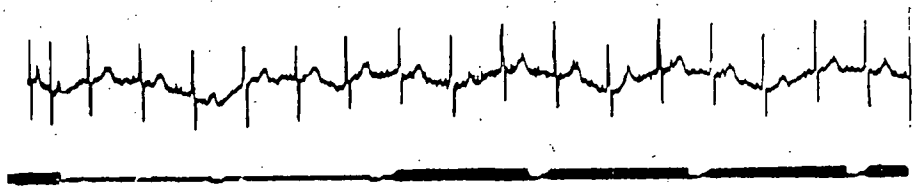

FIGURE 9b EKG RECORDING TAKEN ONE MONTH AFTER IMPLANTATION

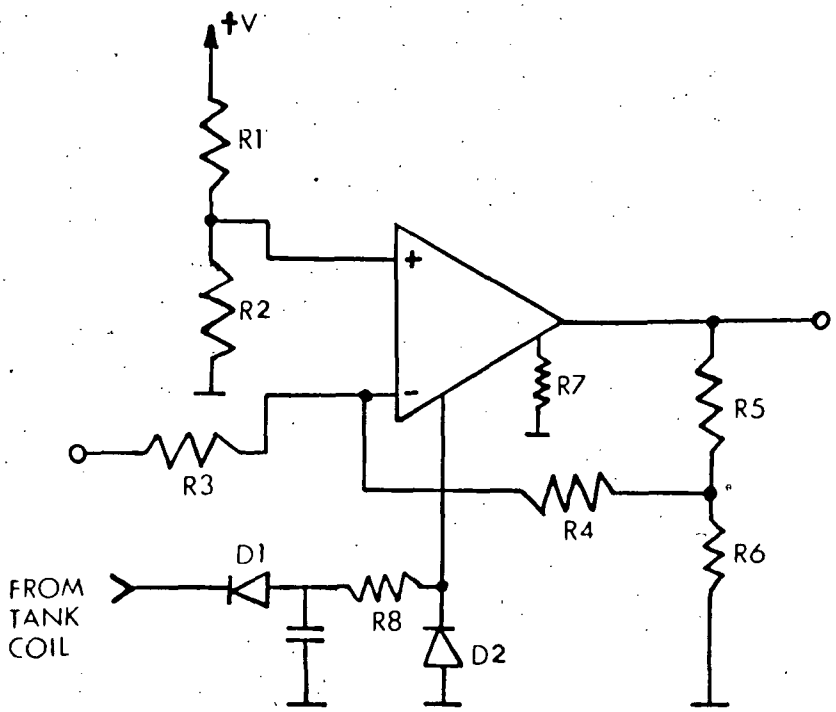

FIGURE 10

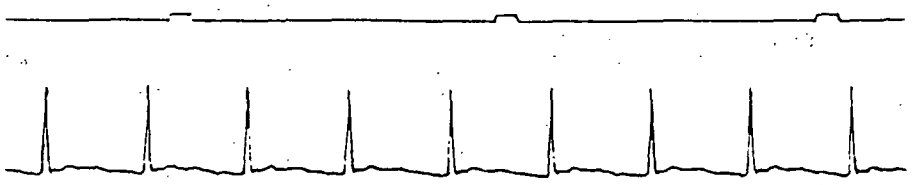

FIGURE 11a EKG RECORDING TAKEN IMMEDIATELY AFTER IMPLANTATION

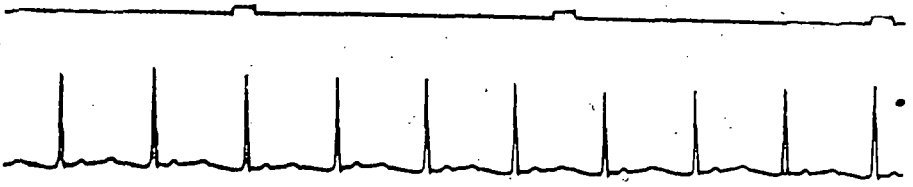

FIGURE 11b EKG RECORDING TAKEN ONE WEEK AFTER IMPLANTATION

Conclusion

The experiments carried out using the RF powered telemetry system demonstrate the feasibility of RF powered systems. After refinements to the electronics, the system is providing good quality EKG recordings. The lifetime of the system is limited only by the lifetime of the implanted electronics and package. The hermetic sealing of the package should provide good protection of the electronics and insure a virtually indefinite lifetime.

Priviledged Communication
Wen H. Ko, Ph. D.

A TELEMETRY CAGE SYSTEM FOR SINGLE FREQUENCY RF POWERING AND RECEIVING

Introduction

The RF cage is modeled as a short-circuit coaxial cable and consists of three major sections: (1) the power driving system, (2) the three axis power detector and (3) the receiving system. The block diagram of the cage system is shown in Figure 1.

The pulsed RF signal, which is generated from a gated oscillator, is applied to the resonant circuit of the cage through a 2W and a 30W power amplifiers. Since the cage is a high Q inductor, an automatic frequency control (AFC) circuit is necessary to compensate for detaining effect due to the movements of the animal inside the cage.

A central conductor passes longitudinally down the center of the cage and is connected to the outer wall at one end of the cage as shown in Figure 2. A twelve watts, 27.5 MHz RF power supplied to the cage generates an RF field inside of the cage which surrounds the central conductor. An RF power detector with three orthogonal coils was designed to pick up and rectify the RF power to d.c. power to supply the implant telemetry system.

The RF power is switched on and off at a rate of 400 Hz. Transmission of the telemetered information from the implant is accomplished by a pulse position modulation scheme during the "power off" interval. The receiving antennas are close to the inside wall of the cage. The receiving system consists of three orthogonal open loops, each of which are connected to an RF amplifier followed by a detector. The three outputs of the detectors are summed and transmitted to a demodulator to obtain the demodulated analog information.

Design of the Rectangular Cage

The configuration of the cage and the magnetic field inside the cage

FIGURE

A DIAGRAM OF AN ADDRESSING AND RECEIVING SYSTEM

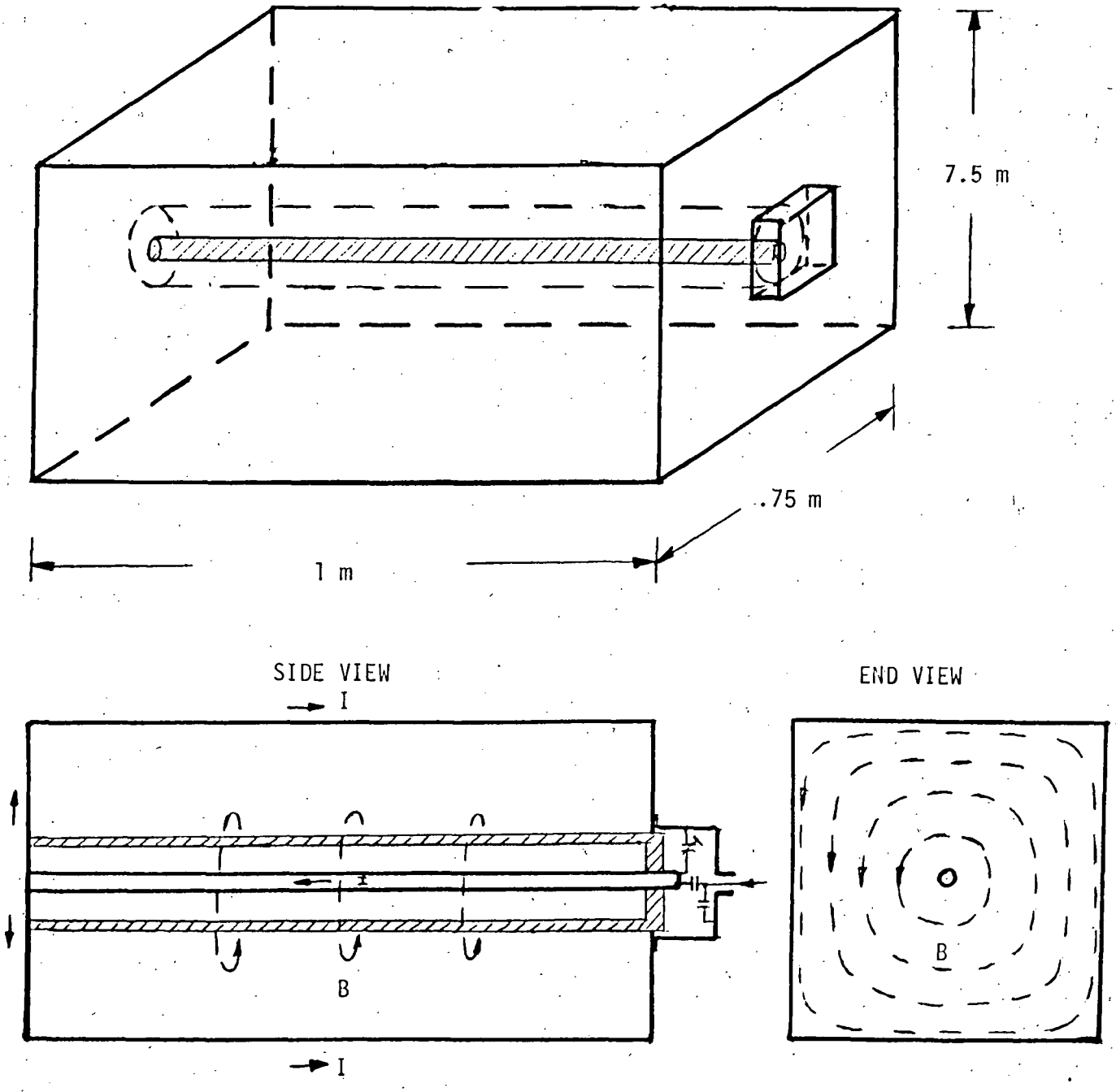

Figure 2. THE CONFIGURATION OF THE CAGE

are shown in Figure 2. The flowing path of the current I builds up a magnetic field B which is inversely proportional to the radial distance from the central rod and is independent of the axial position. B is given by:

$$B=\frac{\mu_o I}{2\pi r}$$

where r is the radial distance from the central rod.

If r is very small, B will be too high and so will DC pick-up voltage (above five times the minimum value required). Then the regulator following the detector will not be able to regulate the detected voltage within the limited range. In addition, the resonant circuit of the cage would be greatly detuned. Therefore, the central rod is surrounded by a plastic tube so that the animal cannot reach this region.

The rectangular cage with a size of 1m x .75m x .75m can be considered as an end-shorted coaxial cable. As the length of the cage is much shorter than the wavelength, the cage is a high Q inductor. The equivalent inductance is given by:

$$L=\frac{\mu_o l}{2\pi}\left(\ln\frac{b}{a}\right)$$

where l is the length of the cage (in meters)

b is the equivalent outer diameter of the cage

a is the diameter of the central rod.

In this case, l = 1m;

$$b = 0.75\text{m} \times \frac{1+\sqrt{2}}{2} = 0.9\text{ m}$$

a = 1 inch

hence, l = 0.79 μh. While the system is operating at 27.5 MHz the tuning capacitance is 42 pf. The tuning circuit of the cage is shown below. The Q of the resonant circuit is 90.

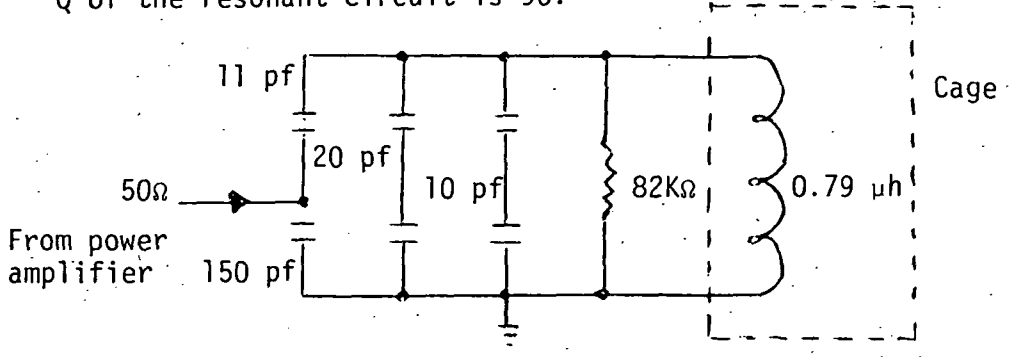

The mechanical construction of the cage is illustrated in Figure 3. RF power is fed into the cage from one end of the cage. The receiver and an electrical fan are mounted on the other end. The fan blows air into the plastic tube through holes on the wall of the cage. Two rows of small holes are drilled on the bottom of the plastic tube. Six pipes are on the top of the cage. The air flow in the cage is shown in Figure 4. The bottom of the cage is hinged at rear. It can be opened while cleaning. A row of rods are set three inches above the bottom for the convenience of cleaning.

Negative Feedback Loop For Automatic Frequency Control (AFC)

The AFC block diagram shown in Figure 5 would miminize the reflected power by minimizing the frequency difference between the RF oscillator and the cage resonant circuit. The d.c. output voltage V_{ref} of the power meter WV-4, which is proportional to the square root of the reflected power, is used as the error signal of the negative feedback loop. Through a low pass filter and a d.c. amplifier, V_{ref} is amplified and the output voltage V_d is applied to the voltage controlled RF oscillator. The circuit diagram of the oscillator and AFC is shown in Figure 6.

Three-axis Power Detector

The circuit and construction diagram of the three-axis power detector are shown in Figure 7. Two perpendicular ferrite-core coils and an air-core coil are utilized to pick up the pulsed RF power. The positions of the three coils and the flat pack of the transmitter are arranged to minimize the mutual inductances and loading effects among them. In addition, a small air core coil is required as the transmitting coil of the implanted transmitter. The pick-up d.c. voltages of the three coils are connected serially so that higher voltage can be obtained and the ripples due to the variation of the direction of the power detector are reduced. The two diodes for each coil make the circuit symmetrical. The three tank circuits resonate at 27.5 MHz and have a loaded Q of 20. The performance of the power detector is shown in Figure 8. For a single channel EKG telemetry, a minimum voltage of 8 volts with a load current 100 μA is required.

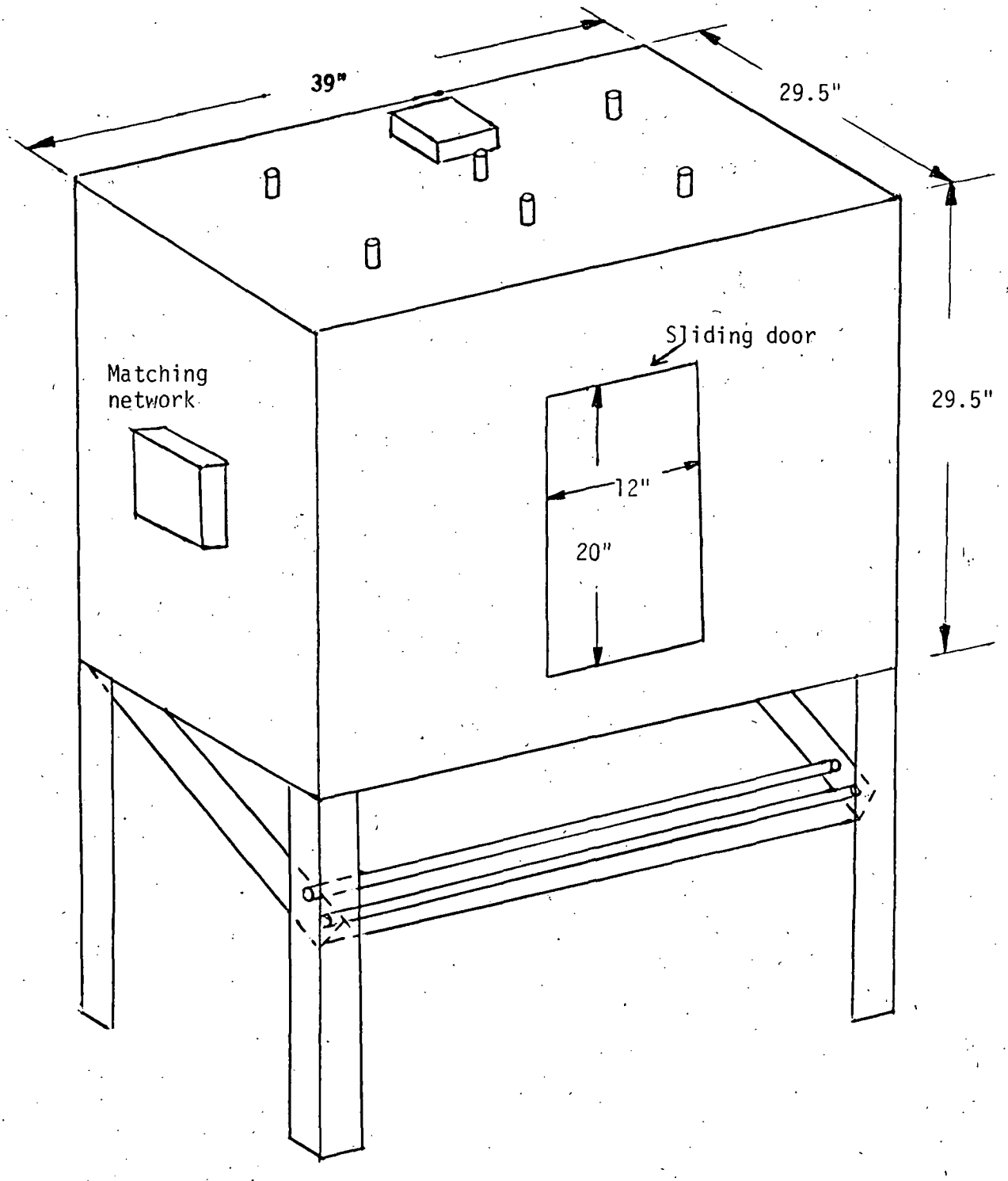

FIGURE 3. MECHANICAL DIAGRAM OF THE RF POWERED CAGE.

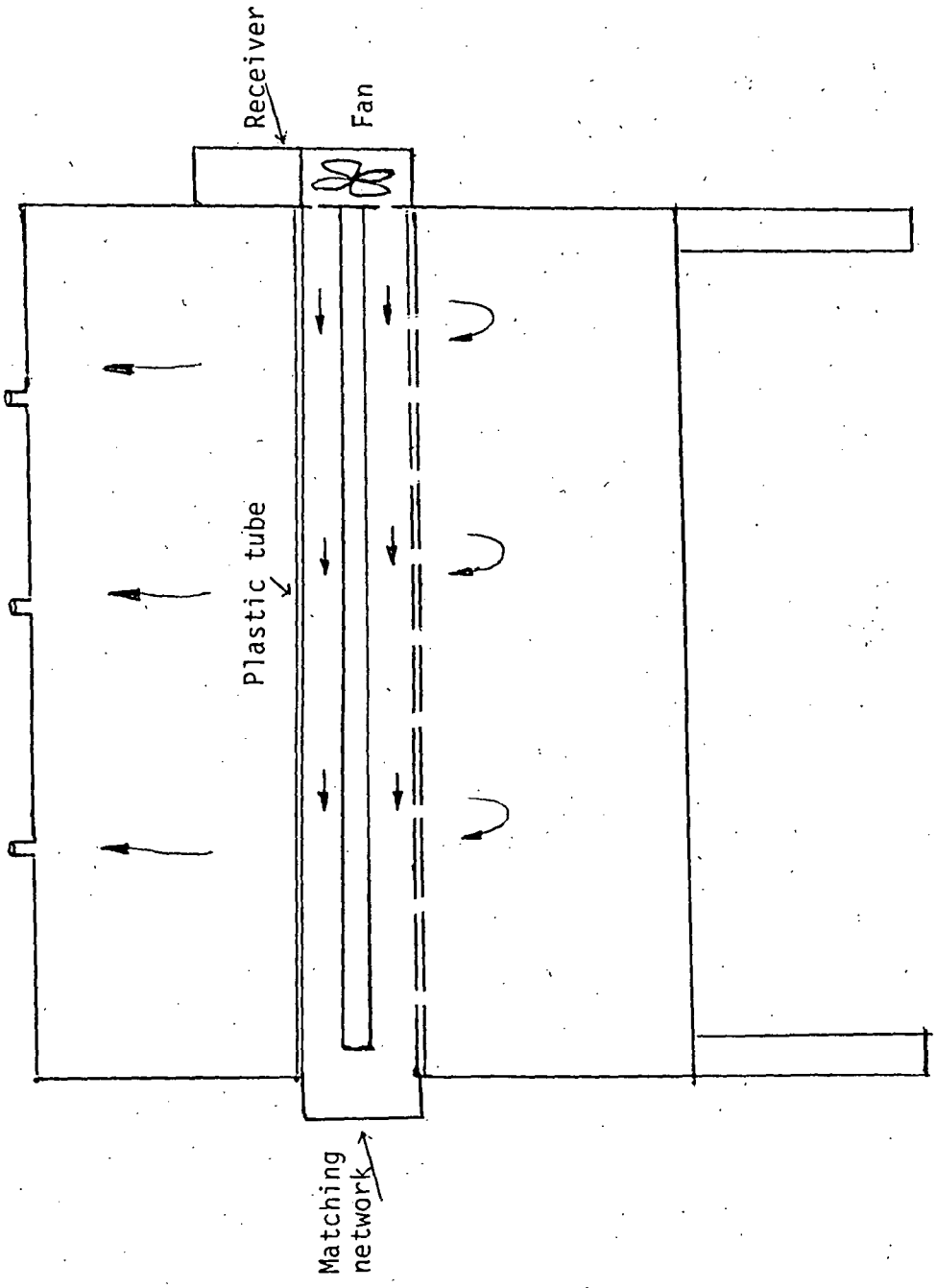

FIGURE 4. THE AIR FLOW IN THE CAGE.

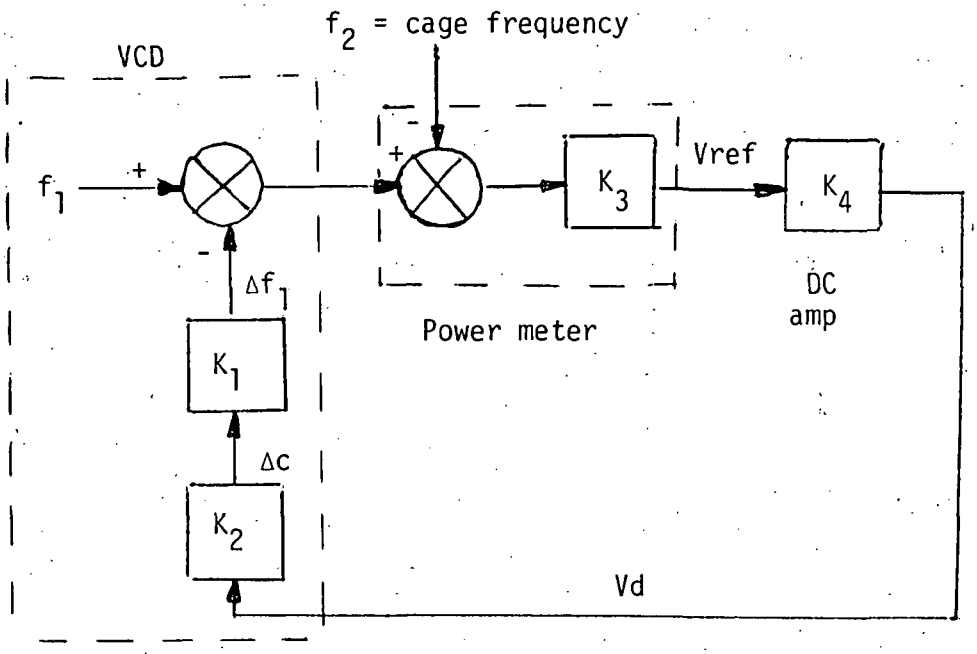

FIGURE 5. BLOCK DIAGRAM OF AFC

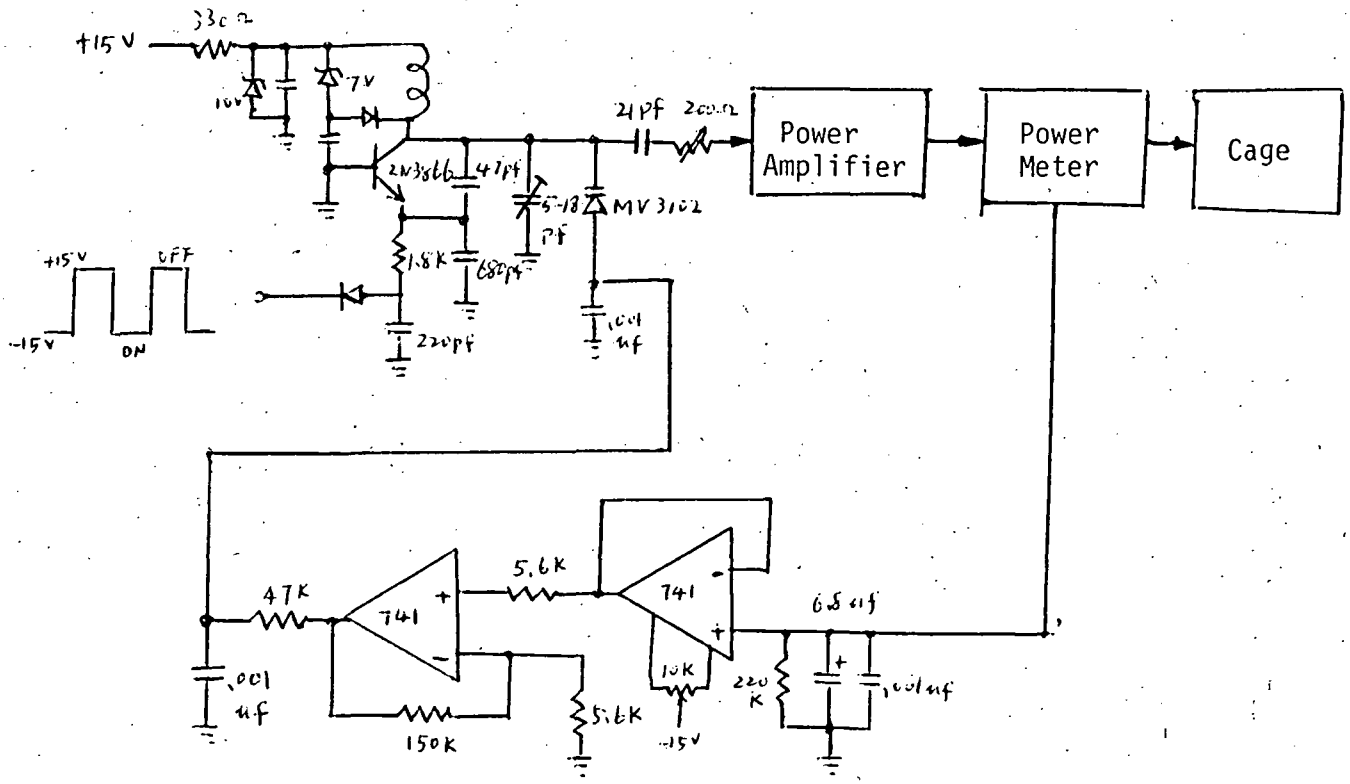

FIGURE 6. CIRCUIT DIAGRAM OF OSCILLATOR AND AFC.

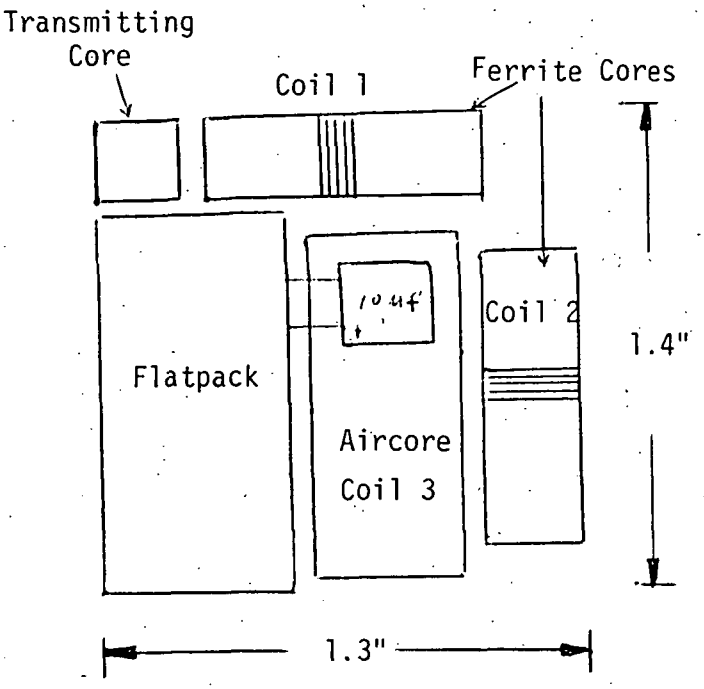

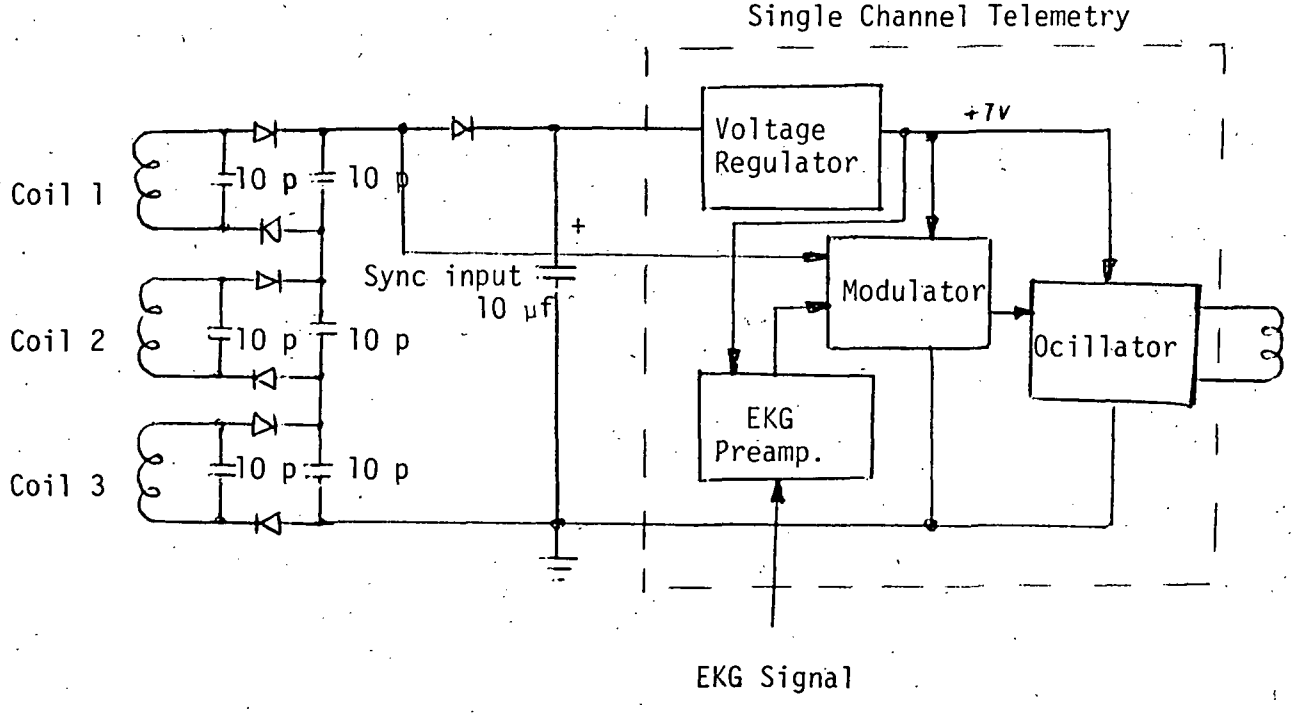

FIGURE 7. CIRCUIT AND CONSTRUCTION DIAGRAM OF THE POWER DETECTOR.

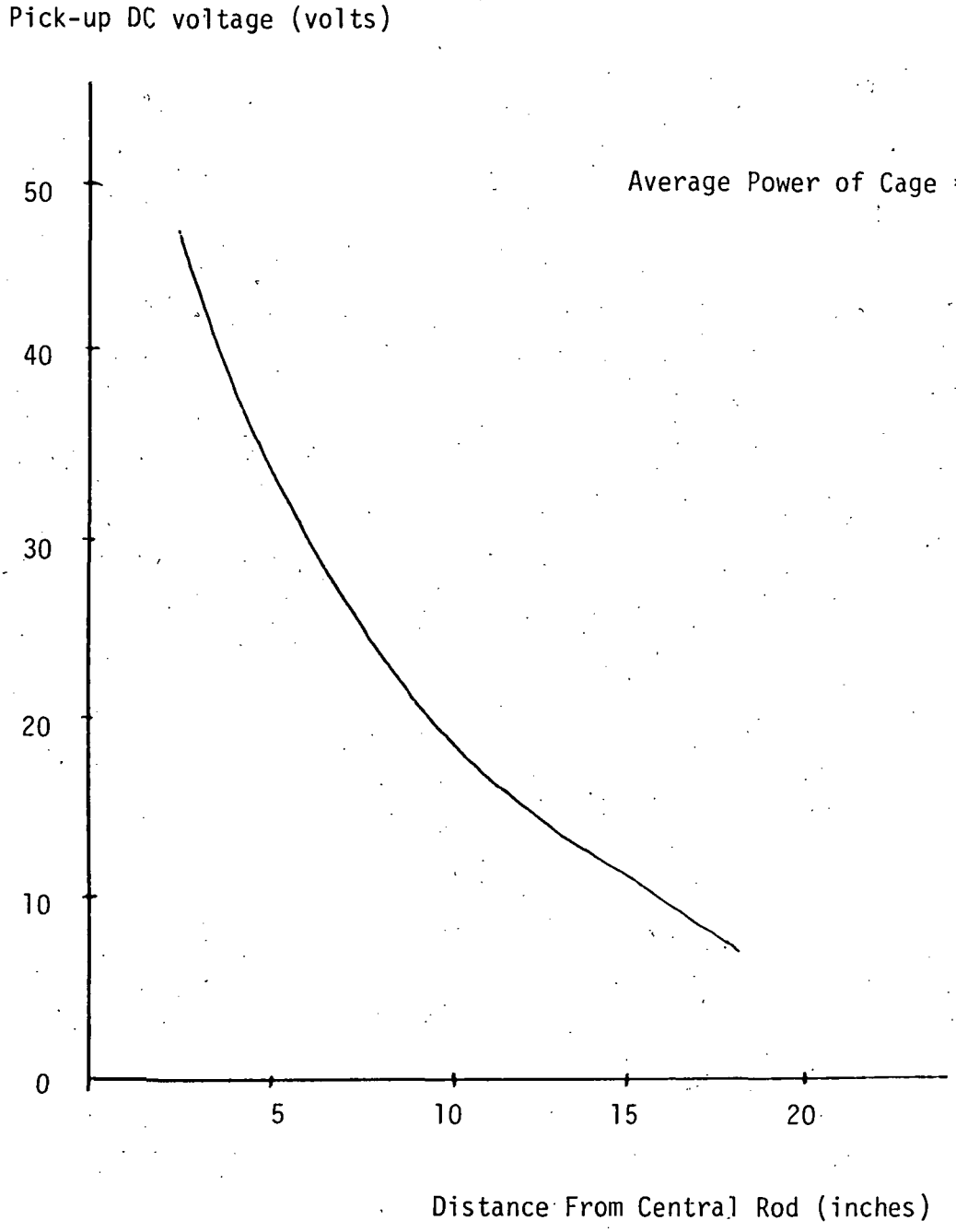

FIGURE 8. PERFORMANCE OF THE POWER DETECTOR.

To obtain the effective permeability as high as possible, the length of the ferrite cores must be at least three times its diameter. In this case, the diameter of the core is 1/4", the length is 3/4", and the permeability of the material is about 30. Hence, the effective permeability, μe, is determined by:

$$\frac{\mu_e}{\mu_o} = \frac{\mu/\mu_o}{1 + 0.1(\mu/\mu_o - 1)} = 7.7$$

Therefore, the area of the air-core is designed to be about eight times the cut area of the ferrite-core. Then the three coils will pick-up equal DC voltage.

The three coils are specified as below:

Coil 1 and 2: Core: Size 3/4" x 1/4" x 3/16"
Permeability = 30 at 30 MHz
Wire: #28
No. of turn: 8 - 1/4
Coil 3: Core: Size 3/8" x 3/4" x 1/8"
Wire: #24
No. of turn: 10

Receiver

To receive strong enough signal independent of the position and orientation of the transmitting coil, three orthogonal antennas of the receiver are constructed as shown in Figure 9. They are made of copper strips with width 1/4" and are built 1/2" apart from the grounded walls of the cage to get high capacitive coupling with the transmitting coil. Through three coaxial cables, the three antennas are connected to the inputs of three RF amplifiers respectively.

A 3N128 and a MC1350 constitute the two stages RF amplifier which has a gain 50 db. The low level detector, MC1330, is a doubly balanced, synchronous detector featuring very linear detection. Its conversion gain is 30 db. The tuning circuits in the receiver are all tuned at the transmitting frequency, 48 MHz, and have a Q of ten.

The three pulse outputs from the three detector are sent to a sum-

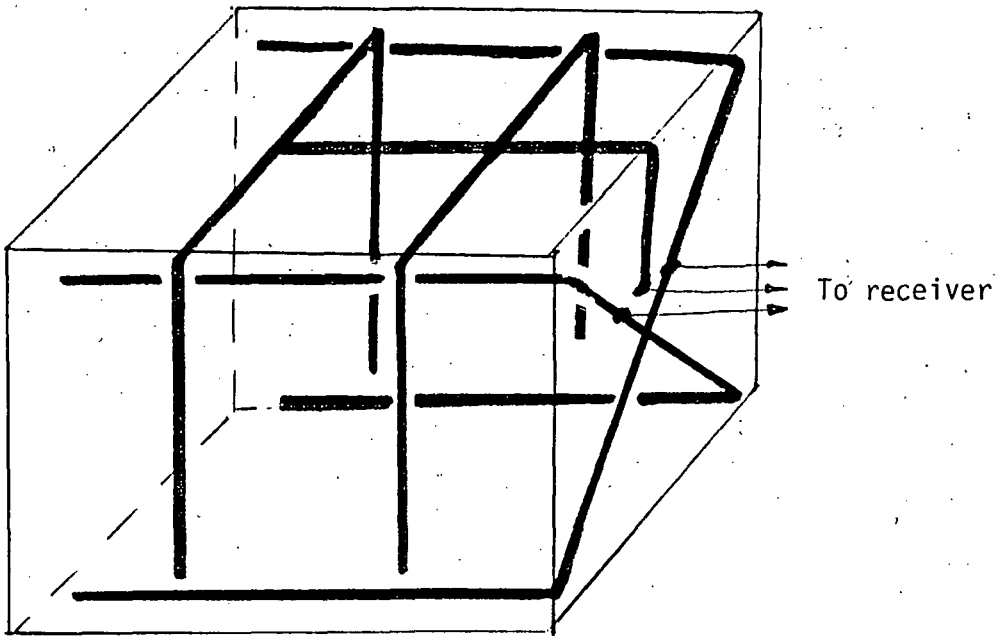

FIGURE 9. ANTENNAS OF THE RECEIVER.

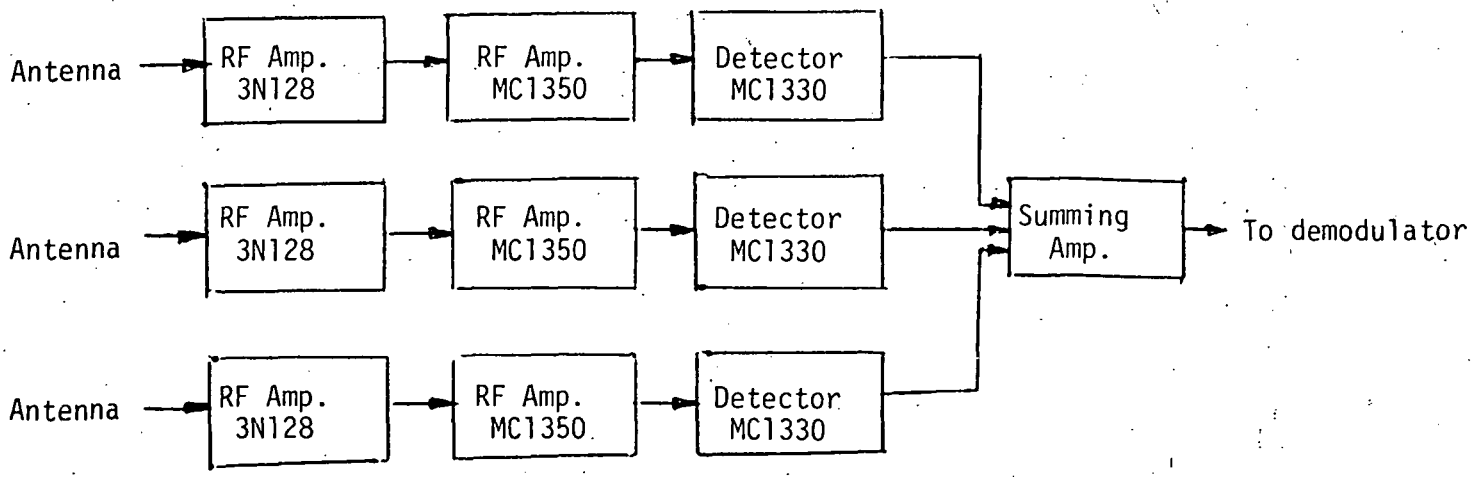

FIGURE 10. BLOCK DIAGRAM OF THE RECEIVER.

ming amplifier. The summed voltage is connected to a pulse position demodulator, and is converted to the analog EKG signals. The block diagram of the receiver is shown in Figure 10.

Priviledged Communication
Wen H. Ko, Ph. D.

A SINGLE FREQUENCY RF POWERED THREE CHANNEL TELEMETRY SYSTEM

Introduction

Because of the relative large size and limited lifetime of conventional battery power, RF has become a very promising means of powering implant units and hence has been extensively studied during the past years. This telemetry system stemmed from the single channel RF powered telemetry system developed use in MEL. In this particular application, a single coil in the implant unit was used for both RF energy absorption and signal transmission and therefore reduces the space needed for the two-coil system - one for RF powering and another for signal transmitting at different frequencies. A time sharing multiplexing technique was used.

The physiological events intended to be monitored includes aortic blood pressure, body temperature and electrocardiograms. Aortic pressure normally requires a frequency range of about 40 Hz for meaningful recording, EKG needs about 80 Hz; while body temperature is understood to be a very slow varying parameter. Work up to now has included the system circuit design and system performance to bench stimulation. The remaining problem lies in the packaging area and further investigation is being carried out.

System description

A system block diagram is shown in Fig. 1. Pulse position modulation is used for coding the information. Since the same frequency is used for RF powering and signal transmitting, signal received by the demodulation unit will also consist of these two components. The signal format is shown in Fig. 2.

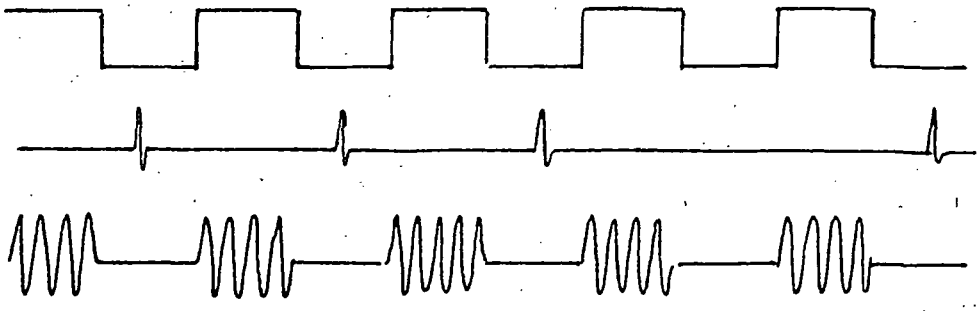

Fig. 2

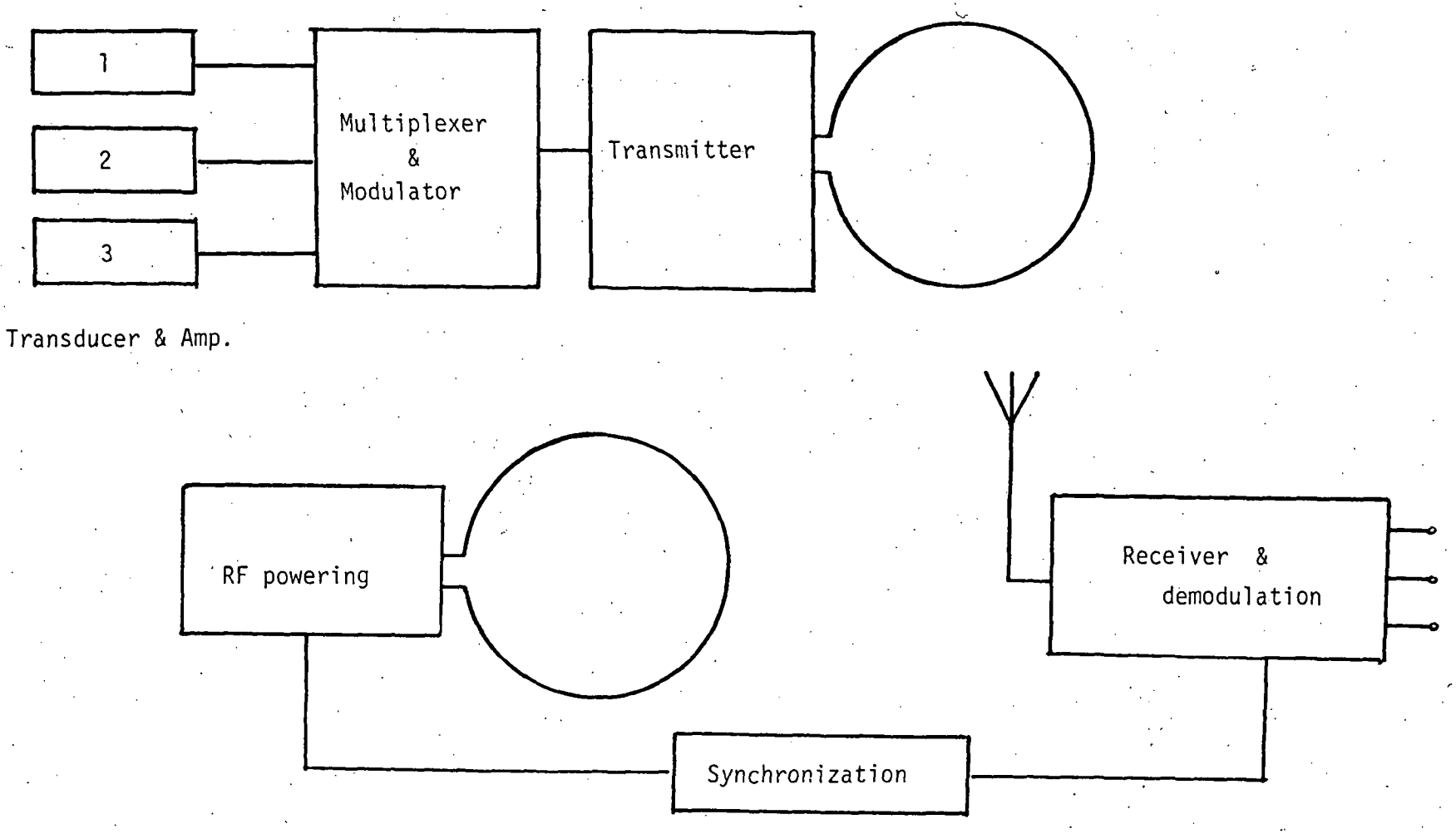

Fig 1. System block diagram

The entire system is synchronized by a clock, as shown in the upper trace. Three sequencing channels are followed by an "empty" channel for channel synchronization purposes. Time lapse between the falling edge of the clock pulse and the signal pulse will then represent the informations -- t_1, t_2 and t_3 in the middle trace. RF powering is delivered during the high periods of the clock as shown in the bottom trace.

The entire system can be divided into an implant unit including transducers, amplifiers, modulator and transmitter; and an external unit which includes the RF powering unit and demodulation unit. They will be discussed separately:

Implant unit. (Fig. 1)

The Implant unit includes the transducers, transducer amplifiers, modulator and transmitter.

(1) Modulator and transmitter.

The modulator is in fact a voltage-to-pulse position converter, the output of which then activates the transmitter. The circuit is shown in Fig. 3, and the timing diagram in Fig. 4. In order to avoid the inter-channel influence, a 470 pF capacitor will be clamped to V+ at every "HI" period of the synchronization clock, through the fourth channel of the 14016 analog gate. The current source for the 470 pF capacitor consists of two 2N3906 transistors shown on top of the capacitor in the diagram.

Fig. 5. shows the circuit diagram of the transmitter, which also acts as the RF power detector. A MPF102 N-channel FET serves as the rectifying diode during RF period. The Colpitts oscillator is activated by pulses from modulator. Clock filtering is achieved through diode detector on the left side of the coil in Fig. D-5. Voltage step down is necessary because of the strong RF induced clock peak-to-peak voltage.

(2) Transducer and transducer amplifier.

Since the pulse position information results from a voltage-to-pulse position conversion, truthful transduction of a physiological event into voltage for the conversion is essential. However, since it is an implant unit; size, power consumption and circuit complexity all have to be taken into account. A compromise of all these concerns will be used to select the final design. For temperature sensing, a YSI thermister (part #44015) with a resistance value of 547K ohms at 37°C is used. The basic idea of the circuit for transduction is that by using the Op. Amp. A1

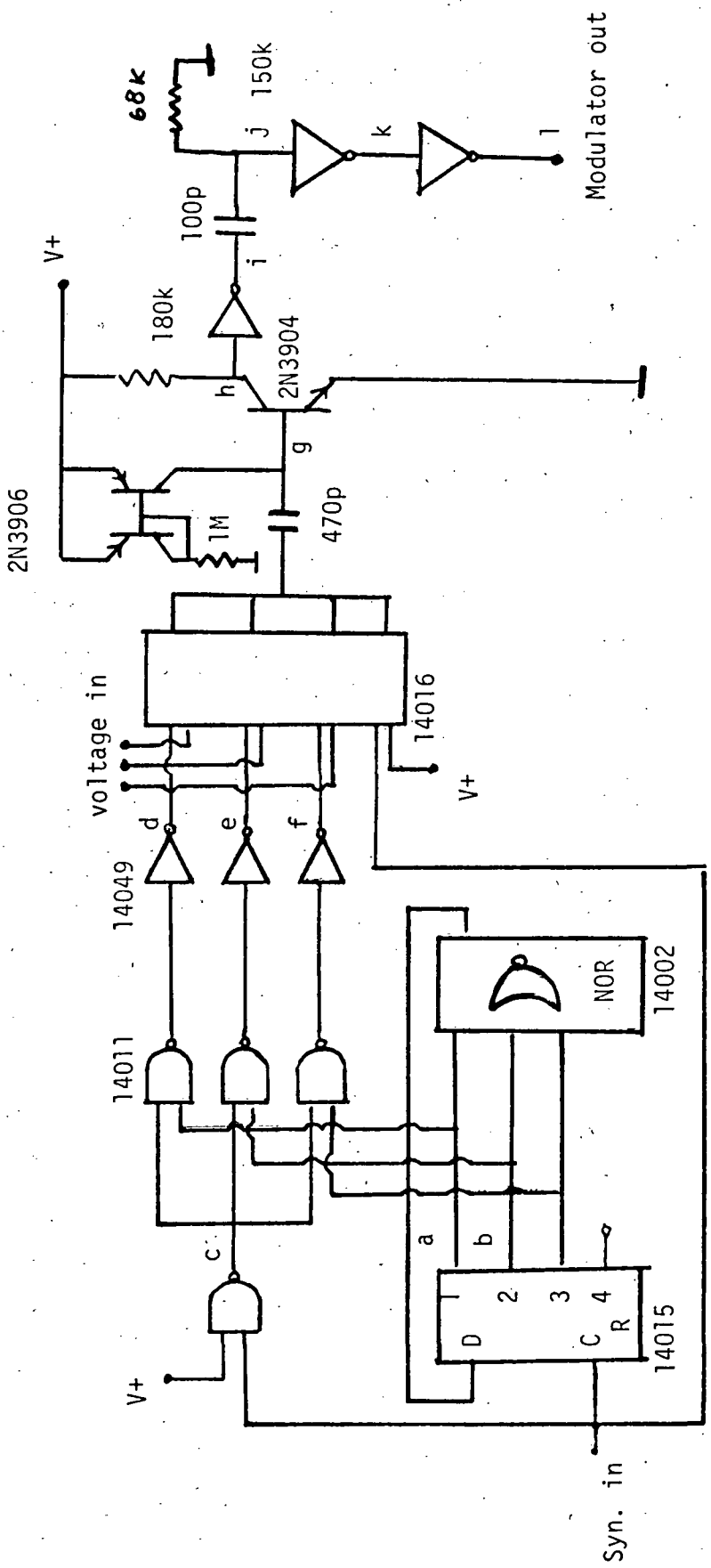

Fig. 3 Modulator - a voltage-to-pulse position converter

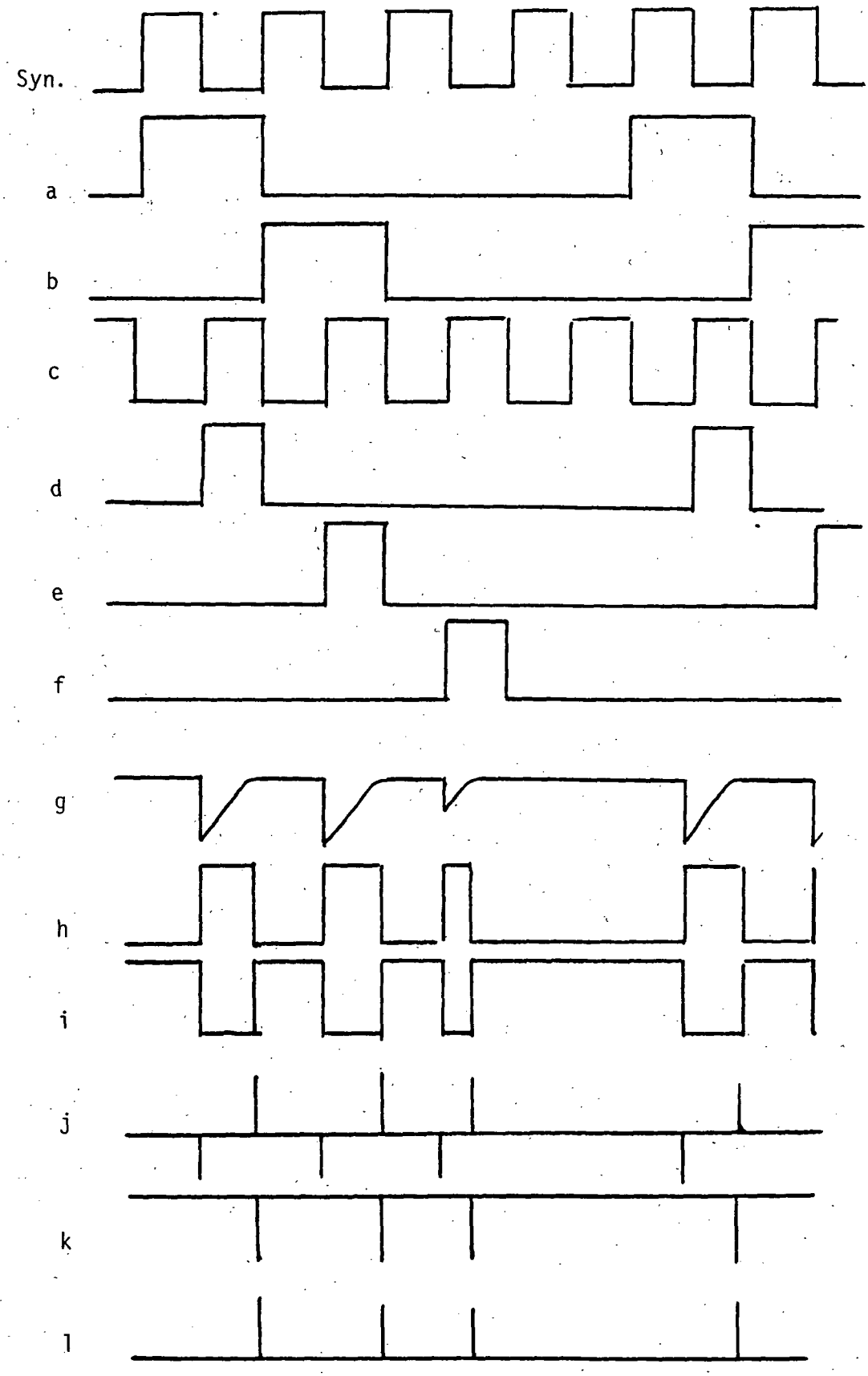

Fig. 4. Timing for modulator

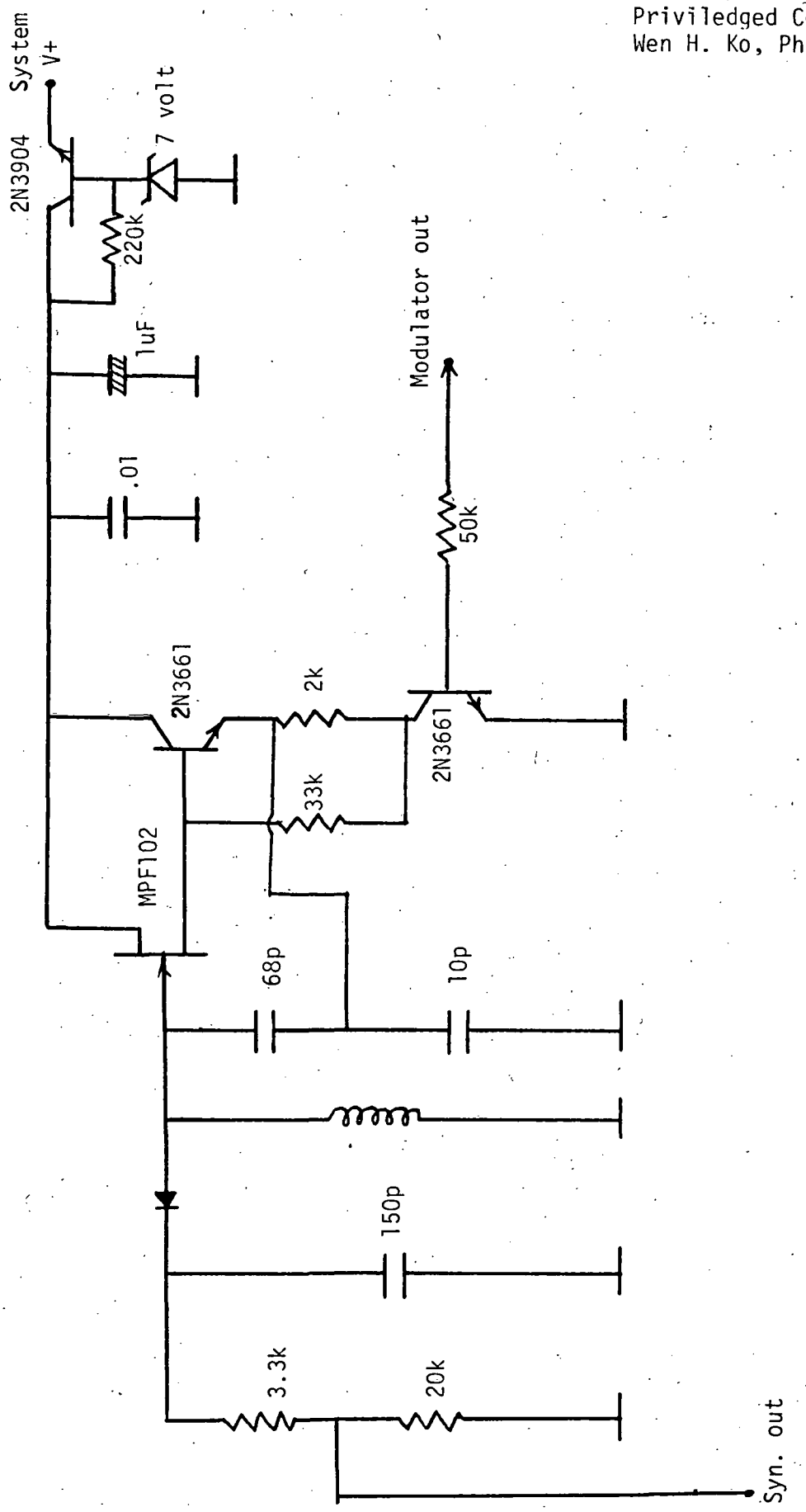

Fig. 5 - RF Transmitter and power detecting circuit

(Fig. 7) as a constant current source, a very linear temperature-to-voltage conversion can then be generated across the feed-back loop in the range of 32° to 43°C. Op.Amp. 2 is used only for amplification and output voltage adjusting purposes. A possible error may occur from the power supply temperature coefficient. However, according to the circuit analysis, $\frac{d\ el}{dVcc}$ is around 0.5. By using a 2N3904 transistor base-emitter reverse breakdown voltage as the power supply regulator, we experienced a temperature coefficient of Vcc around 40 mV over a range of 10°C or about 0.5mV for 0.1°C change(refer to Fig. 6). With the temperature sensitivity of 22 mV/.1°C, assuming an ideal power supply, obtained from the amplifier output e2, one can see that this change due to regulator's temperature coefficient, reflecting at C2 after the second stage amplification of 10, is about 2.5 mV/.1°C and will not be an intolerable problem. When it is also remembered that this temperature effect tends to linearize the thermister's non-linearity at the higher portion of the temperature range, as well as the fact that calibration is done after the demodulation, this temperature effect due to the power supply is not a problem.

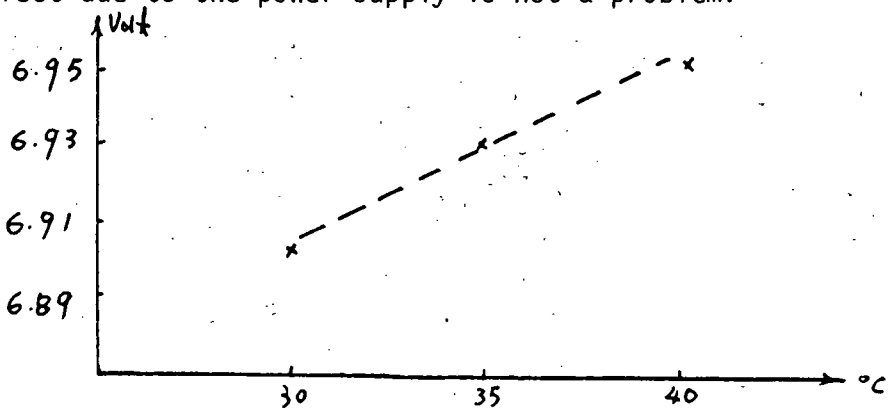

Fig. 6

Fig. 8 shows the amplifier's output voltage plotted against temperature. A good linearity can be observed.

More efforts have expended into the pressure transduction. A small size semiconductor bridge pressure sensor developed in MEL is used for pressure measurement. The amplifier diagram is shown in Fig. 9. A high input impedance amplifier is used for amplification to avoid any loading on the bridge. However, due to the limitation of the RF power source and the low sensitivity with the present semiconductor sensor, a "pulsing" technique has to be utilized to provide a workable signal while keeping the power consumption within range. In other words, the bridge sensor is excited non-continuously during a particular period of time with relatively high current.

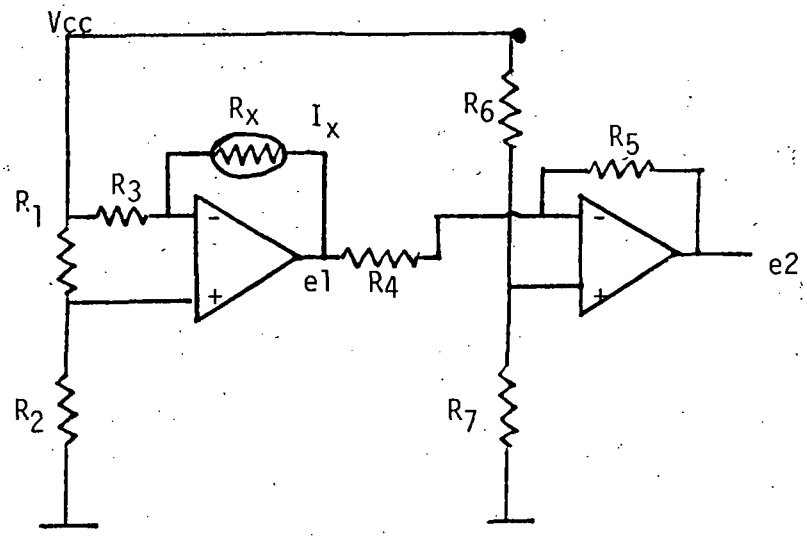

R_1	536K
R_2	953K
R_3	681K
R_4	60.4K
R_5	604K
R_6	649K
R_7	634K

Fig. 7 Temperature sensing amplifier

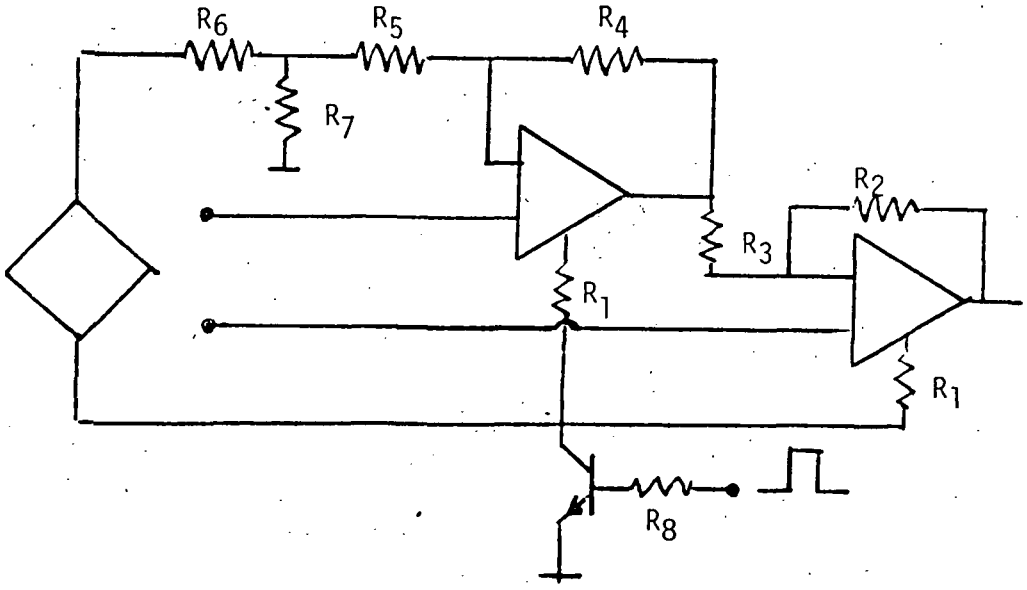

R_1	330K
R_2	1 M
R_3	2.5K
R_4	2.5K
R_5	750K
R_6	750K
R_7	750K
R_8	100K

Fig. 9 Pressure sensing amplifier

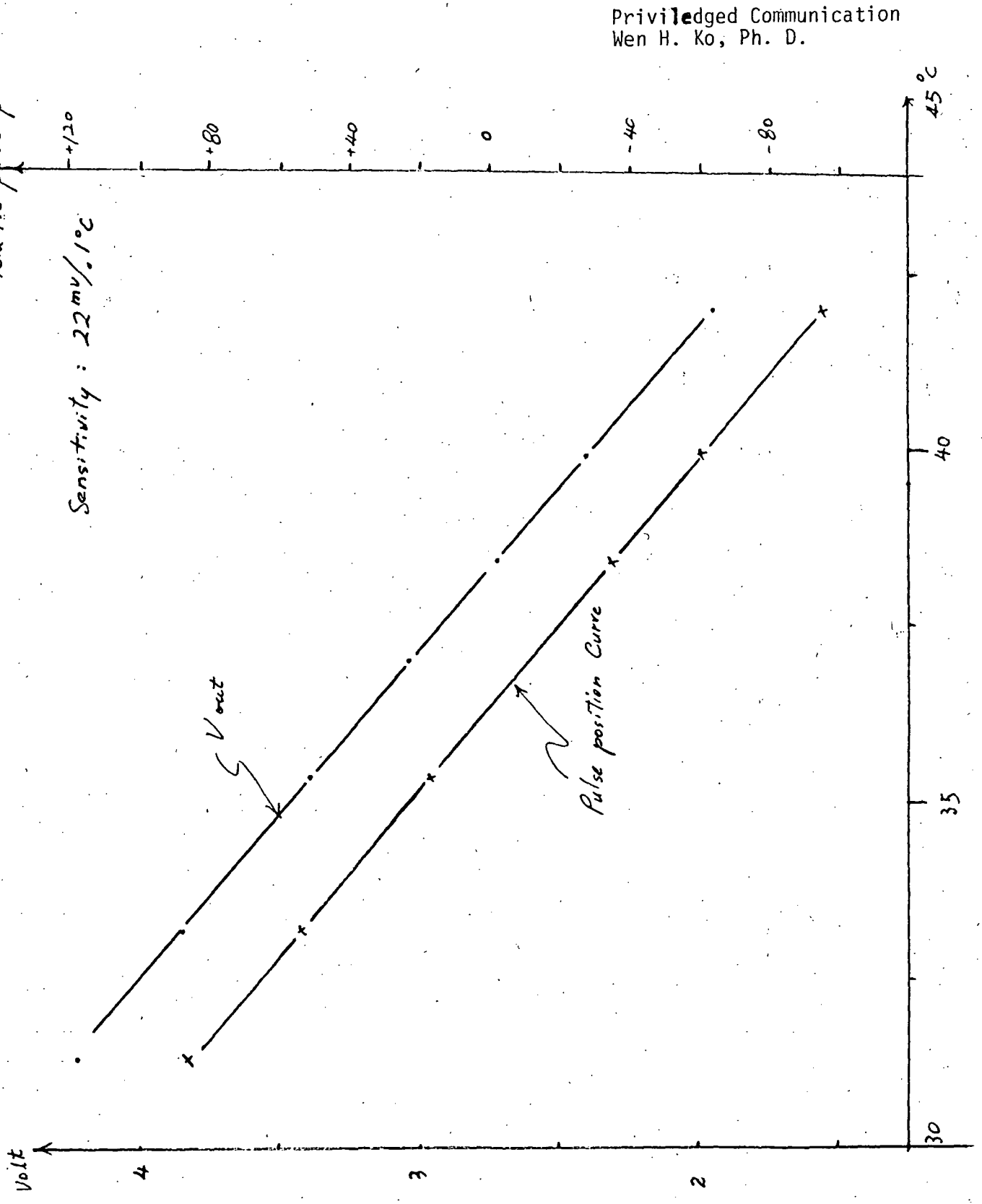
relative pulse position
+120
+80
+40
0
-40
-80
45 °C
40
35
30
Sensitivity : 22mv/.1°C
Volt
4
3
2
V out
Pulse position Curve

FIGURE 8

Sampling and holding is also achieved during this period. Timing for the bridge pulsing is shown below in Fig. 10.

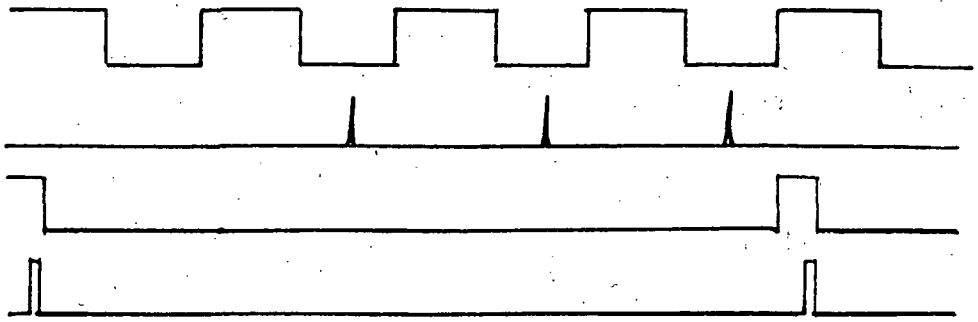

Fig. 10

The pulsing achieved at the synchronous pulse stemmed from the rising edge of this pulse. The bridge's power pulse length is about 100 μsec and the excitation current through the bridge is about 3 mA. A sampling window is opened at the end of this pulse and is about 15 μsec. Pulsing again is applied to the I-set terminal of the amplifier to obtain a fast settling time of the amplifier. Although with this I-set value, the Op. Amp. has a small signal gain band-width product of about 100 KHz, the measured large signal gain bandwidth product is only around 6 to 8 KHz. In view of any sudden disturbance that might occur in the pressure, which may represent a large signal rather than a small one, the amplification of the amplifier is restricted to about 400. The output swing voltage for 200 mmHg ranges about 2 volts . Fig. 11 shows the switching for bridge pulsing and Fig. 12 gives the amplifier's output plotted against 200 mmHg pressure range. The significance of the temperature influence on the transducer can also be seen from this data. The compensation of the temperature effect will be discussed later.

The EKG amplifier is shown in Fig. 13. and is a conventional design.

External Unit

Demodulation and RF powering.

(1) Demodulation.

The signal received by the receiver, as mentioned, consists of the information signal and RF signal. The format is shown below:

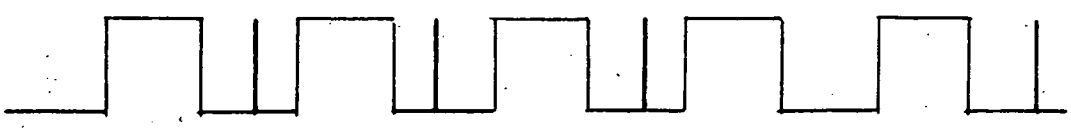

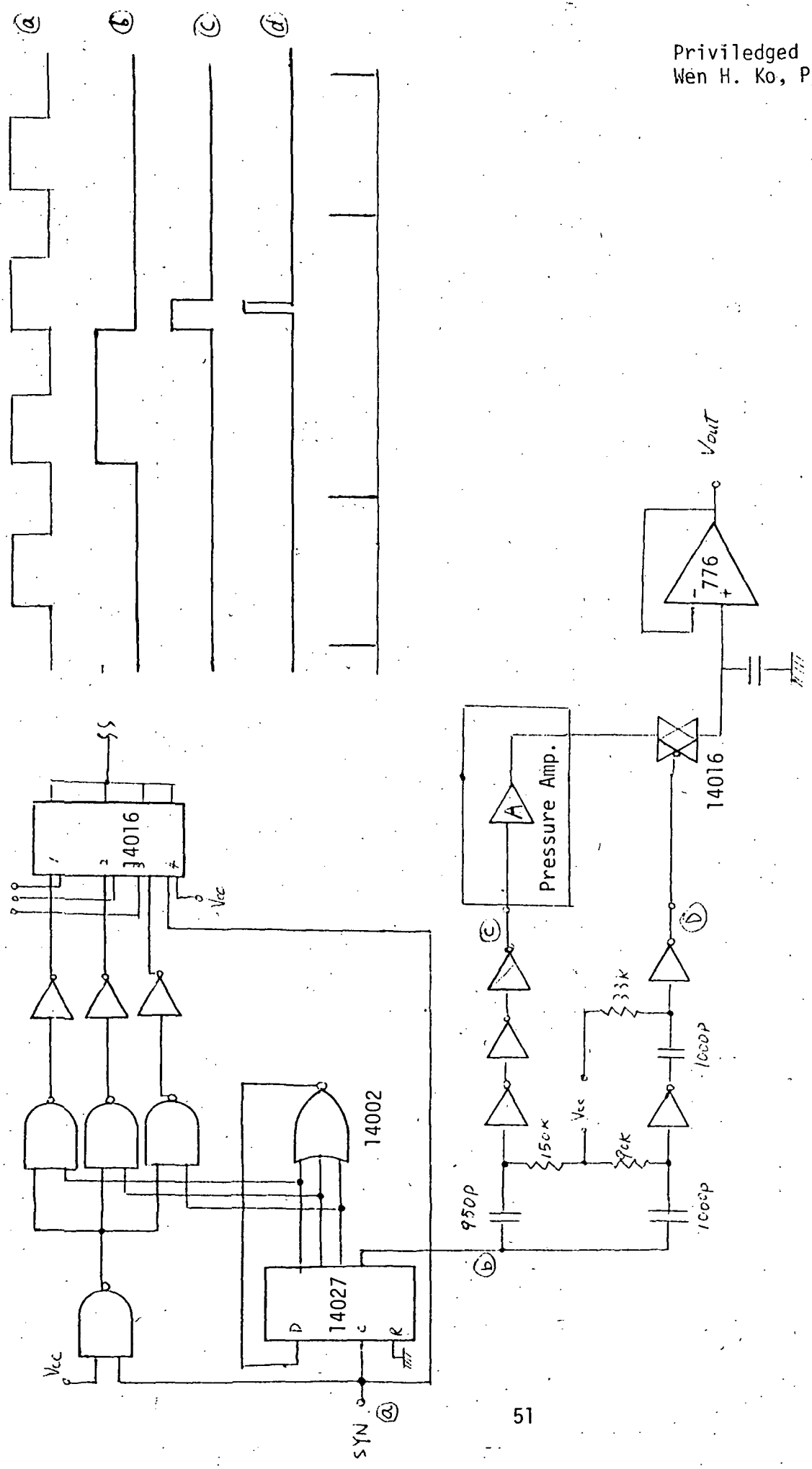

Fig. 11 Logic and timing diagram for bridge pulsing

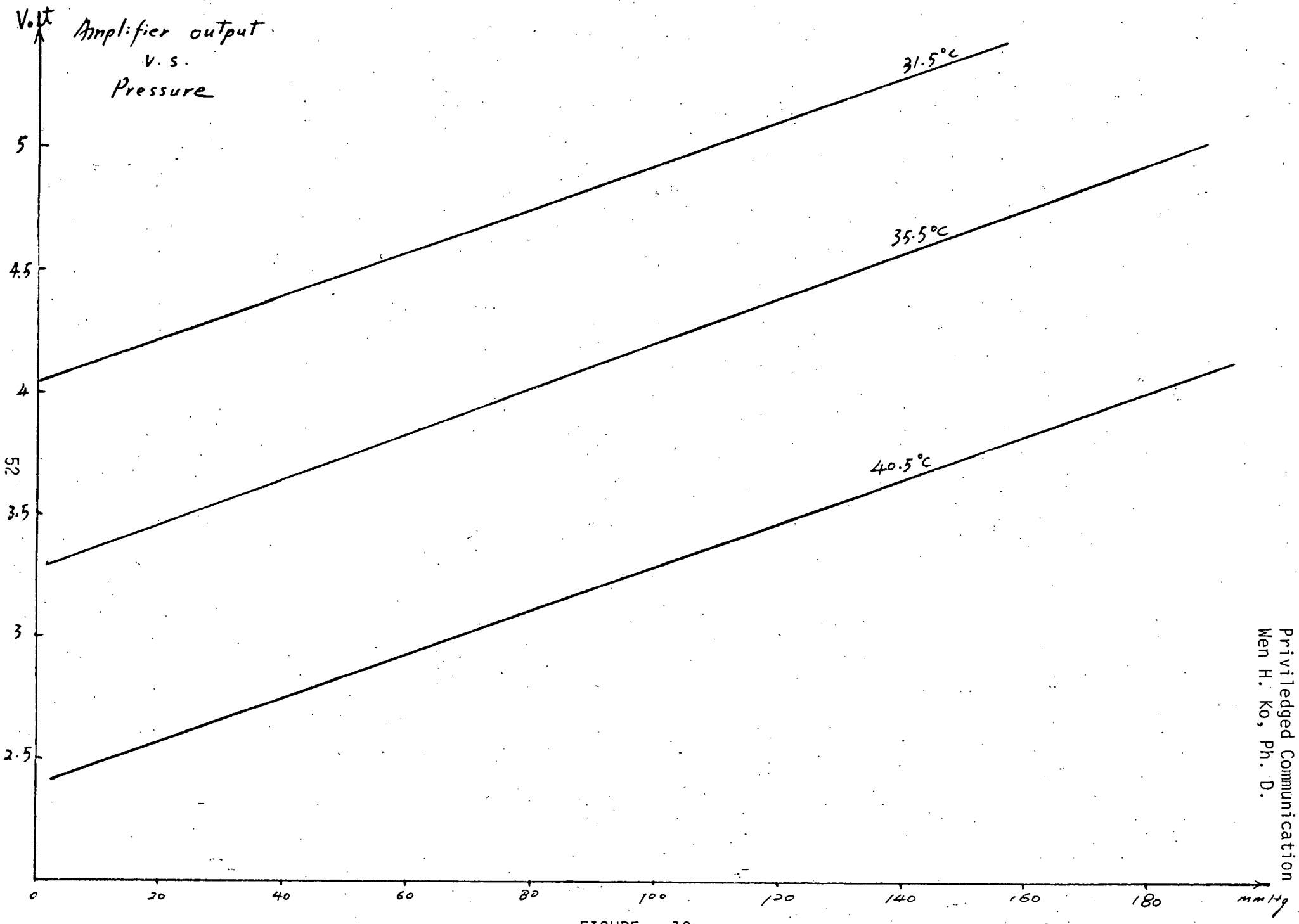

FIGURE 12

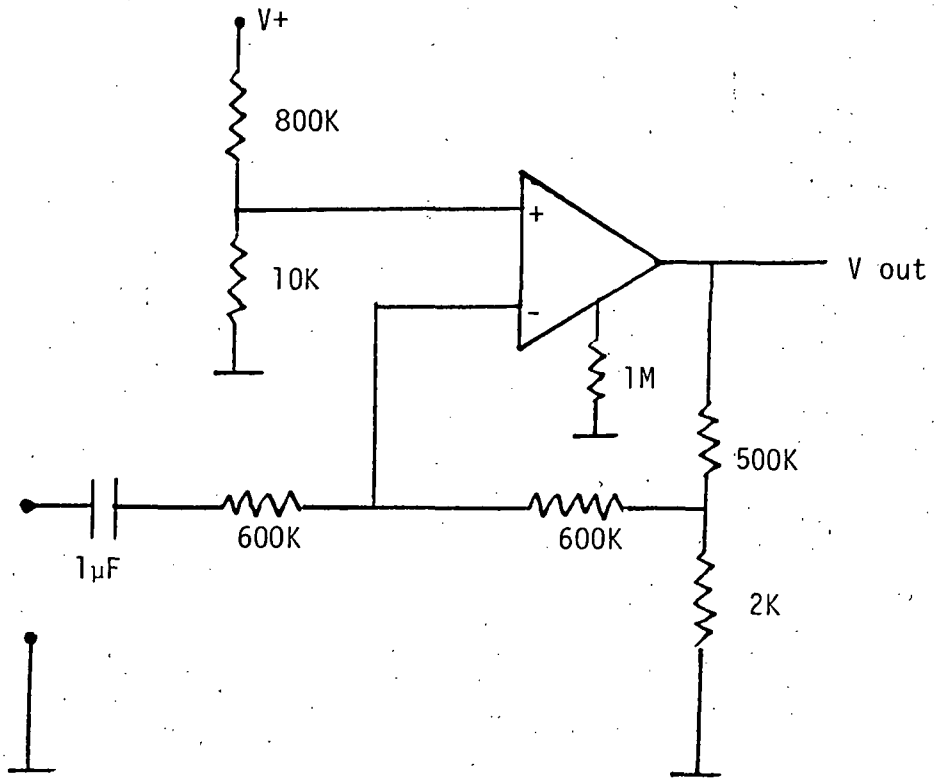

Fig. 13 EKG Amplifier

Multiplexing of the channel is sequential and the period marked "p" is the RF signal.

The block diagram for demodulation is shown in Fig. 14. The function of the individual blocks are described as follows:

Antenna switch. As transmitting and powering are at the same frequency, a great amplitude difference between these two signal sources exists and protection of the AM receiver is necessary. This is achieved by attenuating the RF powering signal received by the antenna with a switching circuit (the circuit is shown in Fig. 15). The control for switching is shown in Fig. 16. Control pulses are generated from the clock. The format is as follows:

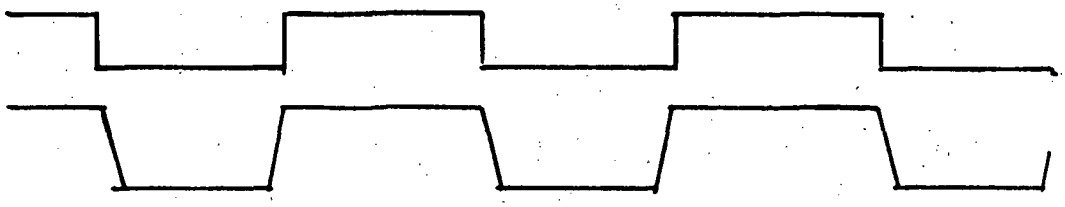

The n-channel MPF102 FET has a typical "ON" resistance at zero gate voltage of about 700 ohms channel resistance, and the typical "OFF" resistance at -7 volts is over 5 Mohms. When the control pulses go to low(-7 volts) level, n-channel FET MPF 102 is turned OFF;while p-channel enhancement mode MOSFET is ON. Conversely, at zero gate voltage the P channel enhancement mode MOSFET has a typical "OFF" channel resistance of greater than 100 Mohms and an "ON" resistance at -7 volts of less than 0.5 Kohms. Consequently, the signal received by the antenna will be attenuated when delivered to the receiver through this circuit if the applied gate voltage to the two FETs is at zero volts, which in this case occurs during the RF powering period. The attenuation was previously measured at about -90dB.

Threshold detector.- Fig. 17. This circuit serves both as a threshold detector and pulse level shifter - due to the fact that the synchronous clock and receiving signal pulses are 0 to Vcc peak-to-peak while the signal processing units operated at $\pm$Vcc. The purpose of this detector is to minimize the noise resulting from transmitting and receiving process. A one shot is followed to adjust the pulse width according to the sampling requirement. The present pulse width is set at 12 μsec.

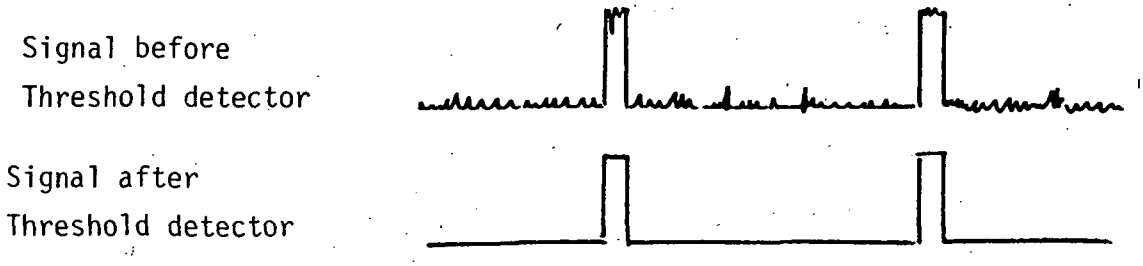

Fig. 18

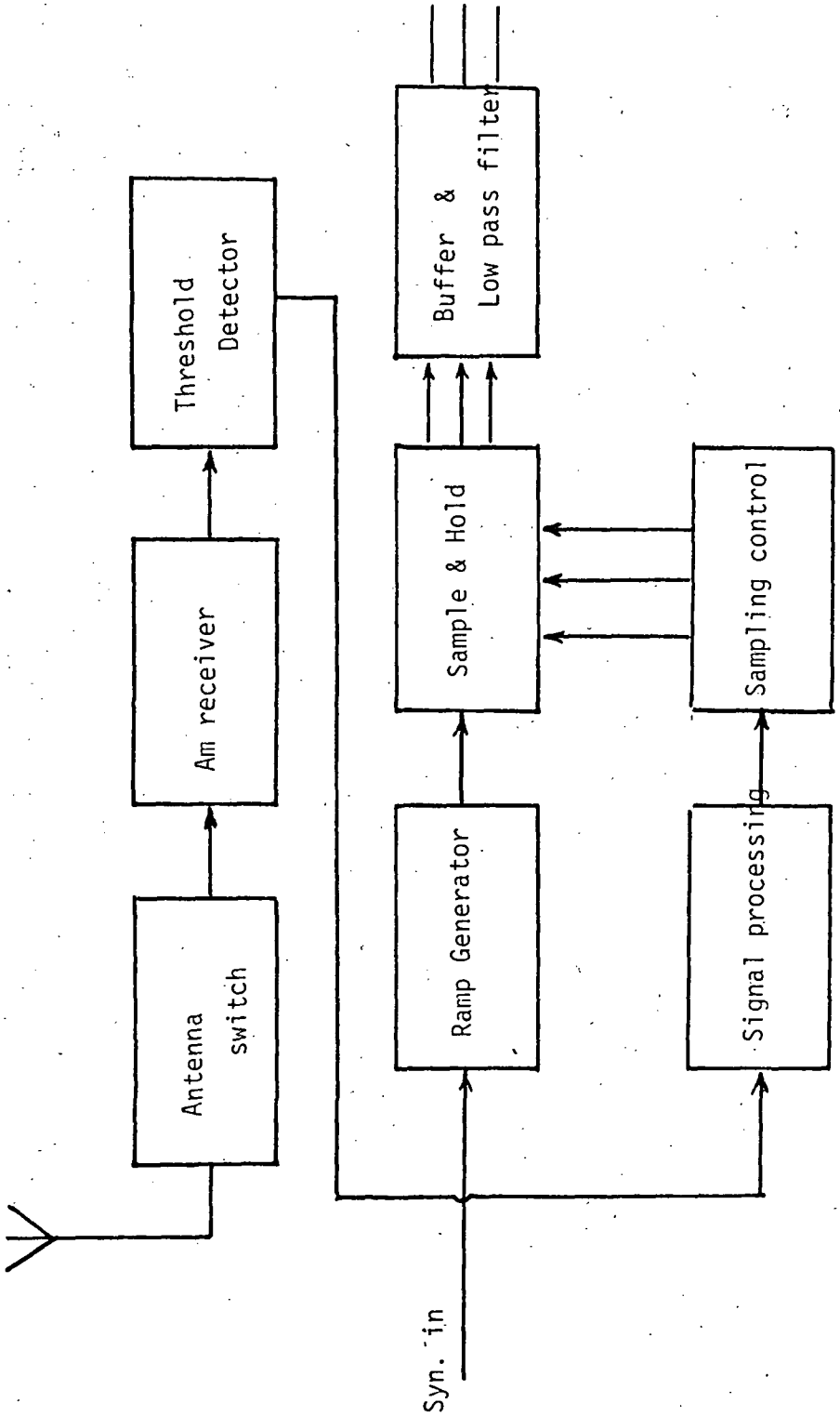

Fig. 14 Demodulation block diagram

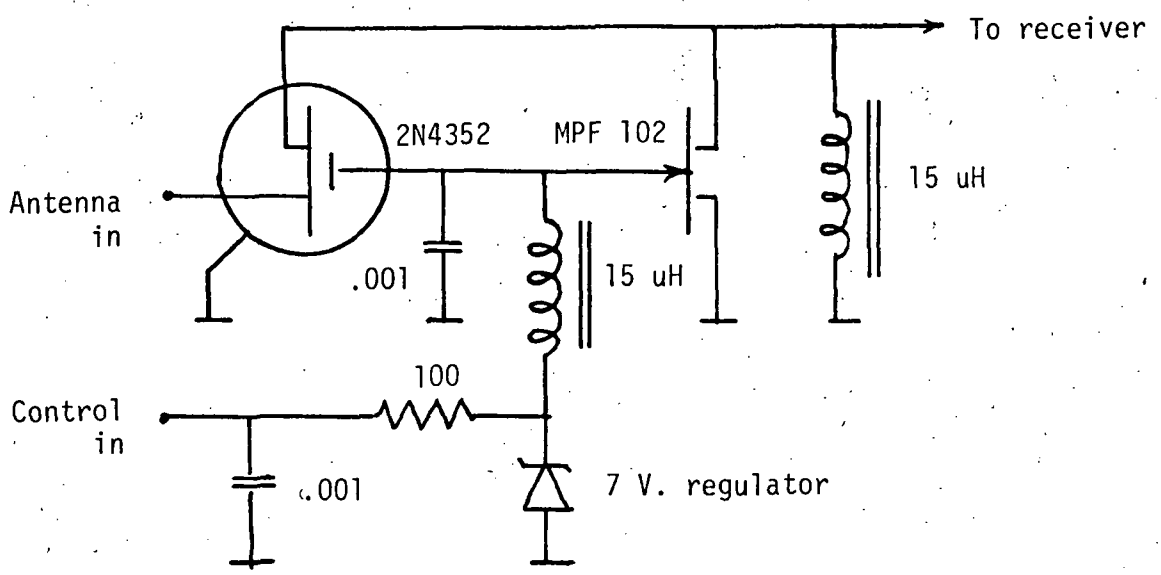

Fig 15 Antenna switch

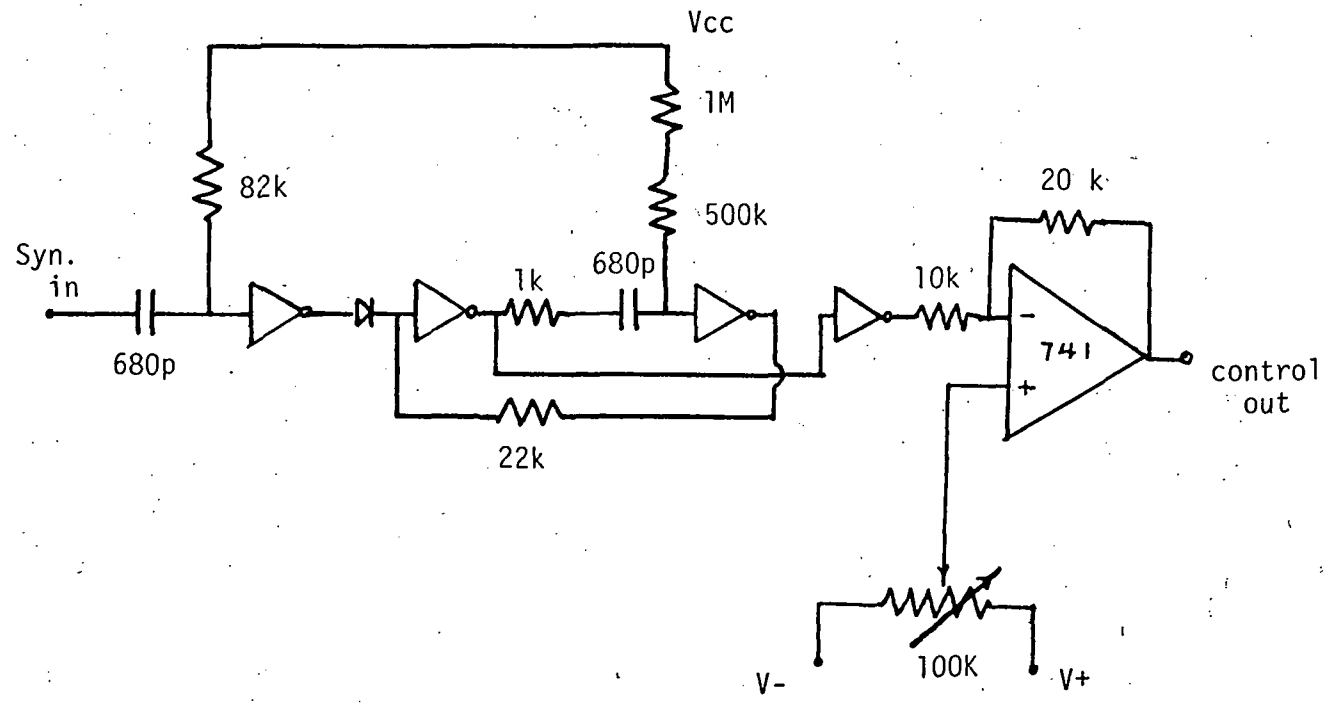

Fig. 16 Antenna switch control

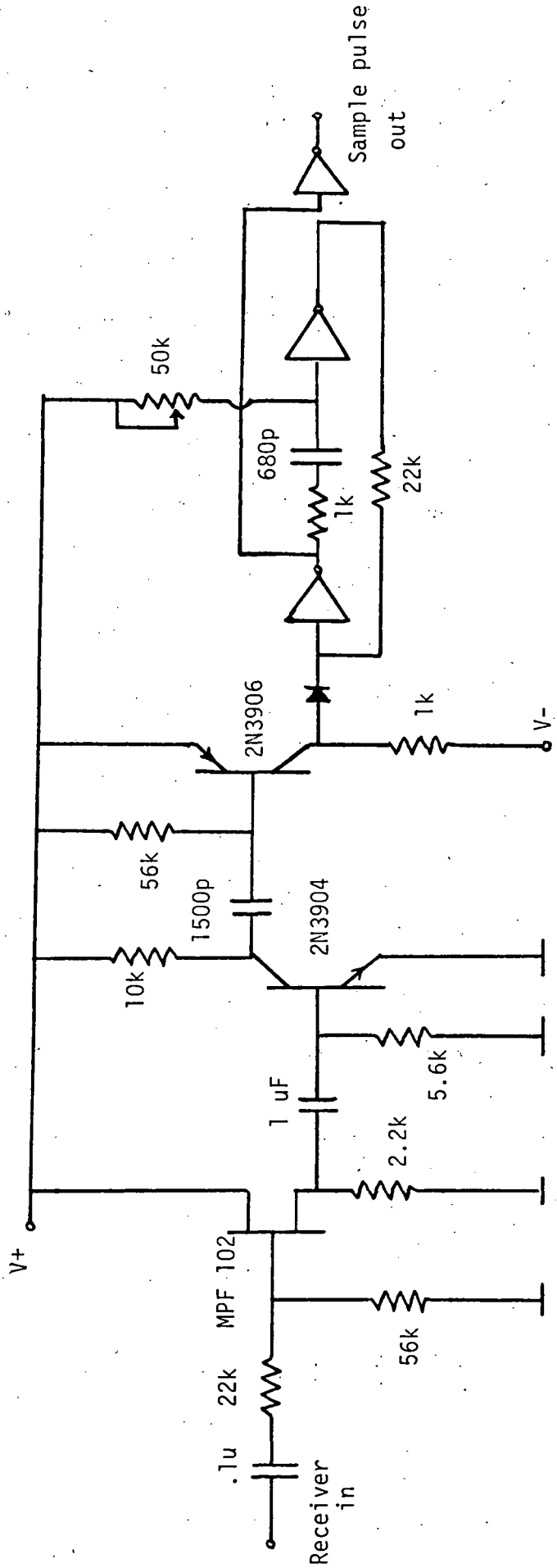

Fig. 17 Threshold detector

Ramp generator. Information will be recovered from pulse position coding by sampling the voltage along a ramp.

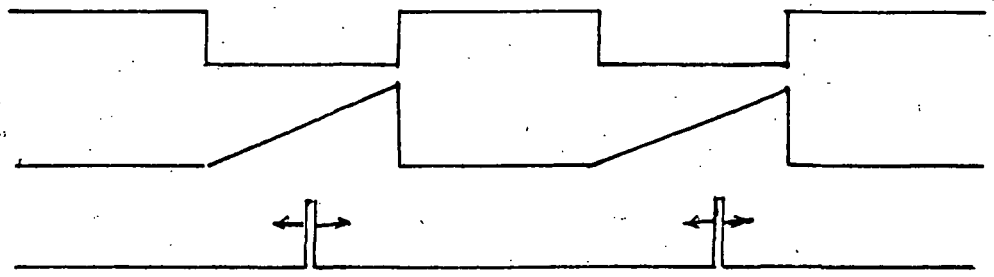

Fig. 19

The ramp generator circuit is shown in Fig. 20. and it uses the stable zener diode functioning voltage as a reference for the constant current supply source to charge the capacitor over the feedback loop. From the circuit analysis, the ratio between the zener's dynamic resistance (R_{dyn}) and R_1 (refer to Fig. 20), R_1/R_{dyn}, should ideally be as large as possible. This means that for each practical zener, only one optimum operating point is available. The zener presently used is a LM 103 2.4 volt regulator which has a very low R_{dyn} in the range 10 μa to 10 ma.

Signal Processing. This part converts the sequencing pulse signal into three independent channel pulses. A CMOS logic device is also used here. The circuit is shown in Fig. 21 and the timing diagram in Fig. 22. Since any signal in the RF period represents errors, that period is blocked totally.

Sampling, holding and buffer stage. - Fig. 23. An analog gate is used for sampling; activated by the sampling pulse resulting from the signal processing block. The CMOS 14016 analog gate has an "ON" resistance of about 400Ω and very high "OFF" resistance. The input - output delay time is in the nanosec range. The holding capacitor is 4700 pF, which during sampling gives an RC constant of about 2 μsec. The sampling time, as previously mentioned, is 12 μsec. For the buffering stage, a 2H0042 FET Op. Amp is chosen because of its 10^{12} Ω input resistance and very low input bias current. A low pass filter with a high-cutoff at 120 Hz is followed to the buffer stage.

Clock. The clock is generated by a 555 timer, shown in Fig. 24. The present clock rate is set at 800 Hz, which gives a 200/sec sampling rate for each channel.

(2) RF Powering

The power for the implant unit is supplied by RF induction from a primary coil, which is the external unit, into the secondary coil, which is also the implant unit's

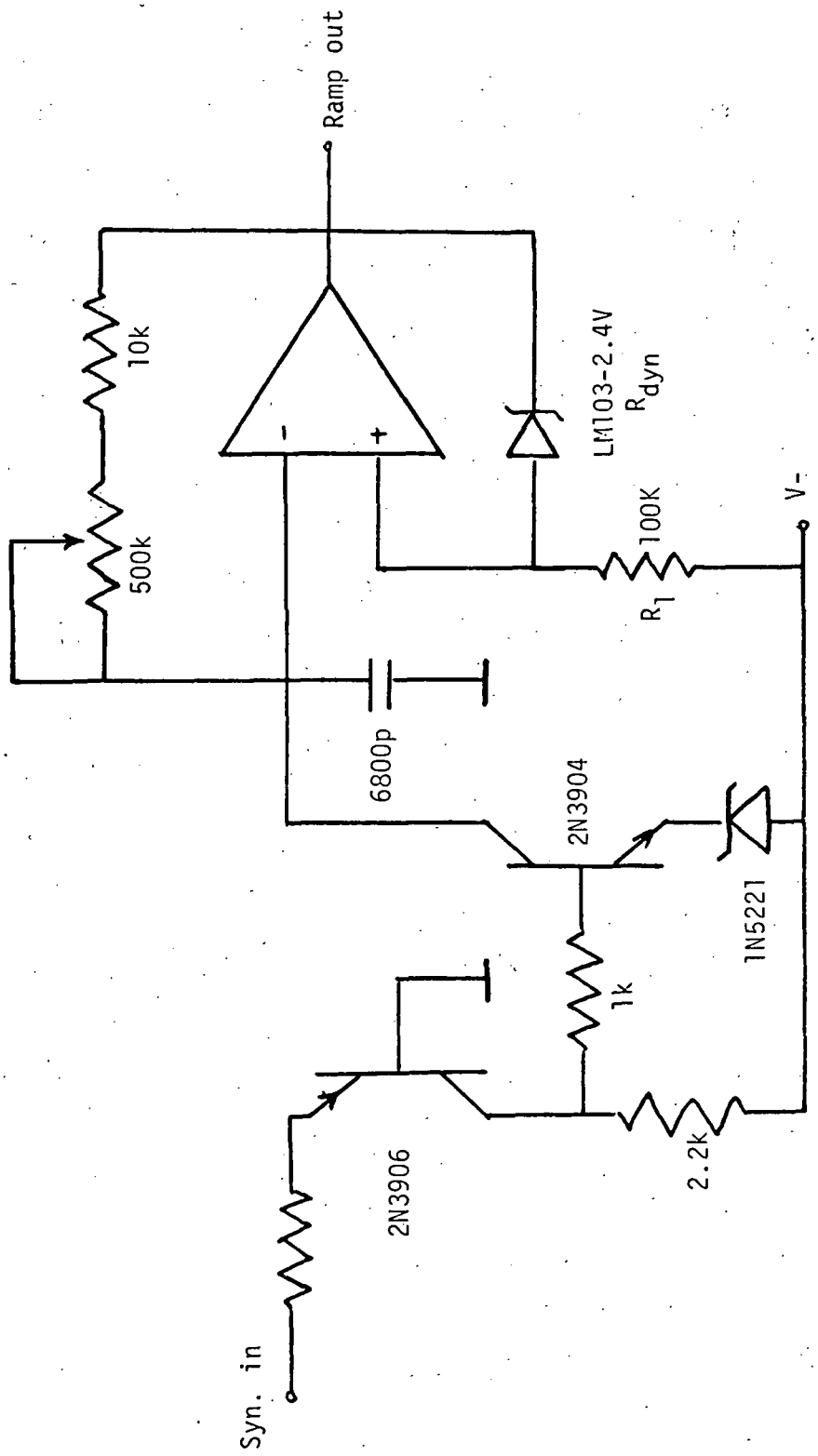

Fig. 20 Ramp generator

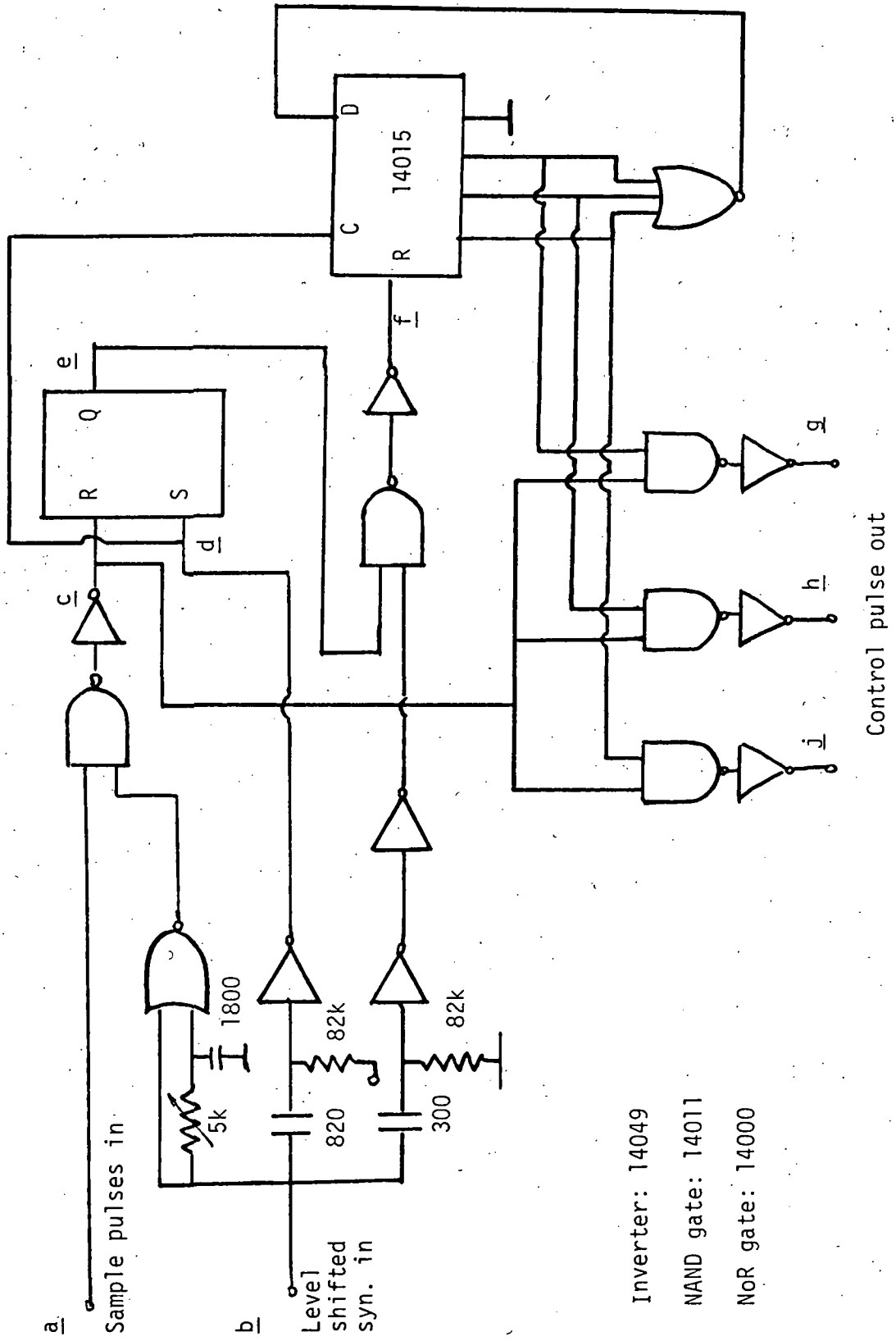

Fig. 21 Signal processing unit

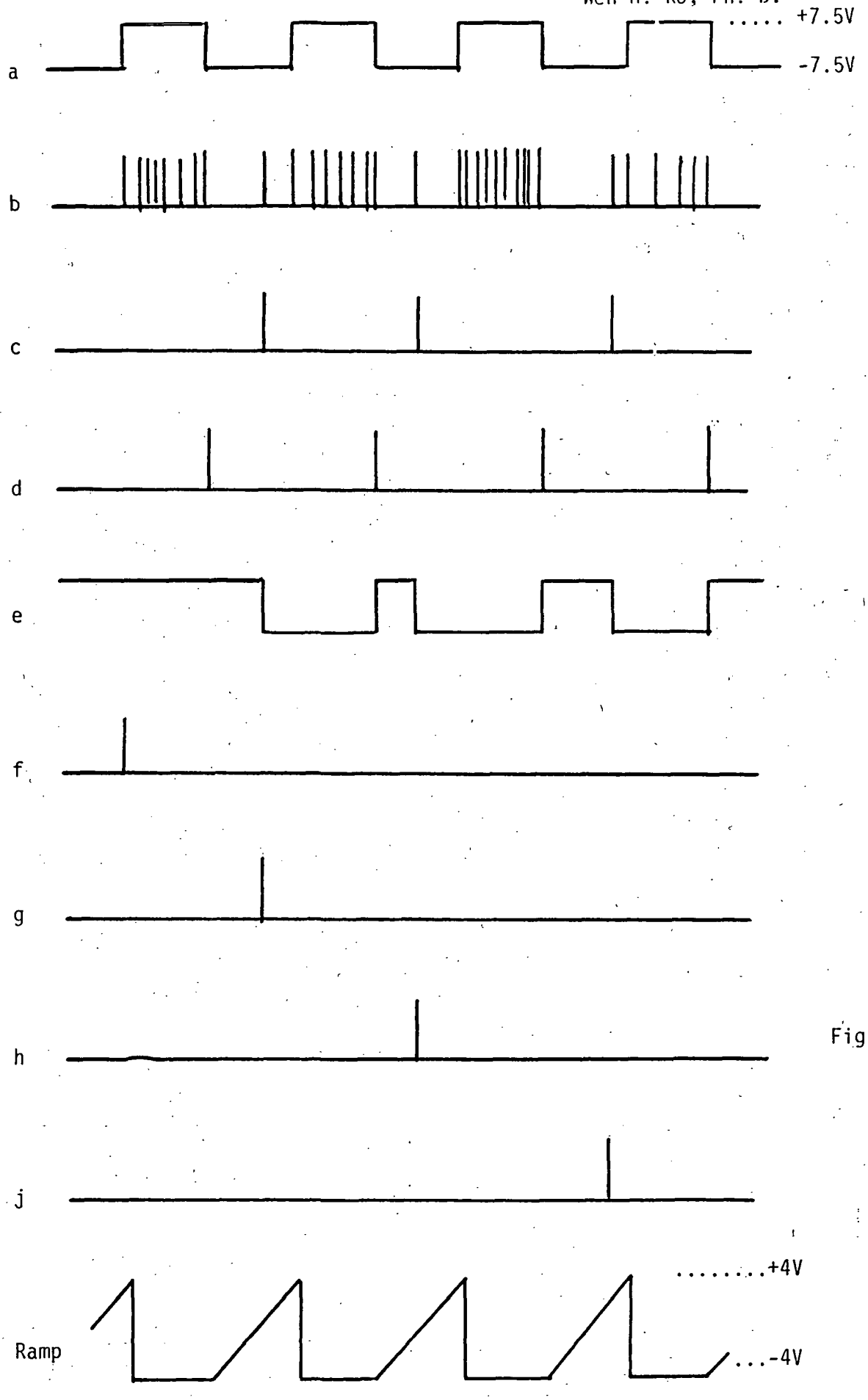

Fig. 22

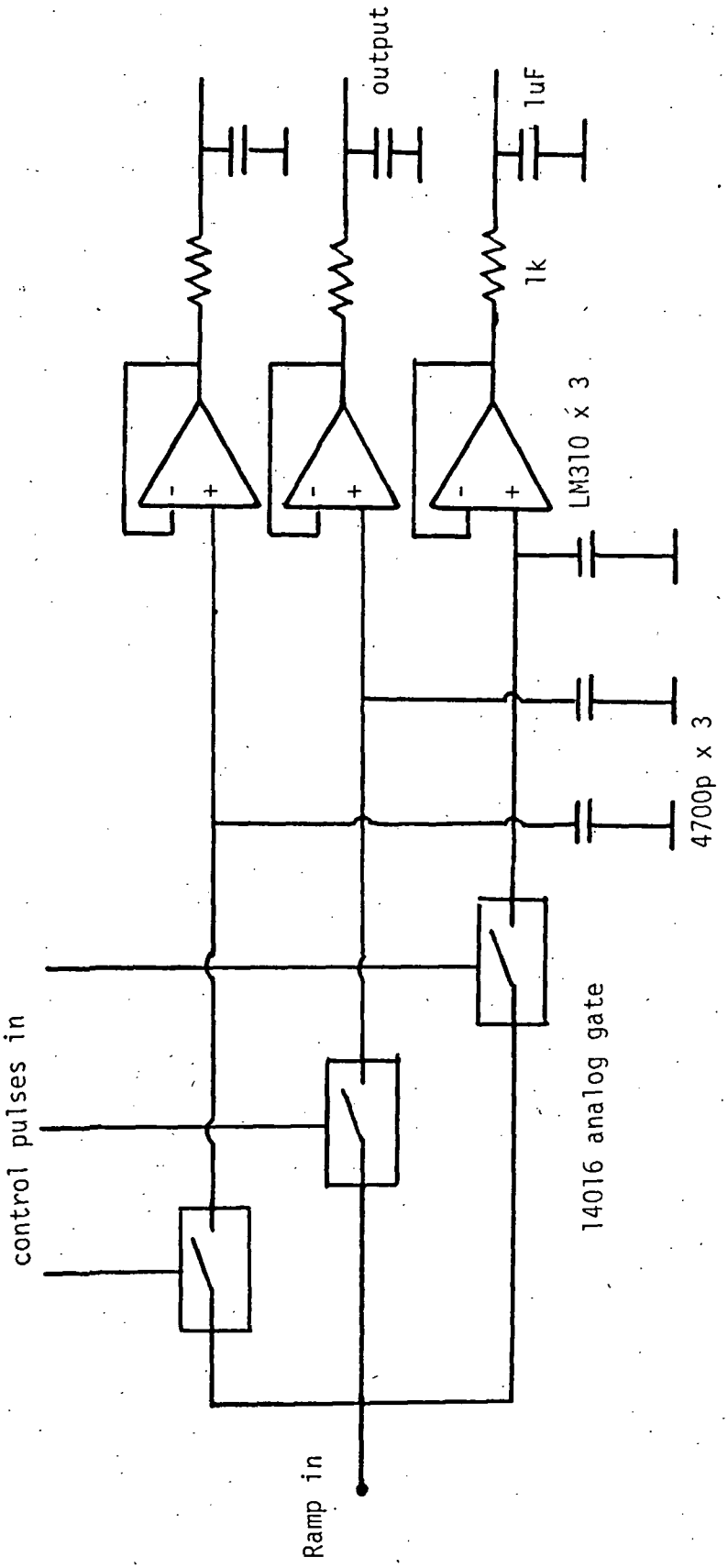

Fig. 23 Sampling, holding and buffer stage

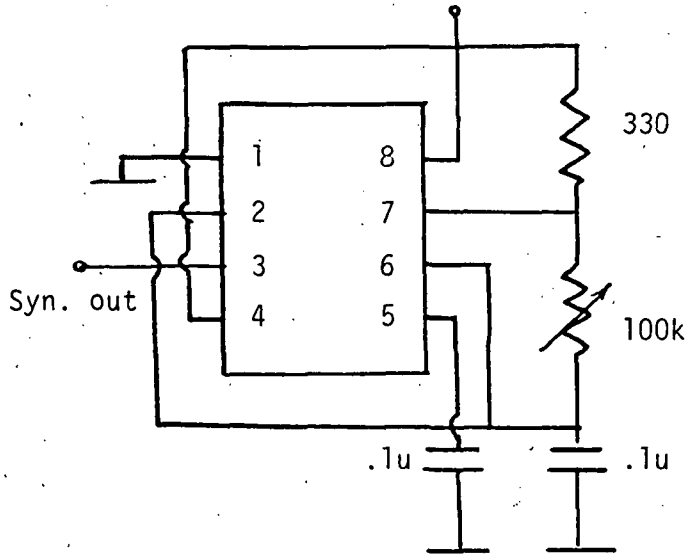

Fig. 24 Clock generating

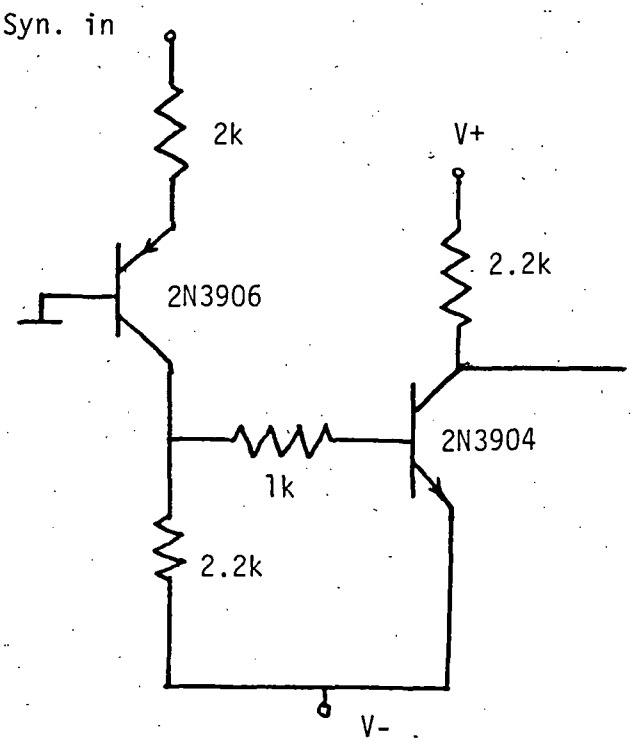

Fig. 25 Syn. level shifting

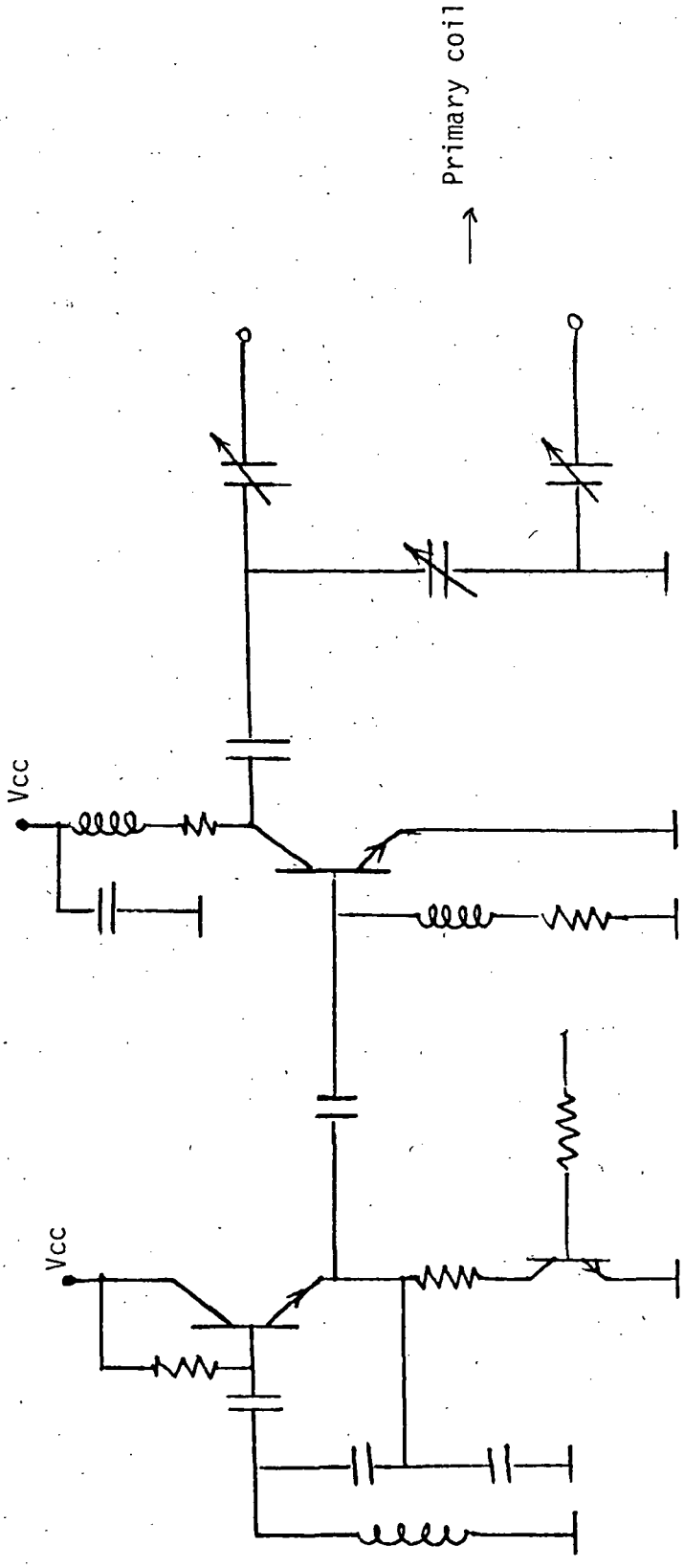

Fig. 25 RF powering circuit

transmitting coil. Main consideration concentrates on the efficiency of the power delivery, which depends on the Q values of the coils and the distance between the two coils. The RF powering unit basically consists of an RF oscillator followed by a power amplifier matched into the tuned primary tank. The circuit is shown in Fig. 25.

System Performance

	Power Supply (Vcc)	Supply Current	Clock rate
Implant Unit	7 volt	250 μA	800 Hz or 200/channel
External Unit	±7.5 volt	45 mA	800 Hz

Two approaches were used to evaluate the system's performance. The first was mainly aimed at the electronic circuits. Instead of using the transduced voltage, signal from the function generator is directly fed into the modulator input and monitors the system's output with a sinusoidal wave. Frequency response is of main interest here. Fig. 26 shows the output recording of two arbitrary channels of the three available channels. The performance of the system can be summarized as follows:

1. 60 cycle noise:

This is mainly due to the power supply ripple of the demodulation circuit. The decoupling circuit had been used for each circuit board. The 60 cycle noise seen at the output is less than 5 mV.

2. Cross talk:

With an input of a 5 volt peak-to-peak sinusoidal wave, the cross talk measured is about -60dB, which is also the typical CMOS multiplexor value.

3. Line coupling noise:

The output of the scope appears as spikes, the amplitude is about 15 - 20 mV. Since it is measured after the 120 Hz High-cutoff low pass RC filter, probe pick-up is of high possibility.

4. Sensitivity:

Sensitivity is defined here as $\frac{\Delta V \text{ out}}{\Delta V \text{ in}}$. It is dependent on the degree of pulse-position modulation and also the slope of the sampling ramp. With the present setting the sensitivity is about 0.75.

5. Frequency response:

Different input frequencies were applied and the system output was recorded. (The sampling rate of the data was set at 300/sec when taking this data). Since the information content is well within 100 Hz, any frequency higher than this was not tested. The attenuation of the higher frequency shown in Fig. 26, is mainly due to the frequency response roll-down of the chart recorder.

6. Sampling, holding drift:

The holding capacitor is 4700 pF. The only discharging pathways are through the buffer amplifier input and the analog gate. Both of these have a resistance value of greater than 10^{10} ohms. RC constant in any event should be larger than 20 seconds. The drift seen at the output is less than 4 mV.

7. The pulse position linearity is shown in Fig. 27. It shows that the conversion factor is 16 mV for 1 μsec pulse position change.

The second approach to test the system has the sense of completion since it includes the transducer stage. The entire implant unit is placed into the oven for controlled temperature testing. The pressure transducer was kept in a well-sealed test tube with a variable pressure arrangement. The EKG channel is grounded. The data monitored at output is plotted in Fig. 28. Sensitivities measured are 10.9 mV/mmHg and 20 mV/.1°C for the pressure and temperature channels, respectively. The temperature coefficient of the pressure channel is about 22 mV/.1°C. A good shielding of the implant unit is necessary to avoid the influence due to the strong RF powering field. Fig. 29 shows the difference seen at pulses received by demodulation unit before and after the shielding. The present discrete circuit form may be the reason for the gittering noise experienced, which limits the resolution to about ±1mmHg and ±.1°C. It is quite certain that after fabrication of the hybrid circuit, this gittering noise will be improved.

Temperature compensation for pressure channel

The temperature coefficient of the pressure transducer is negative for our bridge, i.e. the higher the temperature, the lower the pressure reading for an unchanged pressure. The compensation circuit will add a suitable amount of voltage to the

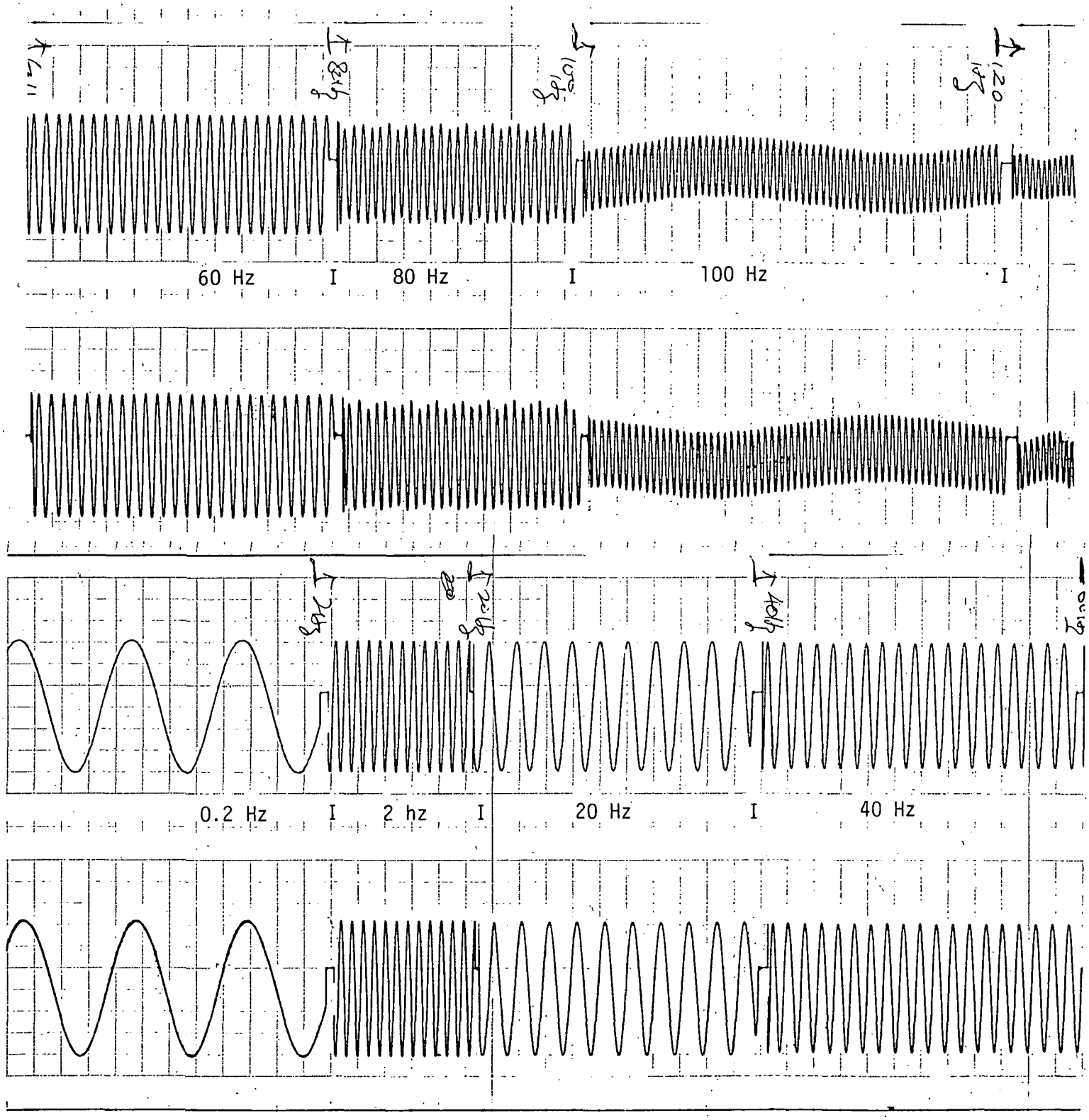

Fig. 26 Frequency test. Recording of arbitrary two channels.

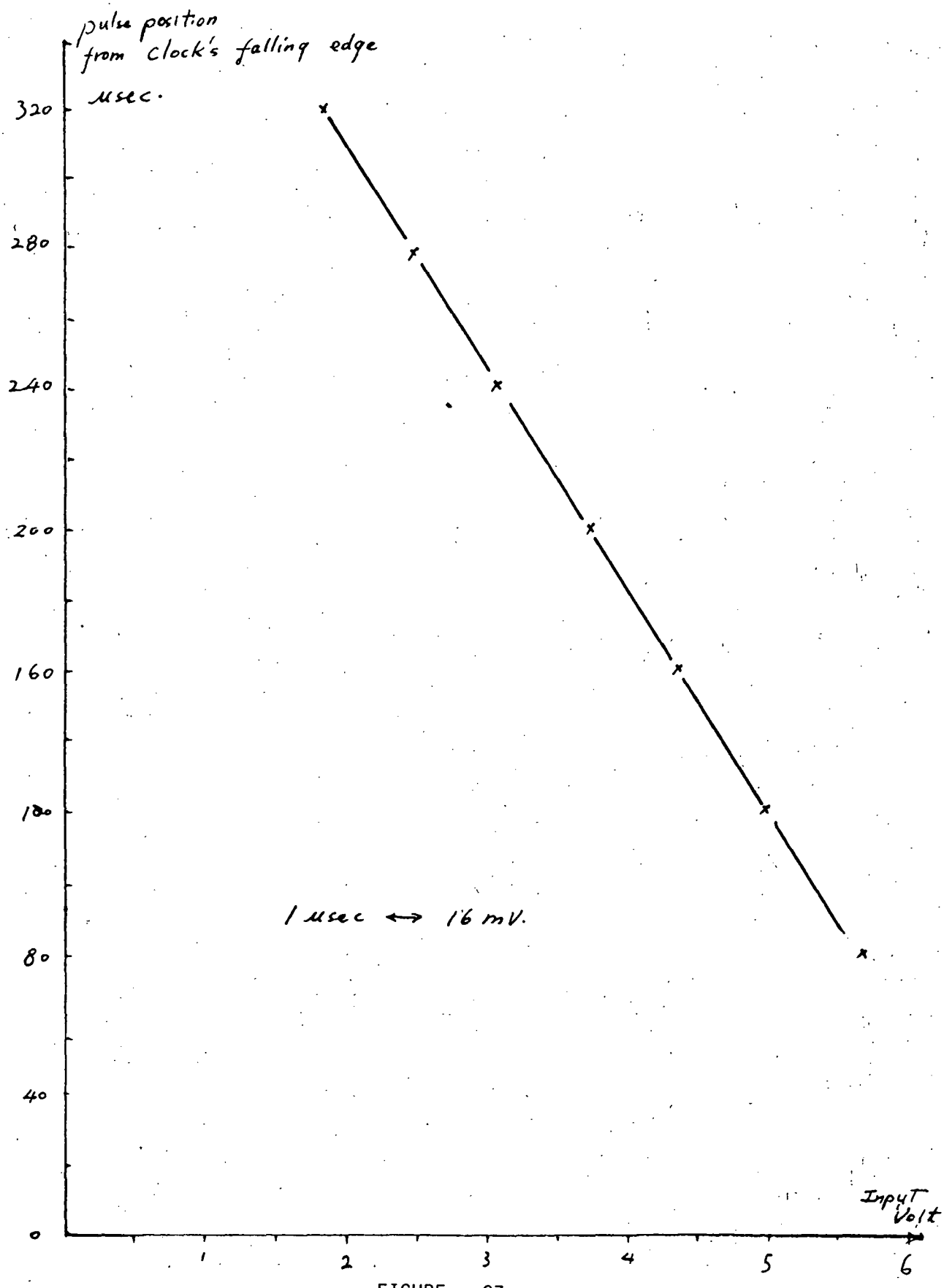
pulse position
from clock's falling edge
usec.
320
280
240
200
160
120
80
40
0
1 usec ↔ 16 mV.
Input Volt
1
2
3
4
5
6

FIGURE 27

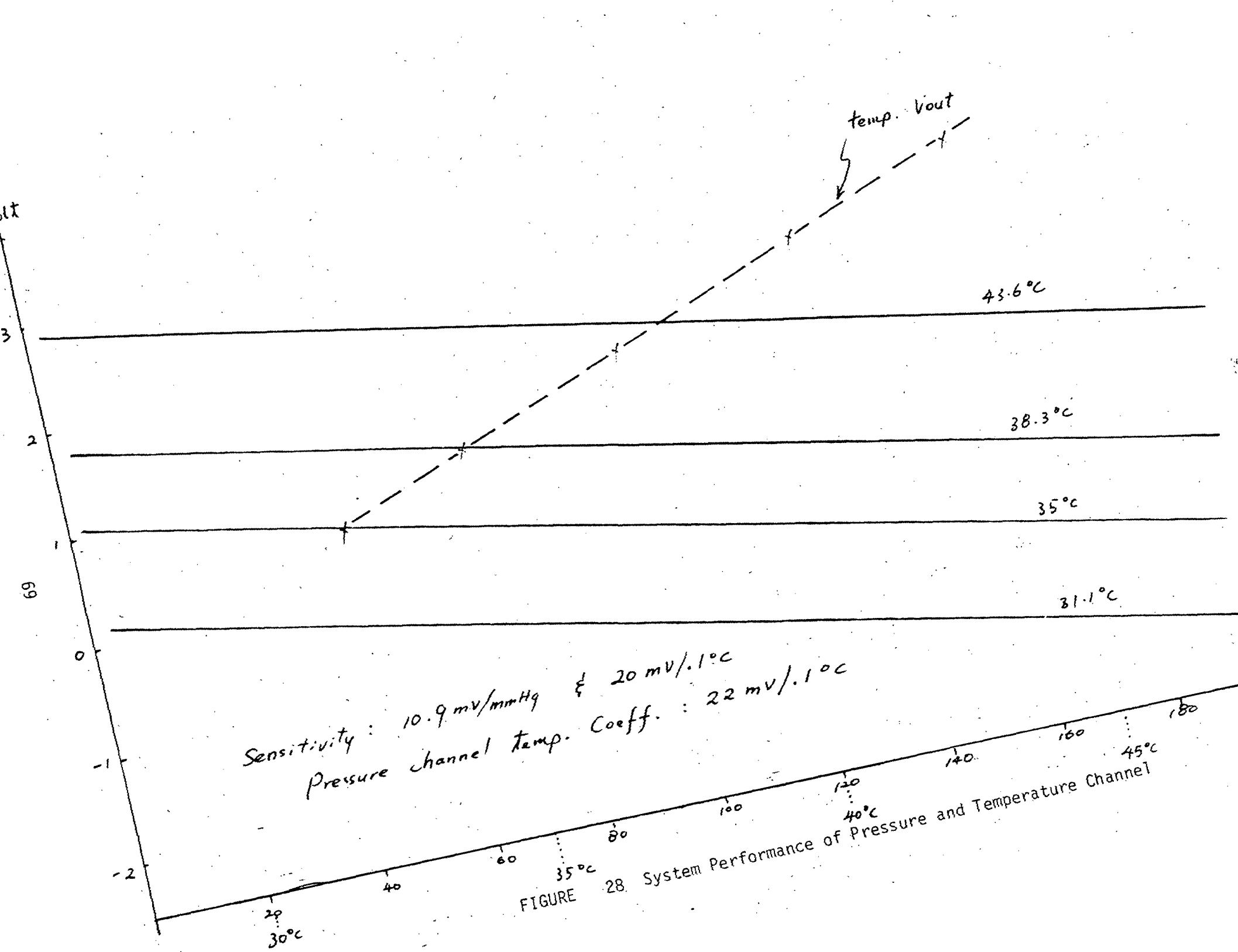

FIGURE 28. System Performance of Pressure and Temperature Channel

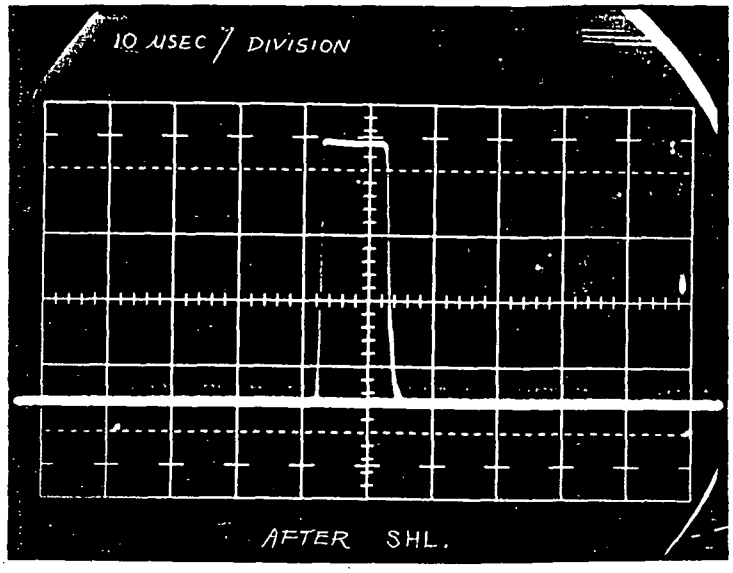

After the shielding

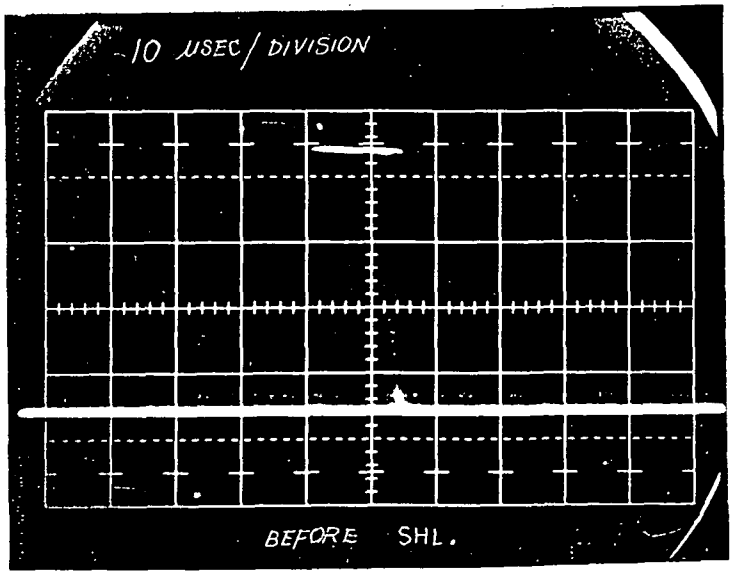

Before the shielding

Fig. 29 Shielding effect of the transducer amplifier

pressure channel output and hence cancel the temperature influence. The idea is shown in the following figure:

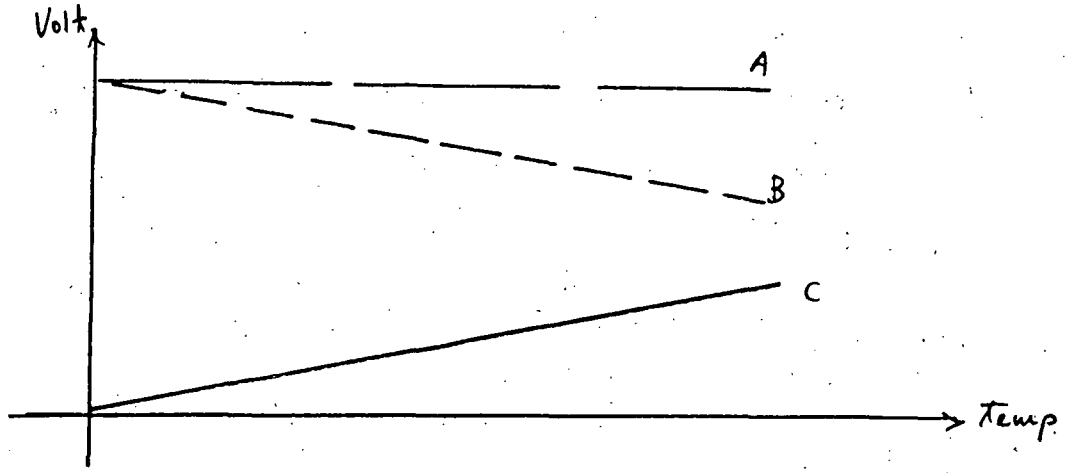

Curve B represents the uncompensated output voltage against temperature range. The compensating curve, curve C, has a slope of the same absolute value as of curve B but opposite in sign. The resultant curve A will then represent a constant pressure over the temperature variation. The offset of curve A will depend on that of curve B and will be adjusted at calibration.

Figure 30 shows the relation of the temperature channel output and the pressure channel temperature variation for a constant pressure source. Both are linearly approximated.

The circuit then consists of a first Op. Amp. to obtain the curve C from the temperature channel output and a second Op. Amp. to add this curve C to the pressure channel output. The circuit is as shown in Fig. 31.

Pressure transducer packaging

The semiconductor pressure transducer fabricated in MEL has the dimensions of 150 x 50 x 10 mils. Various catheter-tip mounting, utilizing the advantage of the small size of the sensor, have been tried and each shows a common problem due to the reaction of body fluid leakage which made contact with the sensor. The proposed packaging is shown in Fig. 32. The basic objective is to separate the transducer from the body fluid by a second fluid which is non-conductive. As can be seen from the drawing in Fig. 32, the package consists of a diaphram made with latex and two stainless steel parts - part A and part B. Half of the wall of part B is cut to provide a larger area for pressure transmitting while still providing mechanical protection to the sensor. A latex diaphram encircles whole of part B and

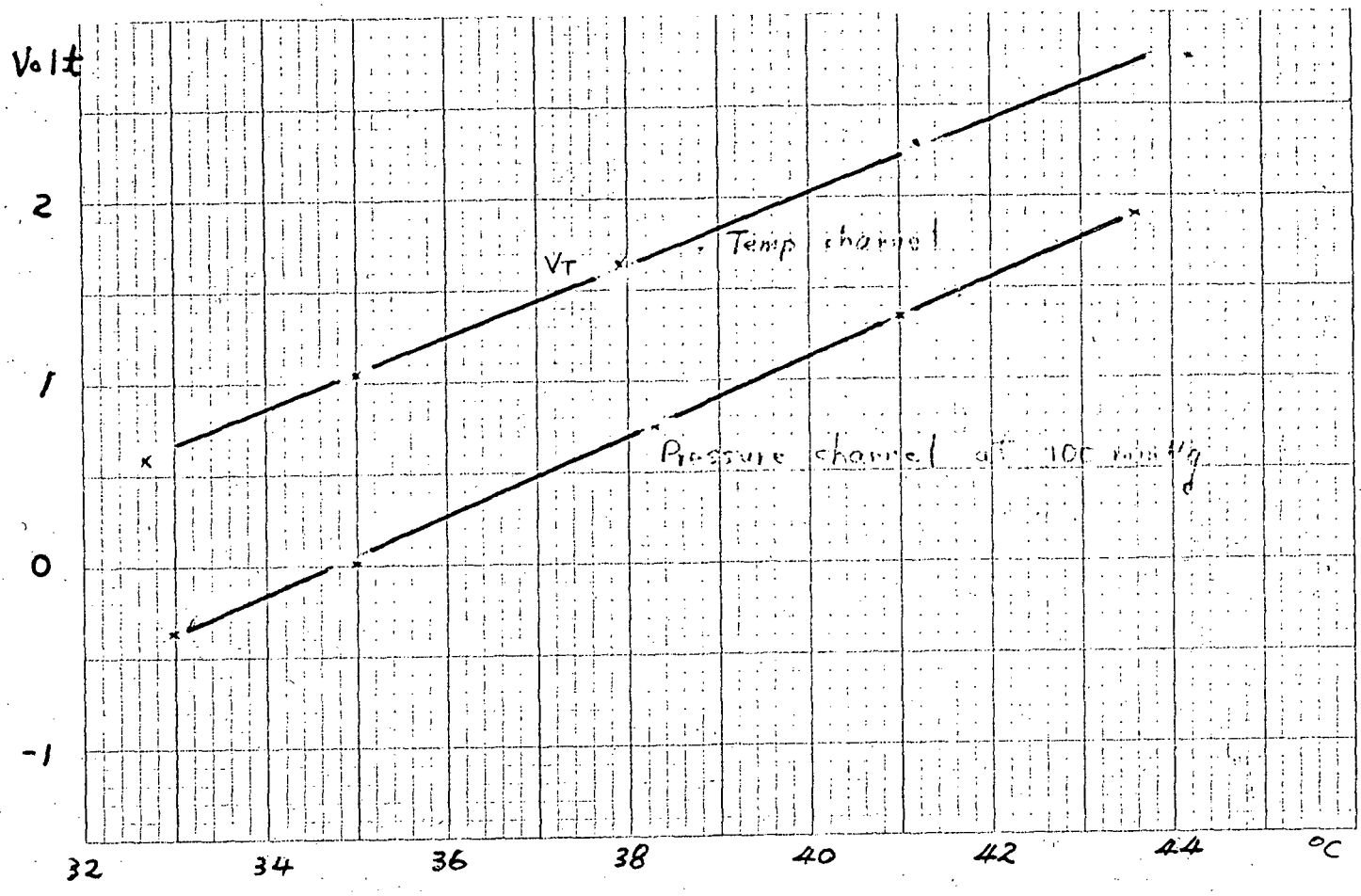

Fig. -30

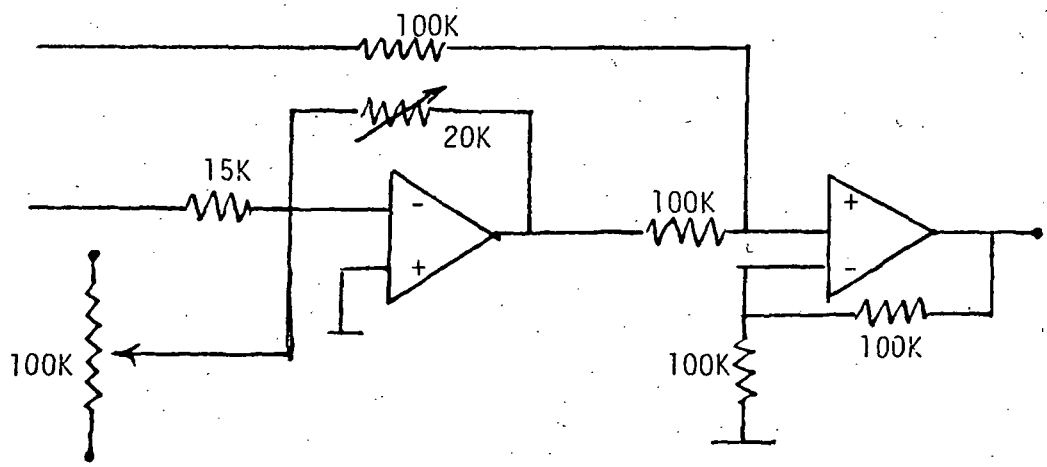

Fig. -31 Compensating circuit

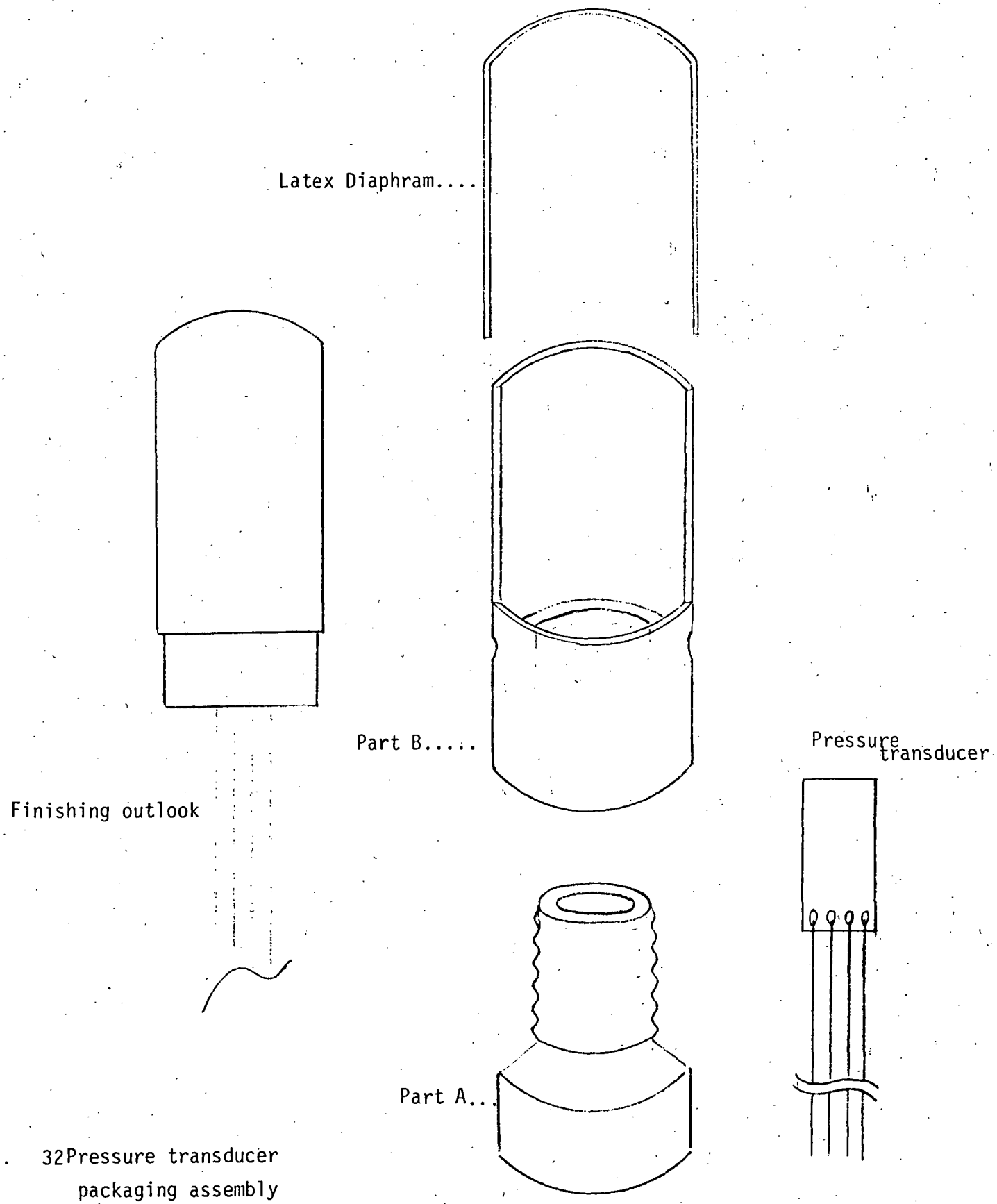

Fig. 32Pressure transducer packaging assembly

is bonded to its base. Sensor leads run through the center hole of part A. The hole is then sealed with RTV. The sensor rests on top of part A with a distance of about 2 mm. Sensor leads also serve as the supporting structure. The inside space is filled with silicon grease, which is the above mentioned "second fluid". The sealing process will be done in the silicon grease in the vacuum to insure that no air bubbles will be trapped inside the package.

The entire unit at present has a diameter of 160 mils and is 500 mils in length. However, it is only the first unit under test and it is believed that further size reduction can be obtained after successful development of the entire procedure.

Priviledged Communication
Wen H. Ko, Ph. D.

A MICROPROCESSOR BASED TELEMETRY DEMODULATION SYSTEM FOR PPM/PWM TELEMETRY SYSTEMS

Introduction

Pulse width-pulse position modulation is a scheme which is commonly used in biomedical implants, due to its low power consumption and high noise immunity as compared to other biotelemetric schemes. Information is transmitted in a succession of time frames, each frame consisting of several pulses of different pulse widths, and is then coded in the time lapsed between the pulses. One pulse is designated as the synchronization pulse and is used to distinquish one frame from another. The transmission scheme is carried out by narrow pulses, and is susceptible to environmental shot noise pickup, which appear as erroneous spikes at the output.

The problem of environmental noise pickup is one of the primary concerns in biomedical telemetry systems. For this reason, a telemetry demodulating unit with an improved built-in noise discrimination scheme was designed. In addition to the noise discrimination scheme, information processing capabilities in the demodulator unit was enabled by the incorporation of a microprocessor, including:

1. Higher reliability against component failure results from reduction in hardware complexity.
2. Addition of the powerful logic and mathematic capabilities of the unit allows for a more precise and complete pulse position discrimination scheme, as well as the addition of data processing capability.
3. Flexibility of system modification for use with various telemetry systems by proper change of system firmware.

A major disadvantage in using a microprocessor; however, is the speed limitation. The present system is designed to handle a data rate of 1200 data per second. This data rate imposes an upper limit on the programming complexity. Allowing half of the computer time for data processing, only 400 μs or less can be used for data logging.

The demodulator unit does not aim at one particular telemetry signal, but aims at a class of signals which are coded in a pulse width-pulse position modulated scheme. To provide such flexibility, three channels of pulse width discriminators are supplied. To insure high reliability, the system initiates a set of self-checking tests during the power up and reset stages. Software has been implemented in the system for a three channel RF powering telemetry unit, which has been developed at the Engineering Design Center. The physiological parameters which are monitored include: ECG, aortic blood pressure and body temperature.

A functional block diagram and a system block diagram of the microprocessor based demodulation system are given in Figures 1 and 2, respectively. Basically, the system performs four distinct funtions: (1) noise discrimination-distinquishes signal from noise, (2) signal demodulation-converts the pulse position modulated signals into physical parameters, e.g. temperature, (3) information processing-processes information for display and recording, and (4) system self-checking. System blocks include the noise discrimination scheme. System clock microprocessor and associated memory, test signal unit, input switches, and system output.

SYSTEM HARDWARE

Noise Discrimination Scheme

The noise discrimination scheme consists of a threshold detector, pulse width discriminator, and pulse rate discriminator. The threshold detector (Figure 3) is used to establish the proper amplitude of the incoming signal. Signals from the radio receiver are buffered by an LM310 voltage follower, which in turn drives the base of an NPN switching transistor (2N3904). The transistor is turned on when the input signal is greater than the sum of V_c and V_{be}, where V_c is the voltage across C_t. When the capacitor is charged to the peak signal value, the difference of the input voltage and V_{be}, the transistor is turned off. During the transistor off time, the capacitor discharges with a time constant R_tC_t, until the next input pulse. To isolate loading effects of the following

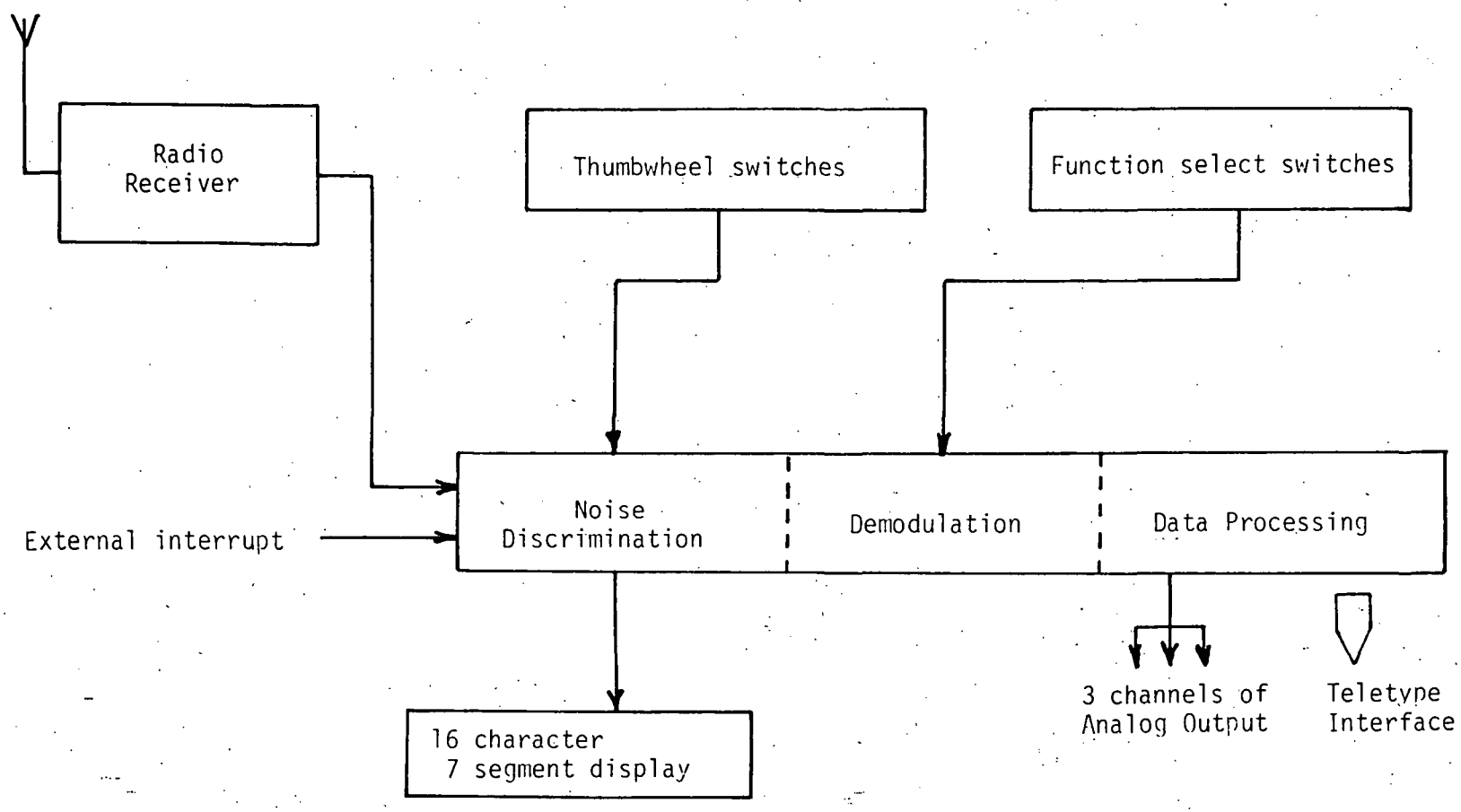

FIG. 1. FUNCTION OF THE DEMODULATION UNIT

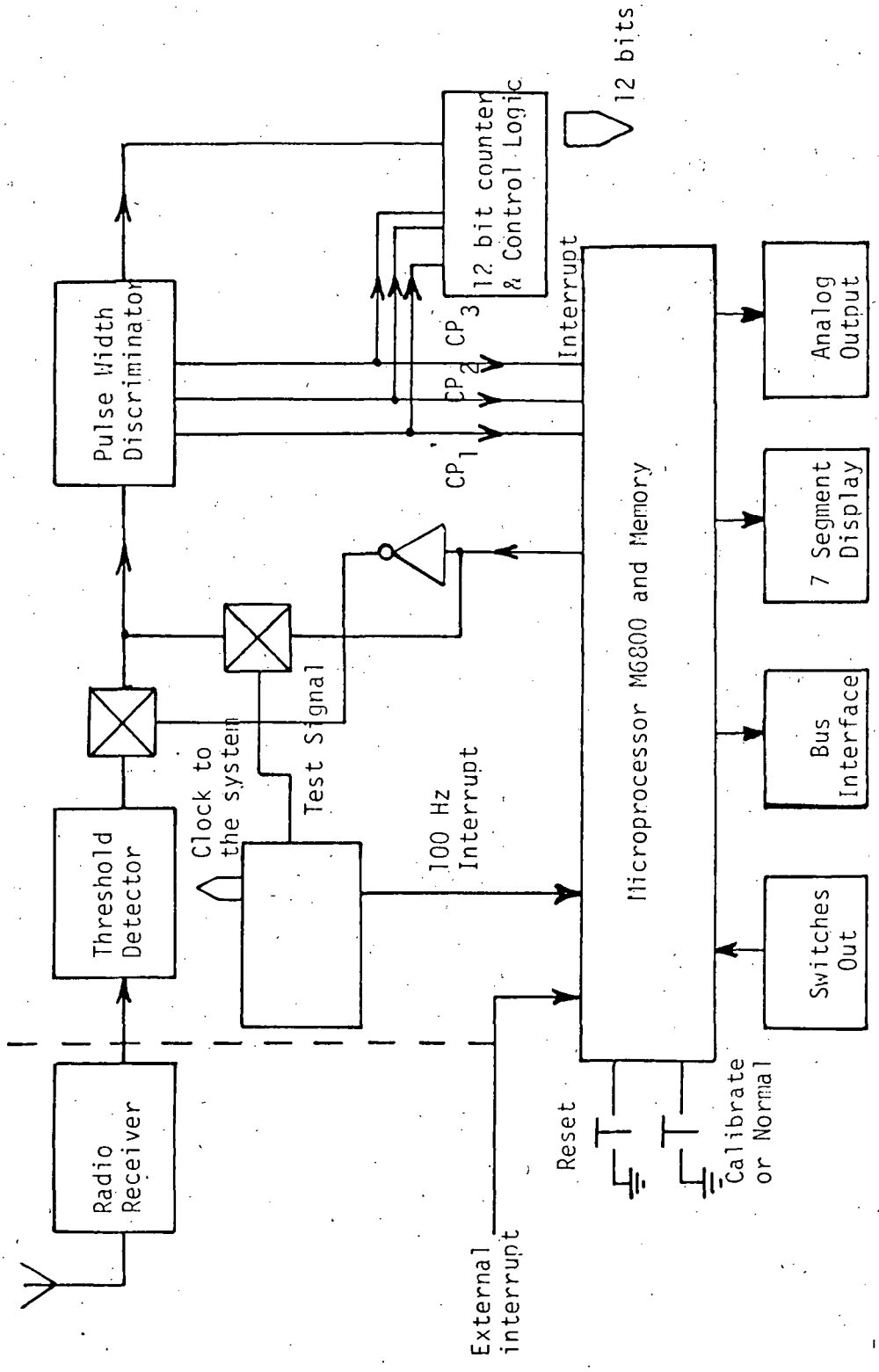

FIG. 2. SYSTEM DIAGRAM OF THE DEMODULATION UNIT

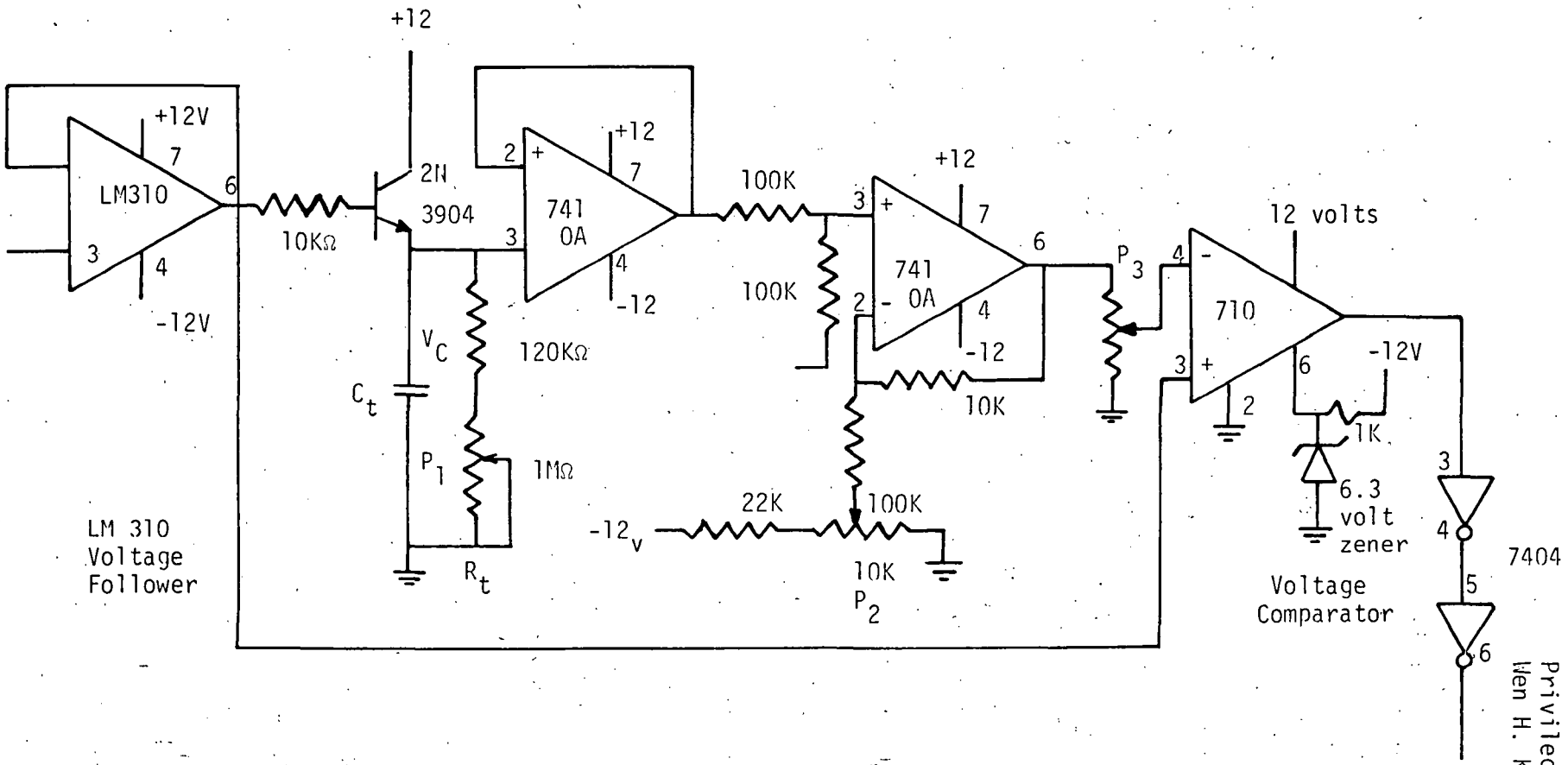

FIG. 3. THRESHOLD DETECTOR CIRCUIT

stages from affecting the decay time, V_c is buffered. The 741 operational amplifier sums V_c and V_{be}m which is defined to be the maximum amplitude. The threshold level is determined by taking approximately two-thirds of the maximum amplitude with potentiometer P_3. A voltage comparator (μA710) is used to compare incoming signals with the threshold level. The threshold detector is limited in that the strength of the incoming signals must be greater than the base-emitter voltage of the NPN switching transistor. It is further limited in that slight distortion and delay of the pulse shape exists due to the finite switching speeds of the transistors and operational amplifiers.

The pulse width discriminators (Figure 4) are used to setup pulse width windows for the incoming signals. This serves the dual purpose of distinquishing the occurrence of different pulses, as well as noise. Only pulses within the pulse width windows are allowed to pass each monostables. The microprocessor is responsible for proper loading of the pulse; widths into a set of D-latches to set the lower limits and tolerance of the discriminator. There are three sets of pulse width discriminator in the system. The first set differs from the other two in that its first monostable has three cascading binary counters; while the others only have two. This provision was made to allow for systems with a wide synchronous pulse. The present system allows for synchronous pulse widths of 0-2048 μs; with a maximum tolerance of 16 μs.

The pulse rate discriminator (Figure 5) is used to compare the pulse rate of incoming signals with the pulse rate of past signals. The pulse position counter is formed by three binary up counters. An on-board dip switch is provided for selection of the counter clock frequency. This provision is made to allow for optimal choice of the clock frequency for various telemetry systems.

System Clock and Microprocessor System

Accurate timing is necessary for counting the time lapsed between pulses. A clocking system was designed based on a 4 MHz crystal and a MC4324 voltage control oscillator. The circuit diagram of the system clock is given in Fig. 6. Output from the voltage control oscilla-

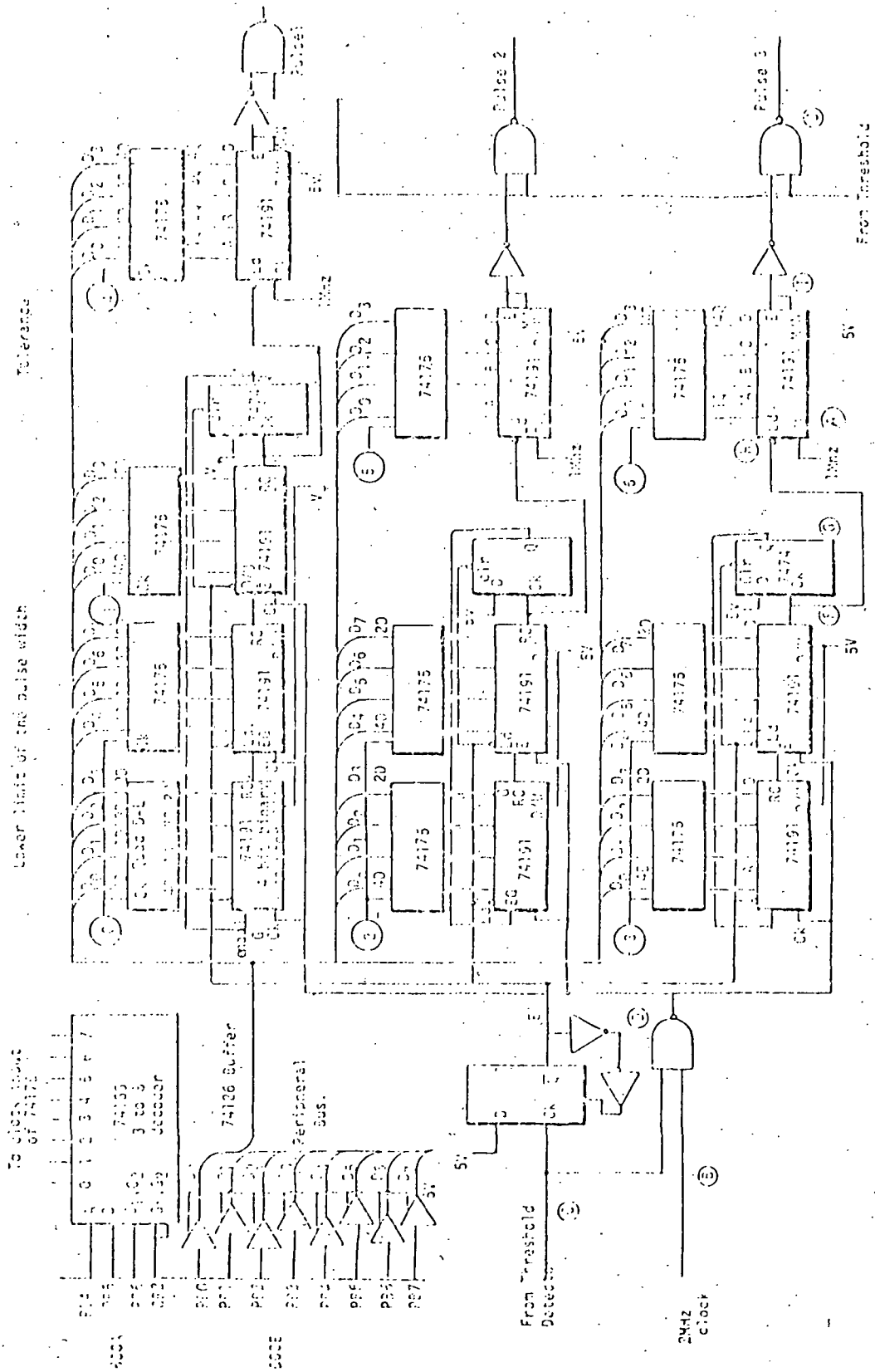

Fig.4 The Three Channels Programmable Pulse Width Discriminator

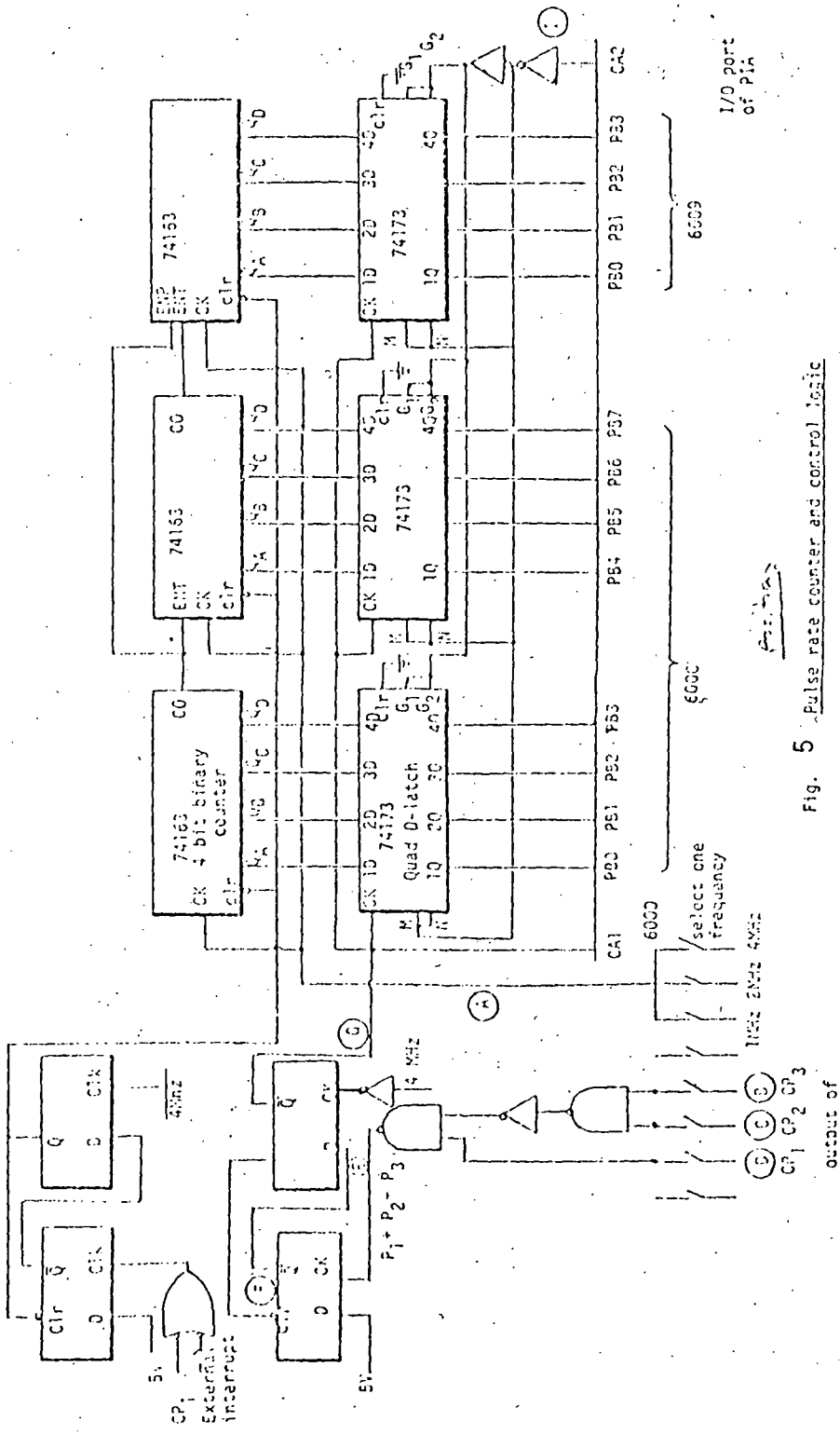

Fig. 5 Pulse rate counter and control logic

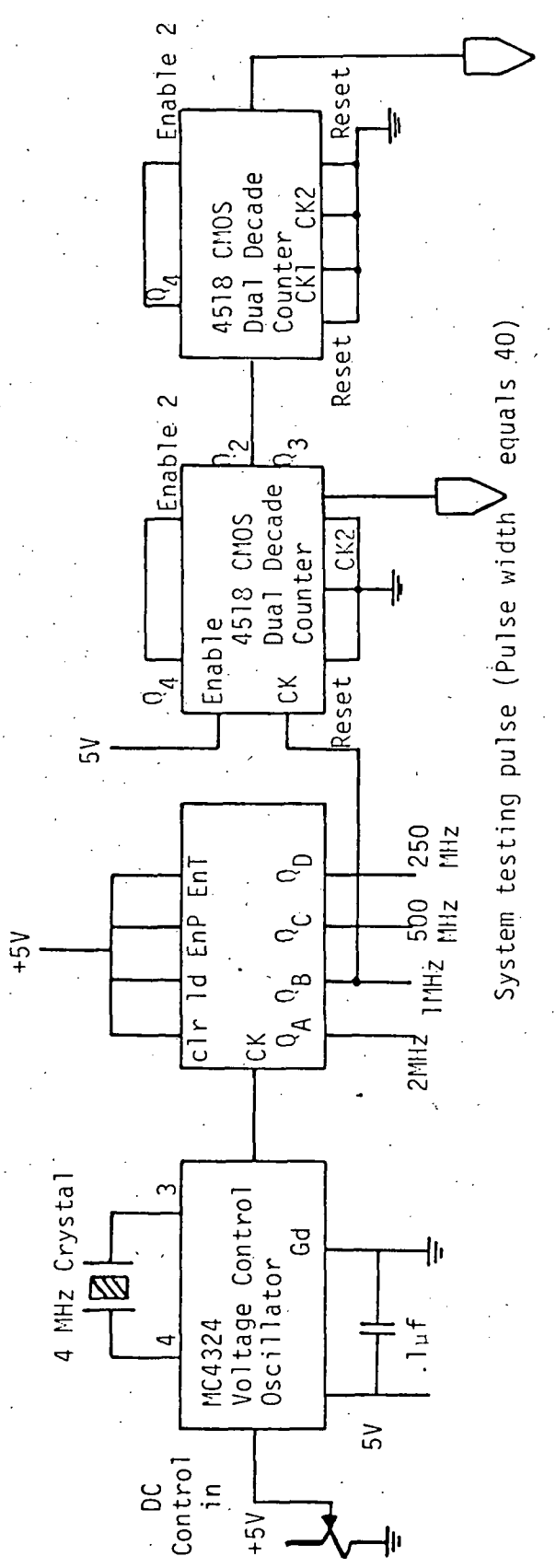

FIG. 6. CIRCUIT DIAGRAM OF THE SYSTEM CLOCK

tor is fed into a 74161 decade counter, providing a 2 MHz, 1 MHz, and 500 KHz clock. The MHz output is fed into two 4518 dual CMOS counters, providing a 100 Hz clock to interrupt the microprocessor and a test signal to the system [40 μsec. at 1 KHz rate].

The microprocessor unit (MPU) was designed with the capability of programming development, field testing and easy system modification. The system block diagram is given in Figure 7. The packaging of the unit is modular, to allow for system expansion, as well as ease in troubleshooting. The peripheral inputs and outputs are divided into two groups. The first group consists of all of the thumbwheel and pushbutton switches which are treated as memory addresses and hang directly on the address bus. The second group of peripheral inputs and outputs require data handling and handshaking and communicate with the microprocessor via two peripheral interface adaptors. These inputs and outputs include the interrupt signals from the pulse width discriminators, inputs from the counters, pulse discrimination setting and D/A converter outputs.

The MPU is controlled by a two phase, non-overlapping clock, which is provided by a retriggerable monostable in an astable configuration. Two potentiometers are used to adjust the pulse widths of ϕ_1 and ϕ_2. The minimum pulse widths for ϕ_1 and ϕ_2 are 430 ns and 450 ns, respectively. As the access time of the PROM 1702 exceeds 1000 ns, ϕ_2 is lengthened to 1000 ns to insure proper data reading. A power up resset circuit is provided to load the MPU and reset all internal registers, as well as to provide system stability during the "power-up" interval. A system bus was designed to insure that the capacitive and current loading does not exceed the driving capabilities of the MPU lines.

The memory module consists of 1K bytes of RAM and 2K bytes of PROM for both software development and fireware storage. As the capacitance load of the module is fairly substantial, both the data and address buses are buffered. An additional 1K byte of PROM occupies another module board with a separate data buffer.

The Peripheral Interface Adaptor (PIA) module forms the main link between the microprocessor and the front end circuitry of the demodulator unit. The PIA's share the same data buffer with the memory module, there-

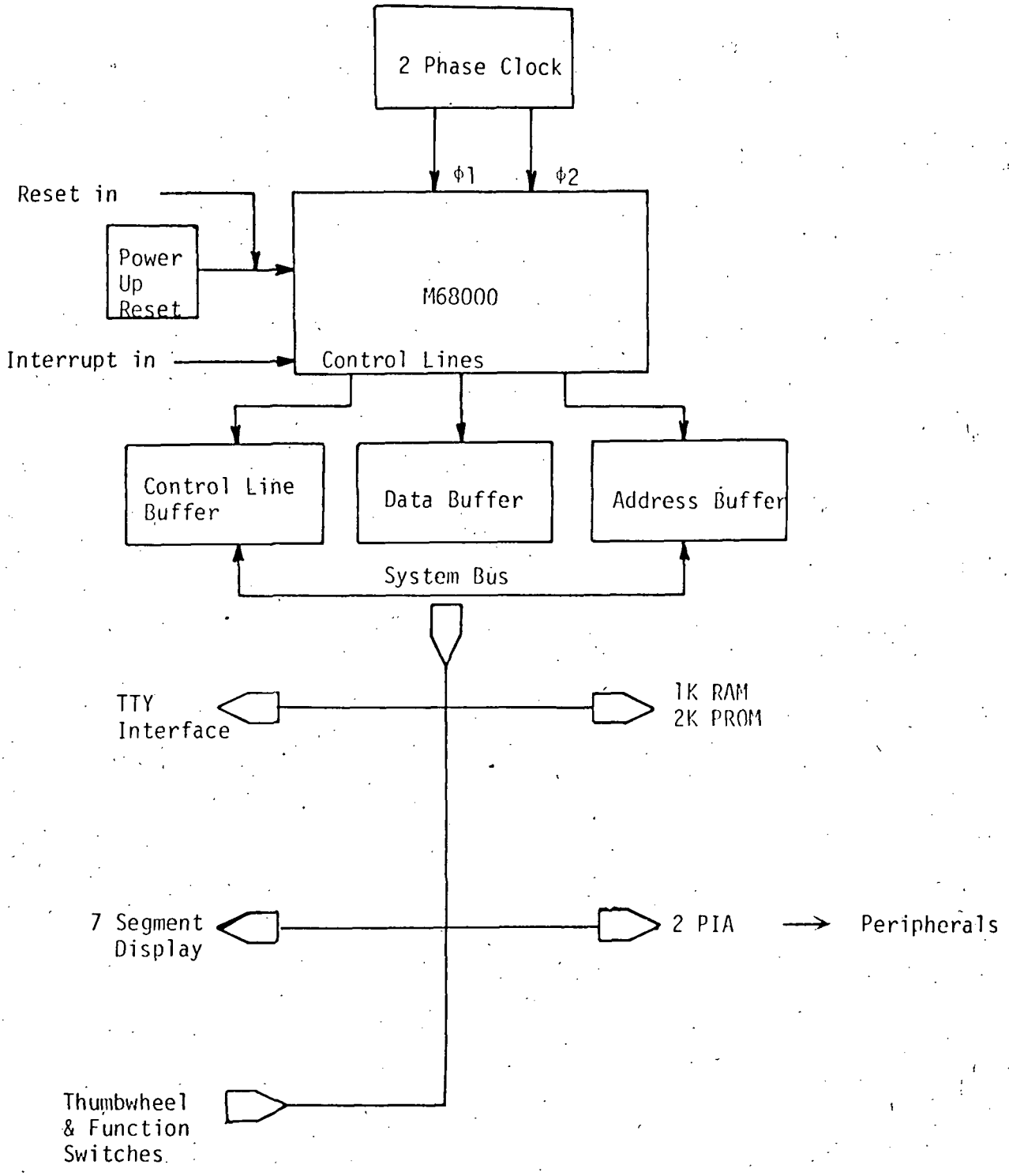

FIG. 7. THE MICROPROCESSOR SYSTEM BLOCK DIAGRAM

fore, removal of the memory module will disable the PIA module as well (a pitfall to be watched for in trouble shooting the unit). Interrupts to the PIA consist of the outputs of the pulse width discriminators, counter control signals, a 0.01 second timer and an external interrupt. It is expected that this set of interrupt signals will satisfy most of the system handling needs.

The teletype interface module consists of a Mikbug ROM, a 128 x 8 bit RAM and a PIA interface to the teletype. The system works in a full duplex mode and transmission timing is provided by a MC14536 programmable timer. The Mikbug teletype monitor has its own interrupt handler program. Upon subjection to any one of the interrupt modes, the microprocessor jumps to a vertor address to fetch a program "start address" and executes the program at that particular address location. Software interrupts gives the programmer breakpoints in the program development, during which the contents of the MPU registers print out the teletype.

SYSTEM SOFTWARE

In programming the demodulation unit for the telemetry system, the major concern was the detailed specification of the signal format and information coding. The implant package information format with a 1 KHZ clock is shown in Figure 8. One signal frame consists of four pulses, including an empty channel for synchronization purposes and three signal channels. In a typical implant package, the position sensitivity of the pulse position versus parameter variation as follows:

Pressure Channel: 1mmHg - corresponding to 0.6 μs

Temperature Channel: 1°C - corresponding to 1.4 μs

EKG Channel: dependent on signal strength.

Due to the input/output structure of the PIA's, the system uses an interrupt scheme to handle the data processing, synchronization to the RF powering signal and channel recognition. Since only one type of pulse exists, only one of the three pulse width discriminators is used. Interrupts to the system consist of the RF powering clock, channel #2's pulse width discriminator output and a 100 Hz timer.

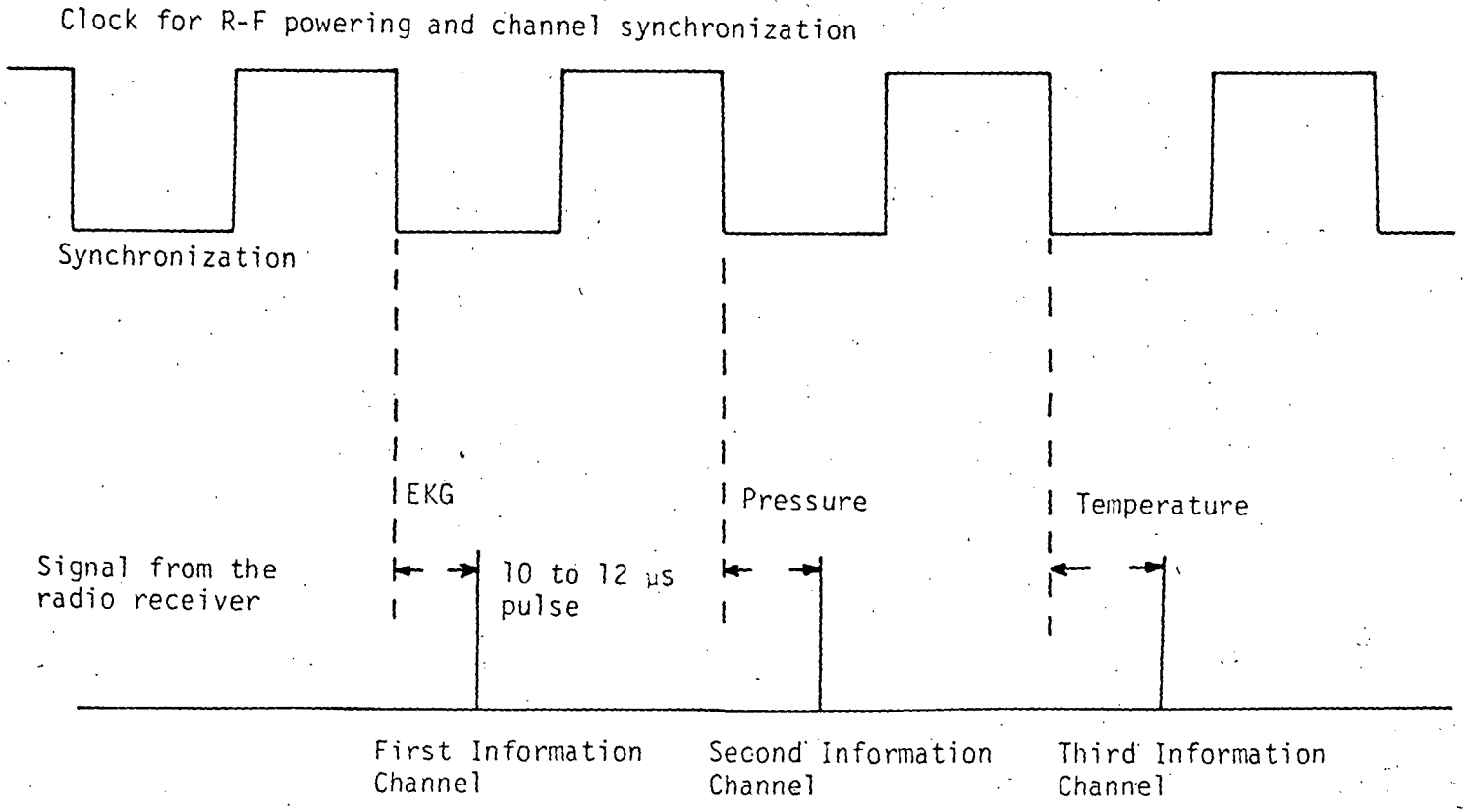

FIG. 8. INPUT SIGNAL FORMAT

The system firmware is organized in the following manner:

1. Initialization program: initialize PIA, stack and temporarily store register in the RAM.
2. System testing program: to test proper operation of the system and send out an alarm signal to the LED display when the system malfunctions.
3. Demodulation start program: set the window width via thumbwheel switches and lock into the proper channel sequence.
4. Processing information program: consists of the interrupt programs and data processing subroutines. Counter data is checked by a noise discrimination program. Valid data is passed to the data processing subroutines and EKG subroutine for further processing.

In order to calculate the EKG rate, the microprocessor has to recognize the periodic appearance of the EKG waveform. A software threshold detector is implemented to discriminate the R-wave in the QRS complex. The threshold is established by taking the maximum amplitude of EKG waveform and subtracting from it the EKG threshold by using the preset in the front panel with S2. The setting of the EKG threshold is calibrated in μsecs. To calculate the pulse rate, a software timer is used to count the time lapsed between two R-waves. This is done while 0.01 sec interrupt occurs.

For the temperature channel, the position of pulse C2 increases linearly with temperature. The pulse position vs. temperature curve can be approximated by the following equation:

$$T_x\ °C = K_3\ (T_{xc} - T_{1c}) + T_1 °C$$

where T_x = Temperature

T_{xc} = Counter Reading of the Temperature Channel at T_x°C

where K_3 will be the slope of the curve and is readily determined by taking the pulse position at T_1 and at another temperature T_2

$$K_3 = \frac{|T_2 - T_1|}{|T_{2c} - T_{1c}|}$$

This is done by microprocessor during system initialization. The typical value is 0.0735°C/μs.

The pressure channel output shows a linear relationship with temperature, i.e. for the same pressure setting, pulse position increases with increase in temperature at roughly 12 μsec/°C. The effect of temperature on the pressure channel count can be approximated by:

$$CP_{xc} = P_x T_y - K_1 (T_{yc} - T_{3c})$$

where P_x = Pressure P_x mmHg eg. 100.0 mmHg

$P_{xc}T_y$ = Pressure count at Temperature T_y°C at pressure P_x

CP_{xc} = Compensated pressure count

where

$$K_1 = \frac{P_{xc}T_3 - P_{xc}T_a}{T_{ac} - T_{3c}}$$

K_1 is positive. Pressure is compensated at temperature T_3. Typical value for K_1 is o.84 mmHg/°C.

After the temperature effect is compensated for, the value of the pressure can be calculated using the following equation:

$$P_x = P_1 - K_2 (CP_{xc} - CP_{1c})$$

Where

$$K_2 = \frac{P_2 - P_1}{CP_{2c} - CP_{1c}}$$

Typical value of K_2 is around 0.44 mmHg/count with a 4 MHz clock.

Values of the constants, K_1, K_2 and K_3 depend on the telemetry implant package. Consequently, a calibration procedure is needed for each package to determine the exact values of K_1, K_2 and K_3. All calculations are done by the microprocessor. The user enters the result of the calibration into PROM and the microprocessor will perform calculations of K_1, K_2 and K_3 during the reset stage.

SYSTEM EVALUATION

Figure 9 shows the setup for testing the operation of the unit. In this unit, the test signal pulse is transmitted with a fundamental frequency of 35 MHz which is picked up with a radio receiver at the third harmonic. The video output of the radio receiver is connected to the "receiver in" output of the demodulation system.

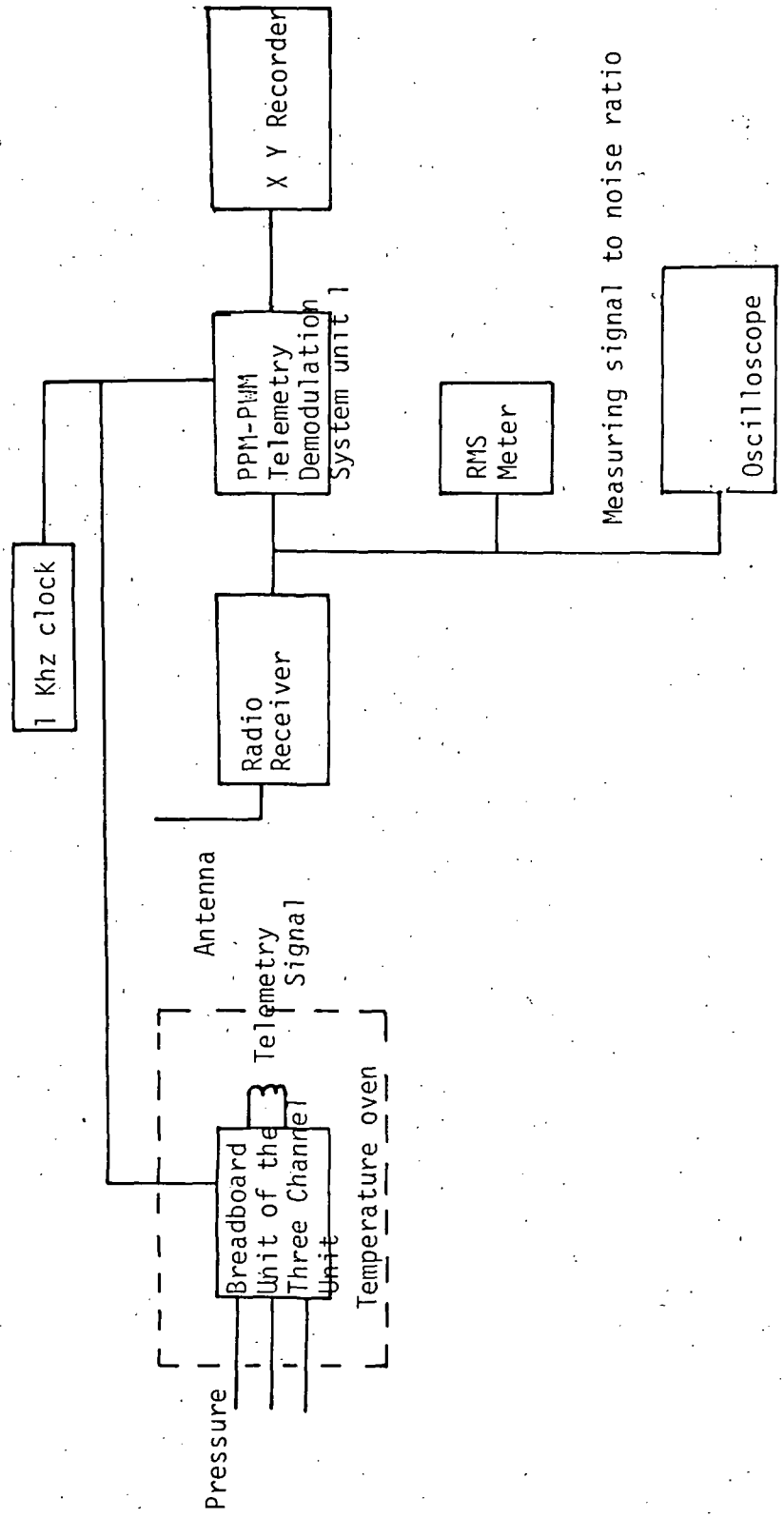

FIG. 9. TEST SETUP FOR THE PWM-PPM TELEMETRY DEMODULATION SYSTEM UNIT 1

The clock for the modulation and demodulation systems is from an NE555 timer running at one KHz. An in-house pressure transducer is used for pressure sensing and a thermistor is used for temperature sensing. A Kronkit signal generator and an EKG signal generator supply test signal to test the frequency response of the system and the EKG recognition scheme.

Noise was derived from a drill. At one time, a white noise generator was used; but the drill proved to be a better shot noise source. The output of the receiver was fed into a RMS meter to give a quantitive measure of the noise level generated.

The three channel telemetry modulation unit was housed in a temperature oven for the calibration of the temperature channel. A water manometer is used to apply pressure transducer.

The output of the EKG channel of the system, when fed with sinusoidal wave of different frequencies is shown in Figure 10. Outputs above 80 Hz begin to show distortion which can be ascribed to the sampling frequency of the signal. Figure 11 shows the output of the EKG channel of the system with an EKG input. The EKG signal observed by the seven segment display agreed with the signal period.

The implant package was calibrated in the temperature range of 30°C to 40°C. Within this range, the calibration is accurate up to 1/2°C, however, beyond this range, the thermistor begins to exhibit nonlinearity. The pressure channel calibration is accurate only on a short term basis. Investigation of the pressure transducer indicates that there is a constant drift in the pressure transducer.

The effectiveness of the system is discriminating environmental shot noise was investigated. Typical signal input from the radio receiver with noise is shown in Figure 11. Without the discrimination scheme, the output of the demodulation unit a substantial amount of noise leaks through the threshold detector. Nevertheless, with the first two stages, most of the noise is eliminated.

The pulse rate discriminator discriminated signal from noise to within a certain tolerance of the previous pulse position and shut off data processing under sudden occurence of noise after the first two stages. The output is held constant until noise passes away.

Signal amplitude = 60 us

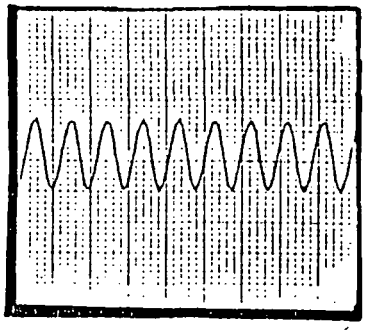

20 Hz

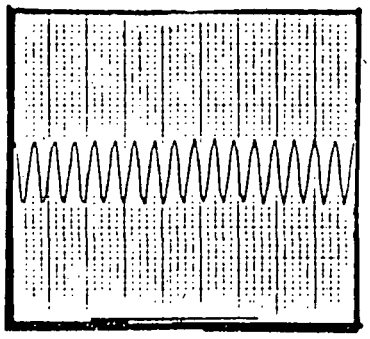

40 Hz

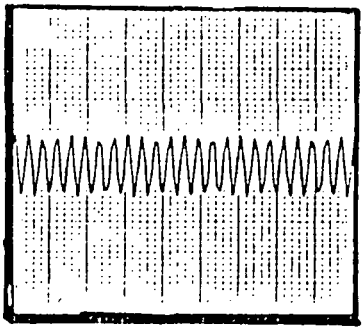

60 Hz

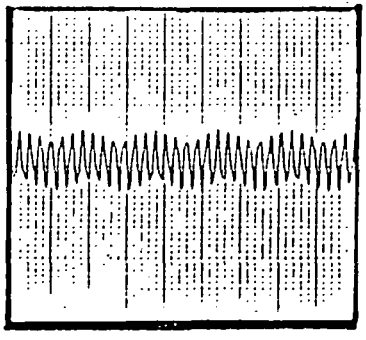

80 Hz

Fig. 10 System reponse to different frequencies.

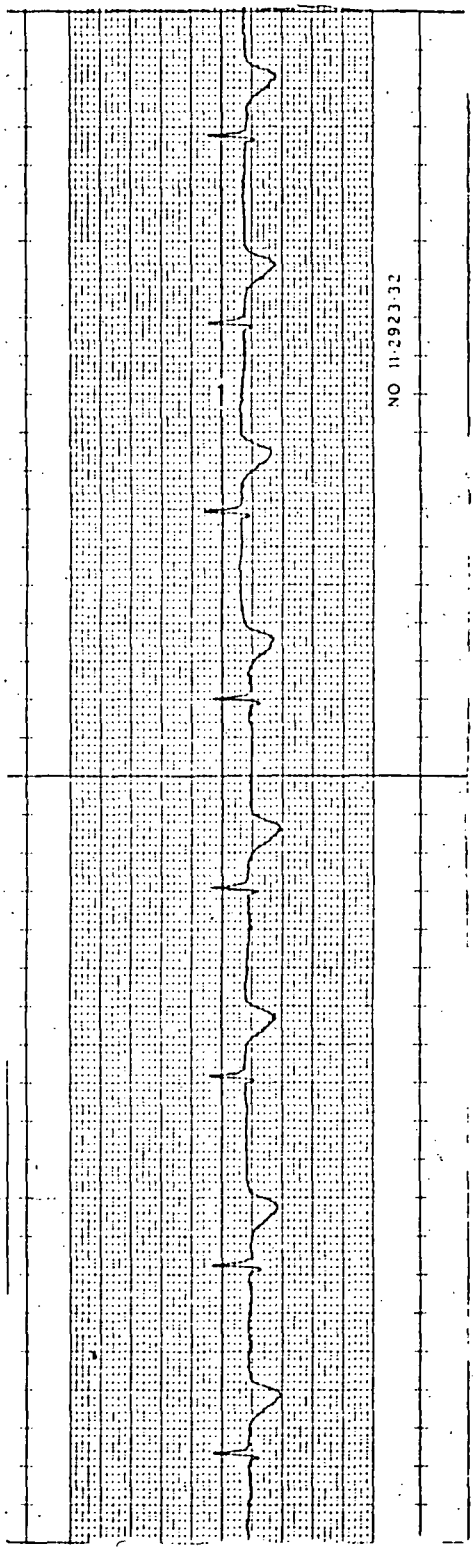

Signal amplitude from peak of the R wave to the bottom is around 5 us

Horizontal axis : 25 mm / sec.

Fig. 11 The output of the EKG channel

PUBLICATION AND THESIS LIST

Ahn, B.K.; Liu, C.C. and Wist, A.O., "Development of a Miniature pH Glass Electrode with Field Effect Transistor Amplifier for Biomedical Application," Medical and Biological Engineering, May, 1975.

Ko, W.H.; Liang, S.P.; and Fung, C., "Design of the PR Powered Coils for Implant Instruments," submitted to Medical and Biological Engineering, 1977.

Ko, W.H.; Hynecek, J.; and Homa, J., "Single Frequency RF Powered ECG Telemetry System," submitted to IEEE Trans. BME, 1977.

Liu, C.C.; Ahn, B.K.; and Brown, E.G., "Engineering Development and Evaluation of Implantable pO_2, pH, pCO_2 Sensors, " 1st Pacific Chemical Engineering Congress, Kyoto, Japan, October, 1972.

Ko, W.H.; Hynecek, J.; Poon, C.W.; and Greenstein, E., "Ingestible Telemetry System for Low Frequency Signals," 26th ACEMB, Minneapolis, Minn., October 1973.

Vamvakas, S., "Miniature Three Channel Tape System for Physiological Monitoring," 10th Annual Meeting of the Association for the Advancement of Medical Instrumentation, Boston, Mass., March, 1975.

Hynecek, J. and Ko, W.H., "Single Frequency RF Powered Telemetry System," 28th ACEMB, New Orleans, Louisiana, September 20-24, 1975.

Ko, W.H.; Hynecek, J.; and Kou, A., "An Implantable Single Frequency RF Powered Telemetry System," 3rd International Symposium on Biotelemetry, May 17-20, 1976.

Ko, W.H. and Kou, A., "A Single Frequency RF Powered Implantable Multichannel Telemetry System in Cardiovascular Application," 29th ACEMB, Boston, Mass., November 6-10, 1976.

Ko, W.H. and Liang, S.P., "RF Powered Cage System for Implant Telemetry," submitted to the 30th ACEMB, 1977.

Vamvakas, Spiro. *Miniature Three channel Tape System for, Physiological Monitoring,* M.S., August, 1974.

Poon, Chie Wan. *An Ingestible Temperature Telemetry System,* M.S., September, 1974.

Todd, Steven Gerald. *The Control and Demodulation for a Single Channel R. F. Powered Telemetry Transmitter,* M.S., January, 1975.

Kou, Abraham. *A Single Frequency RF Powered Three Channel Telemetry System,* M.S., June, 1976.

Yau, K.K. *A Microprocessor Based Telemetry Demodulation System for PWM/PPM Telemetry Signals,* M.S., June, 1977.